Targeted alpha therapy for epithelial ovarian cancer

Author:
Song, Emma Yanjun

Publication Date:
2007

DOI:
https://doi.org/10.26190/unsworks/6662

PLEASE TYPE

THE UNIVERSITY OF NEW SOUTH WALES
Thesis/Dissertation Sheet

Surname or Family name: **Song**

First name: **Emma** Other name/s: **Yanjun**

Abbreviation for degree as given in the University calendar: **PhD**

School: **St George Clinical School** Faculty: **Medicine**

Title: **Targeted Alpha Therapy for Ovarian and Other Cancers**

Abstract 350 words maximum: (PLEASE TYPE)

Purpose: Control of micrometastatic ovarian cancer in peritoneal cavity remains a major objective in post-surgical treatment. The purpose of this project was to investigate the efficacy and toxicity of targeted alpha therapy (TAT) for ovarian cancer in intro and in vivo in animal model and select optimal targeting vector for ovarian cancer clinical trial; to develop animal model of ovarian cancer for further TAT.

Methods: The expression of the tumor-associated antigens (Her2. MUC1, uPA/uPAR) on cancer cell line, animal model and human ovarian cancer tissue was tested by immunostaining. MTS and TUNEL assay were used to evaluate cell killing of alpha conjugates in monolayer and spheroids growth cells. In vivo, toxicity and maximum tolerance doses for different vectors were tested and determined. The pharmacokinetics was studied for different time points and different parameters. The antiproliferative effect of ^{213}Bi-C595, and ^{213}Bi-PAI2 was tested at 9 days post-peritoneal cell inoculation of ovarian cancer cell OVCAR3. The treatment efficacy of ^{213}Bi-Herceptin was tested at a 2 days post-subcutaneous breast cancer cell BT474 inoculation. Mice were injected (i.p) with various concentrations of alpha conjugates. Changes in tumor progression were assessed by girth size and tumor size.

Results: uPA/uPAR and MUC1 are expressed on ovarian cancer cell lines and more than 30% ovarian cancer tissue, while HER2 was only positive in one cell line and less than 15% positive was found in ovarian cancer tissues. The ACs can target and kill cancer cells in vitro in a dose dependent fashion. TUNEL positive cells were found after incubation with the different ACs. PAI2 and C595 vectors were selected for in vivo ascites model study of OVCAR3 cell with high expression. Delayed and acute toxicity in animal model showed that radiation nephropathy was the cause of body weight loss. Biodistribution studies showed that kidney and ascites was the major uptake organs. L-lysine can induce kidney uptake for ^{213}Bi-PAI2, but no statistics different was found. A single ip injection of ^{213}Bi-C595 or ^{213}Bi-PAI2 can inhibit ascites growth, whereas, ^{213}Bi-Herceptin can inhibit breast cancer growth in a nude mice model. There were no toxicity was found in clinical trial patient up to 1.5 years.

Conclusion: ^{213}Bi labelled targeting vectors can specifically target cancer cells in vitro and inhibit tumor growth in vivo. These ACs may be useful agents for the treatment of ovarian and breast cancer at the minimum residual disease stage.

FOR OFFICE USE ONLY Date of completion of requirements for Award:

4/7/07

THIS SHEET IS TO BE GLUED TO THE INSIDE FRONT COVER OF THE THESIS

TARGETED ALPHA THERAPY

FOR EPITHELIAL OVARIAN CANCER

Emma Yanjun Song

A Thesis Submitted in Fulfillment of The Requirements for The

Degree of Doctor of Philosophy

Faculty of Medicine

University of New South Wales

March 2007

ORIGINALITY STATEMENT

'I hereby declare that this submission is my own work and to the best of my knowledge it contains no materials previously published or written by another person, or substantial proportions of material which have been accepted for the award of any other degree or diploma at UNSW or any other educational institution, except where due acknowledgement is made in the thesis. Any contribution made to the research by others, with whom I have worked at UNSW or elsewhere, is explicitly acknowledged in the thesis. I also declare that the intellectual content of this thesis is the product of my own work, except to the extent that assistance from others in the project's design and conception or in style, presentation and linguistic expression is acknowledged.'

Date 27.08.07

ABSTRACT

Purpose: Control of micrometastatic ovarian cancer in the peritoneal cavity remains a major objective in post-surgical treatment. The purpose of this project was to investigate the efficacy and toxicity of targeted alpha therapy (TAT) for ovarian cancer in vitro and in vivo in animal models and to select the optimal targeting vector for an ovarian cancer clinical trial. Animal models of ovarian, breast and prostate cancer were developed and for further TAT; a phase I melanoma clinical trial was supported, paving the way for an ovarian cancer clinical trial.

Methods: The expression of the tumor-associated antigens (Her2, MUC1, uPA/uPAR) on cancer cell line, animal model xenografts and human ovarian cancer tissue was tested by immunostaining. MTS and TUNEL assays were used to evaluate cell killing of alpha conjugates in monolayer and spheroids. Toxicity and maximum tolerance doses for different vectors were tested and determined in vivo. Pharmacokinetics was studied for different time points and different parameters. The antiproliferative effect of ^{213}Bi-C595 and ^{213}Bi-PAI2 was tested at 9 days post-peritoneal cell inoculation of the ovarian cancer cell line OVCAR3. The treatment efficacy of ^{213}Bi-Herceptin was tested at a 2 days post-subcutaneous breast cancer cell BT474 inoculation. Mice were injected (i.p) with various concentrations of alpha conjugates (AC). Changes in cancer progression were assessed by girth size and tumor size.

Results: uPA/uPAR and MUC1 are expressed on ovarian cancer cell lines and more than 45% ovarian cancer tissue, while HER2 was only positive in one cell line and was positive in less than 15% of ovarian cancer tissues. The ACs can target and kill cancer cells in vitro in a dose dependent fashion. TUNEL positive cells were found after

incubation with the different ACs. PAI2 and C595 vectors were selected for in vivo ascites model study of OVCAR3 cell with high expression. Delayed and acute toxicity in animal models showed that radiation nephropathy was the cause of body weight loss. Biodistribution studies showed that kidney was the major uptake organ. L-lysine can reduce kidney uptake for ^{213}Bi-PAI2, but no significant differences were found. A single ip injection of ^{213}Bi-C595 or ^{213}Bi-PAI2 can inhibit ascites growth, whereas, ^{213}Bi-Herceptin can inhibit breast cancer growth in a nude mice model.

Conclusion: ^{213}Bi labelled targeting vectors can specifically target ovarian cancer cells in vitro and inhibit tumor growth in vivo. These ACs may be useful agents for the treatment of ovarian cancer at the minimum residual disease stage.

Dedicated to

My parents and husband (Changfa Qu) – the people who brought me to life and continue to be a light through any dark moment

ACKNOWLEDGEMENT

I would like to express my appreciation to people who provided great assistance during this study.

I am so pleased and feel so lucky to be a PhD student under the supervision of Professor Barry J Allen, who not only has a deep knowledge in the research field, but is modest, easy to talk with humble, and has an encouraging personality, providing a good example for my future career development. He made research and life much easier for a migrant PhD student. I enjoyed every moment to stay with his group and the scientific discussion arising between us. I would like to acknowledge and thank Professor Allen for all his support for my work and me through all these years.

I am grateful to Shirley Edwards Foundation for a medical research scholarship, which eased my financial difficulties.

Thanks are also due to Dr Greg Robertson, Gynaecology Oncologist, Department Gynaecology, St George Hospital, my co-supervision for the research work, as well as the great help while I was ill.

Dr Rizvi and Dr Li from Centre for Experimental Radiation Oncology need special mention for their technical support to this work. Dr Rizvi is a specialist in radiation chemistry in addition to being a helpful and wonderful person. He helped throughout the study, particularly in the radiation labelling aspect. Dr Li is a specialist in

Immunohistochemistry and I would like to acknowledge his assistance in scoring staining density. I would also like to thank Dr Raja for her help and encouragement in the clinical trial and also to acknowledge her great help in English correction and thesis writing.

I would also thank my husband Dr Changfa Qu for his great emotional support and encouragement, as well as his technical support in animal handling and modelling. He has been through the entire thick and thins over the years, but has always been supportive and a wonderful partner. Without his help, I would not have been able to finish this work.

I would like to thank Professor J Kearsley, Director, Division of Cancer Services, St George Hospital for his support. I would also like to express my appreciation for assistances by Dr Qi, Department Immunology; Dr Fang, Department Cancer Services; Dr Feng, Department Medicine; Dr Mohammad, Department Surgery.

The research work described in this thesis was carried out at Division of Medicine, the St George Hospital, and the University of New South Wales. I gratefully acknowledge the support of both organizations in this work.

Thank you all.

Emma Yanjun Song

LIST OF PUBLICATIONS

1. Song YJ, Qu CF, Rizvi SMA, Li Y, Robertson G, Raja C, Morgenstern A, Apostolidis C, Perkins AC, Allen BJ. Cytotoxicity of PAI2, C595 and Herceptin vectors labeled with the alpha-emitting radioisotope Bismuth-213 for ovarian cancer cell monolayers and clusters. Cancer Letters 2006; 234:176-83.

2. Song EY, Rizvi SMA, Qu CF, Raja C, Brechbiel MW, Morgenstern A, Apostolidis C, Allen BJ. Pharmacokinetics and toxicity of 213Bi-labeled PAI2 in preclinical targeted alpha therapy of cancer Cancer Biol Ther 2006; in press

3. Qu CF, Songl YJ, Rizvi SMA, Li Y, Smith R, Perkins AC, Morgenstern A, Brechbiel M, Allen BJ. In vivo and in vitro inhibition of pancreatic cancer growth by targeted alpha therapy using 213Bi-CHX.A"-C595. Cancer Biology & Therapy 2005; 4:848-53.

4. Qu CF, Song EY, Li Y, Rizvi SMA, Raja C, Smith R, Morgenstern A, Apostolidis C, Allen BJ. Pre-clinical study of 213Bi labeled PAI2 for the control of micrometastatic pancreatic cancer. Clin Exp Metastasis 2005; 22:575-86.

5. Qu CF, Li Y, Song YJ, Rizvi SMA, Raja C, Zhang D, Samra J, Smith R, Perkins AC, Apostolidis C, Allen BJ. MUC1 expression in primary and metastatic pancreatic cancer cells for in vitro treatment by (213)Bi-C595 radioimmunoconjugate. British Journal of Cancer 2004; 91:2086-93.

6. Rizvi S, Qu C, Song Y, Raja C, Allen B. In vivo studies of pharmacokinetics and efficacy of Bismuth-213 labeled antimelanoma monoclonal antibody 9.2.27. Cancer Biol Ther 2005; 4:763-8.

7. Rizvi SMA, Li Y, Song EY, Qu CF, Raja C, morgenstern A, Apostolidis C, Allen BJ. Preclinical studies of bismuth-213 labeled plasminogen activator inhibitor

type 2 (PAI2) in a prostate cancer nude mouse xenograft model. Cancer Biol Ther 2006; 5:386-93.

8. Allen BJ, Raja C, Rizvi S, Li Y, Tsui W, Zhang D, Song E, Qu CF, Kearsley J, Graham P, Thompson J. Targeted alpha therapy for cancer. Phys Med Biol 2004; 49:3703-12.

9. Raja C, Graham P, Rizvi S, Song E, Helen G, John T, Anja B, Alfred M, Christos A, John K, Ralph R, Barry J A. Interim analysis of toxicity and response in a Phase 1 trial of systemic targeted alpha therapy for metastatic melanoma
Cancer Biol Ther 2007; in press.

LIST OF ABBREVIATIONS

AC	—	Alpha Conjugate
ACEC	—	Animal Care and Ethics Committee
AIC	—	Alpha-Immunoconjugate
APAAP	—	Alkaline Phosphatase Anti-Alkaline Phosphate
ARC	—	Animal Resources Centre
ATCC	—	America Type Culture Collection
Bi	—	Bismuth
BSA	—	Bovine Serum Albumin
CBMN	—	Cytokinesis block micronucleus assay
CC	—	Cold control
cDTPA	—	Cyclic Anhydride of Diethylenetriaminepentacetic Acid
CML	—	Chronic Myelocytic Leukaemia
CO_2	—	Carbon Dioxides
CT	—	Computer-Aided Tomography
DAB	—	Diaminobenzidine
DMEM	—	Dulbecco's Modified Eagle's Medium
DMPS	—	D,L-2,3-dimercapto-propane-I-sulfonic acid
DMSA	—	Meso-2,3-dimercaptosuccinic acid
DMSO	—	Dimethylsulphoxide
DNA	—	Deoxyribonucleic Acid
DPBS	—	Dulbecco's Phosphate Buffered Saline
DTPA	—	Diethylenetriaminepentacetic Acid
ECM	—	Extracellular Matrix
EDTA	—	Ethylene Diamine Tetraacetic Acid
EGFR	—	Epidermal growth factor receptor
ELISA	—	Enzyme-Linked Immunosorben Assay
FACS	—	Fluorescence Activated Cell Sorting

FBS	—	Fetal Bovine Serum
FITC	—	Fluorescein Isothiocyanate
HAMA	—	Human Anti-Mouse Antibody
HER2	—	Human Epidermal Growth Factor Receptor
HI	—	Hydriodic Acid
HRP	—	Horse Radish Peroxidase
i.p	—	Intraperitoneal
i.v	—	Intravenous
Ig	—	Immunoglobulin
IMDM	—	Iscove's Modified Dulbecco's Medium
ITLC	—	Instant Thin Layer Chromatography
ITU	—	Institute for Transuranium Elements
LET	—	Linear Energy Transfer
MAb	—	Monoclonal Antibody
MRD	—	Minimal Residual Disease
MTD	—	Maximum Tolerated Dose
MTS	—	3-(4,5-dimethylthiazol-2-yl)-5-(3-carboxymethoxyphenyl)-2-(4-sulfophenyl)-2H-tetrazolium, inner salt
MUC1	—	Human Urinary Epithelial Mucin
NIH	—	National Institute of Health
PAI-1	—	Plasminogen Activator Inhibitors Types 1
PAI2	—	Plasminogen Activator Inhibitors Types 2
PC	—	Pancreatic Cancer
PCR	—	Polymerase Chain Reaction
RBC	—	Red blood cell
RBE	—	Radiobiological Effectiveness
RIC	—	Radioimmunoconjugate
RIT	—	Radioimmunotherapy

RT	—	Room Temperature
s.c	—	Subcutaneous
scFvs	—	Single-Chain Fvs
TAAs	—	Tumor Associated Antigen
TAT	—	Targeted Alpha Therapy
TBS	—	Tris Buffered Saline
TUNEL	—	Terminal Eoxynucleotidyl transferase [TdT]-Mediated Deoxyuridinetriphosphate
UNSW	—	University of New South Wales
uPA	—	Urokinase Plasminogen Activator
uPAR	—	Urokinase Plasminogen Activator Receptor
VEGF	—	Vascular Endothelial Growth Factor
WBC	—	White blood cell

TABLE OF CONTENTS

LIST OF FIGURES

LIST OF TABLES

APPENDICES

CHAPTER 1

Introduction

1.1 Current problems of ovarian cancer

Ovarian cancer is the most lethal of the gynecological cancers. This is due to late detection and the fact that most patients have disease outside the pelvis at diagnosis. Cytoreductive, surgery and systemic therapy have improved the overall survival of these patients. However, relapses occur even after apparent complete remission because of an occult spread of single tumor cells or small tumor cell clusters. Late-stage ovarian cancer is often characterized by metastatic seeding of the peritoneal surface and accounts for 75-85% of all of the newly diagnosed ovarian cancer patient (McGuire, 1993). Peritoneal spread is an important feature in the natural history of the disease. Failure to control disease within the peritoneal cavity is a major cause of treatment failure. Half of those patients later relapse with chemoresistant disease and are not adequately rescued by additional therapy (Creemers et al., 1996). Therefore, there is an urgent need for new therapeutic approaches for metastatic ovarian cancer. To kill single tumor cells in the peritoneal cavity, a new locoregional radioimmunotherapeutic strategy based on tumor-specific MAbs conjugated to high linear energy transfer α-emitters seems highly promising (Aurlien et al., 2000; Imam, 2001; McDevitt et al., 1998).

1.2 Radioimmunotherapy

Interests in radioimmunotherapy (RIT) for various cancers are growing rapidly. The field was clinically established by the recent introduction of the first two U.S. Food and Drug Administration–approved drugs, ibritumomab tiuxetan (Zevalin; Biogen Idec Inc.) (Wiseman et al., 1999) and tositumomab (Bexxar; GlaxoSmithKline) (Press et al., 2000), for the treatment of non-Hodgkin's lymphoma.

The development of strategies with different targeting agents, such as antibodies and other ligands, continues. In the search for increased efficacy and lower toxicity for normal tissues, α-emitters may play an important role in the treatment of micrometastases and small tumors. Initial clinical trials have been carried out with the α-emitters ^{213}Bi (Jurcic et al., 2002), (Allen et al., 2005) and ^{211}At (Zalutsky, 2005). Novel therapeutic approaches are urgently needed that can kill cancer cells in transit or at the pre-angiogenic stage and so change the course of the disease. One potential approach is the use of radiolabelled antibodies that can target metastatic as well as primary tumor sites with minimal reactivity to normal tissues. Radiolabelled antibodies have been used with some success in different cancers (Allen et al., 2001; Couturier et al., 2005), such as leukemia (Couturier et al., 1999; Goldenberg & Sharkey, 2005; Jurcic et al., 1995; Sgouros & Scheinberg, 1993; Zhang et al., 2002), melanoma (Hamby et al., 1998; Liewendahl & Pyrhonen, 1993; Rizvi et al., 2000; Safa & Foon, 2001), metastatic colorectal and pancreatic cancer (Almqvist et al., 2005; Behr et al., 2002; Gold et al., 2004; Liersch et al., 2005; Song et al., 2006; Wong et al., 2003); ovarian cancer (Back et al., 2005; Song et al., 2006). Specific MAbs against an appropriate molecular target can potentially be employed as delivery vehicles for radioactivity, drugs, or toxins. Antibodies that recognize tumor-associated antigens are

conjugated to potent beta and alpha emitting radionuclides can provide selective systemic radiotherapy to primary and metastatic tumor sides. This approach has already achieved success in highly radiation-sensitive disease such as lymphoma, leukaemia and melanoma (Allen et al., 2005; DeNardo et al., 1999; Jurcic et al., 2002).

1.3 α particles

Alpha particles are of considerable interest for radioimmunotherapy applications since their short range in soft tissue is limited to only a few cell diameters. The delivery of such high energy in such a small volume, or high-linear-energy-transfer (LET), makes alpha particles especially well suited for targeting micrometastatic disease and single cancer cells such as leukaemia and other blood-borne disease.

1.3.1 Bismuth-213

The bismuth-213 radioisotope is of special interest because of its unique nuclear properties, which include a short 46 minute half-life and high energy (8.4 MeV) alpha-particle emission. Its availability from the actinium-225/bismuth-213 generator system makes this radioisotope particularly well suited for medical use. Bismuth –213 is produced from decay of Ac-225, as shown in Figure 1-1. Actinium-225 is formed from radioactive decay of radium-225, the decay product of thorium-229, which is obtained from decay of uranium-233.

Figure 1-1 Bi-213 generation scheme

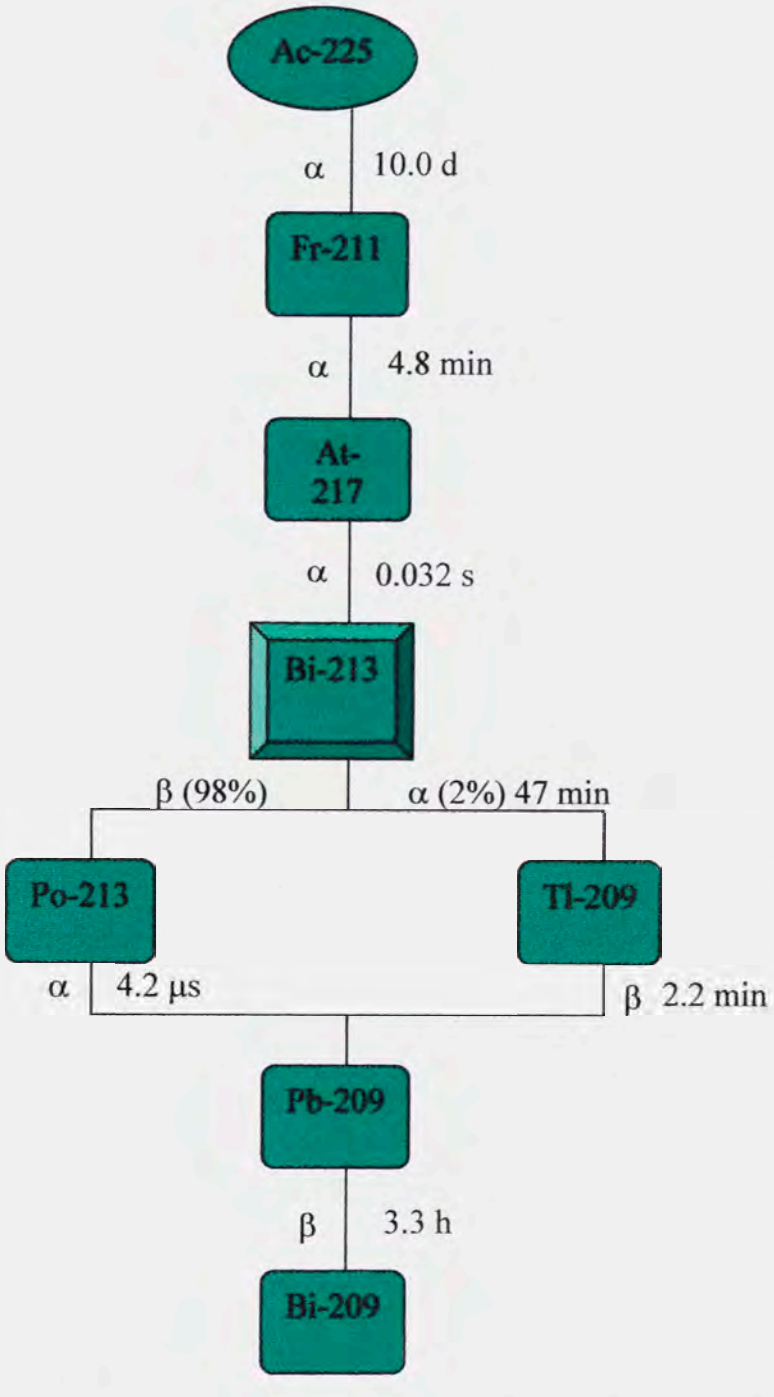

Figure 1-1 The diagram shows the decay steps and energy emitted from Ac-225 via Bi-213 to stable Bi-209.

The very short 46 minutes half-life of bismuth-213 limits its use, however, only when attachment to a carrier molecule can be conducted very quickly and the targeting is rapid following intravenous administration, such as the clinical treatment of acute myeloid leukemia, where trials are being conducted at the Memorial Sloan Kettering Cancer Center in New York. Radioimmunotherapy with alpha particles has the advantages of high energy deposition (~ 100 keV/μm) in a short path length (80 μm), which produces significant cellular damage close to the site of radioisotope deposition.

For an equivalent quantity of radio-immunoconjugate fixed on cancer cells, the cytotoxicity of α-particles is 5–100 times that of β -particles: α-particles have a mean path length of 50–100 μm in biological tissue and a linear energy transfer (LET) of ~100 keV/μm, resulting in a higher absorbed activity and a larger number of ionisations in a range corresponding to cell diameter (Figure 1-2). The result is cell-specific targeting with a high probability of non-repairable DNA double-stranded breaks, because of the high density of ionisation across the double strand of DNA. Thus, the cytotoxicity of α-particles may be extremely effective and less activity dependent than that of β-particles, and cell death may occur after a single or a few α-particle emissions (Raju et al., 1991).

Figure 1-2 alpha versus beta radiation

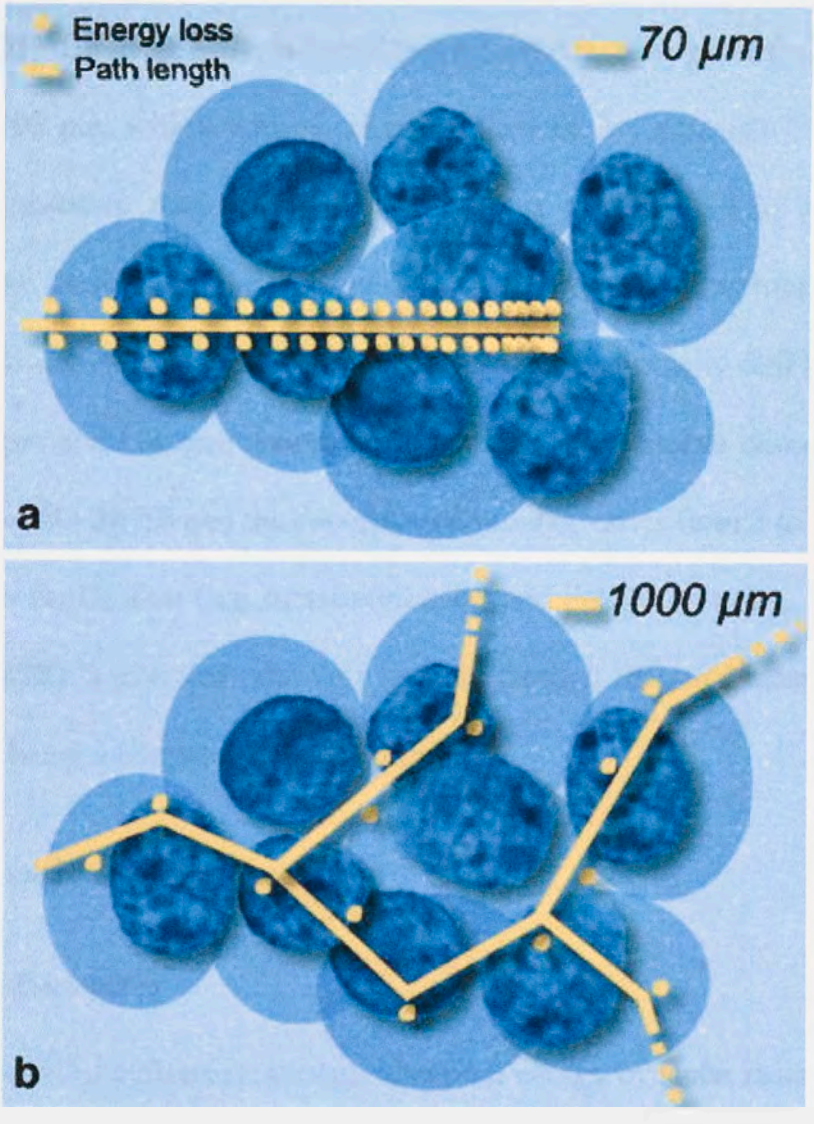

a Short path length of α-particles, in the range of a few cell diameters, compared with **b** the longer path length of β -particles. (Couturier et al., 2005)

1.3.2 Chemistry of Bi(III)

The chemistry of Bi(III) has been reviewed recently (Briand & Burford, 1999; Hassfjell & Brechbiel, 2001). Bismuth is the heaviest stable element in the periodic table with an ionic radius of 103 pm, with a normal oxidation state of 3+, although 5+ species are well-known as oxidative reagents. Stable bismuth is widely used in antiulcer and antibacterial drugs. Besides having a string affinity for oxygen and nitrogen donors, Bi forms very stable complexes with sulphur and halogens, especially iodide. Chelating agents with oxygen and nitrogen donors or compounds with thiolate donors form very stable complexes with Bi(III) and the coordination number varies from 3 to 9. Bi (III) is known to bind to Zn(II) sites (e.g..metallothionein) and Fe(III) sites (e.g. trasferrin) in proteins. Free Bi(III) is excreted relatively quickly through the renal clearance system with the kidneys being a temporary deposit organ.

1.3.3 Physical and Biological Dosimetry

1.3.3.1 Physical Dosimetry

The absorbed dose (D), defined as average absorbed energy of alpha radiation per unit mass, is an important parameter in conventional radiotherapy. Both tumor response and normal tissue damage are reported as a function of activity. In targeted radionuclide therapy, dosimetry is complicated by several factors:

(i) heterogeneous radionuclide distribution,

(ii) short-range particulate radiation, and

(iii) few radioactive events per cell (Zanzonico, 2000).

The first factor results from several biological and chemical variables, i.e., heterogeneous radionuclide conjugation, heterogeneous antigen (target molecule)

expression, antibody avidity, poor tumor vascularization, and high interstitial pressure in the tumor (Adams & Schier, 1999). Very often the targeting agent is not able to penetrate multiple layers of tumor cells (Kennel et al., 1990).

The second factor is that α-particles have a mean path length of 50–100 μm in biological tissue and a linear energy transfer (LET) of ~100 keV/μm, resulting in a higher absorbed activity (Allen & Blagojevic, 1996).

The third factor is that small numbers of α-particle traversals of cell nuclei result in a broad distribution of specific energies individual cell "dose", with some cell nuclei receiving very few or even zero α-particle traversals (Humm, 1987). To achieve curative cancer treatment, very low survival probability for all cancer cells should be obtained, otherwise undamaged cells will lead to repopulation of cancer cells.

The Medical Internal Radiation Activity (MIRD) committee produced principles for activity calculations in radionuclide therapy (Howell et al., 1999). The absorbed dose fraction is the fraction of energy absorbed in the organ. The mean absorbed activity from given radionuclides from a source to a target region was calculated, assuming homogeneous radionuclide distribution within a region. The concept of region extends to the subcellular level (Howell et al., 1999). Some models for inhomogeneous radionuclide distribution in tumors have also been proposed (Goddu et al., 1994). The MIRD model and a Monte Carlo transport code for electrons and photons have been used in *in vivo* experiments for activity determination after α-particle irradiation (Behr et al., 1999b; Gratz et al., 1999; Kennel et al., 1999b). None of the above models take into account the width of the specific energy distribution and hence cannot provide the probability of zero hit cells for a specific treatment plan. In microdosimetry, the stochastic variations of energy deposited within small targets (e.g., cell nuclei) are considered (Humm et al., 1993; Stinchcomb & Roeske, 1992). Estimates of the average

activity and the fraction of cells receiving zero (or any number of) α-particle traversals may be obtained from microdosimetric calculation of the specific energy distribution. Cells with zero or low traversal rates will survive for tumor regression. Since such microdosimetric computations for actual clinical situations may be difficult to perform due to the unknown cellular microdistribution of the radionuclide, a dosimetric framework is required where microdosimetric moments are implemented in the MIRD formalism (Roeske & Stinchcomb, 1997).

To improve current dosimetry models, more accurate estimates of the radionuclide microdistribution should be provided. Autoradiography and histological samples of tumor models and normal tissue would improve on this (Devys et al., 1996; Yokota et al., 1992). Along with improvement of dosimetry for the clinical situation, cell survival probabilities for given numbers of α-particle traversals require a more accurate determination.

1.3.3.2 RBE

Much effort has been devoted to determining the relative biological effectiveness (RBE) of α-particle irradiation and other types of high-LET (linear-energy-transfer) radiation. **RBE (relative biological effectiveness)** is a factor used to compare the biological effectiveness of absorbed radiation activities from different types of ionizing radiation; more specifically, the experimentally determined ratio of an absorbed activity of a radiation in question to the absorbed activity of a reference radiation (250 kV X ray) required produce an identical biological effect in a particular experimental organism or tissue. For example, if 10 mGy of fast neutrons equaled in lethality 20 mGy of 250 kVp x-rays, the RBE of fast neutrons would be two. Most studies have focused on the effect on cancer cells in vitro, with various endpoints such as cell death or the induction of

double strand breaks. Although a wide range of RBE values (from 1 to 20) has been proposed (Andersson et al., 1993; Barendsen, 1994), a number in the interval from 3 to 5 is generally agreed on (Aurlien et al., 2000; Ballangrud et al., 2001). Barendsen et al (Barendsen, 1994) reported that single-track lethal damage was composed in part of a type of damage that was not repaired by delayed plating and was very strongly dependent on LET with maximum RBE values up to 20. Another component consists of potentially lethal damage that was weakly dependent on LET with maximum RBE values less than 3. Azere et al reported that the RBE of Pb-212 for 37% cancer cell survival in vitro is 2-4 (Azure et al., 1994). Vandenbulcke et al. (Vandenbulcke et al., 2003) compared the RBE of ^{213}Bi for cancer and non-cancer cells by using an α-emitter RIT model in vitro, reporting values of 2–5, whereas Thomas et al. (Thomas et al., 2003) reported a range of 7–14 for the lethality of ^{210}Po for bovine endothelial cells by using cellular damage endpoints. The RBE of 4.3 was reported for the induction of micronuclei of ^{241}Am for rat alveolar epithelial cell line (SV40T2) (Yamada et al., 2002).

Reports on the RBE of α-radiation for tumors in vivo are very limited, whereas for normal tissues there are some data. For example, Howell et al. (Howell et al., 1997) reported values in the range of 3–9 for various α-particle emitters in their mouse testis model, and Elgqvist et al. (Elgqvist et al., 2005) reported an RBE of 3.4–5 for myelotoxicity in nude mice after injection of ^{211}At-labeled antibodies. The RBE in a tumour growth inhibition model was 4 – 5.5 (Back et al., 2005), and reported values of 1–2 for myelotoxicity in mice (Behr et al., 2002) . These data are consistent with data reported from clinical human studies with the α-emitter ^{213}Bi using the humanized murine monoclonal antibody (mAb) HuM195 (Palm et al., 2000).

Knowledge of the RBE for cancer cells is essential in the development and validation of cancer-seeking substances for therapy as well as for prediction of the therapeutic outcome in clinical practice. In combination with the RBE for normal tissues, it provides a tool with which α-particle radiation can be validated, in terms of the width of the therapeutic window. This window may be broader for high-LET radiation than for conventional low-LET radiation (Back et al., 2005). Furthermore, this effect may be especially pronounced for cancer cells with low radiosensitivity.

1.3.3.3 Biological Dosimetry with Micronuclei

A micronucleus (MN) is formed during the metaphase/anaphase transition of mitosis (cell division). It may arise from a whole lagging chromosome (aneugenic event leading to chromosome loss) or an acentric chromosome fragment detaching from a chromosome after breakage (clastogenic event) which do not integrate in the daughter nuclei. MN are a direct measure of the biological effective dose (is RBE x absorbed dose) as the induced radiation damage (in the number of MN) is a biological end point. Direct exposure to alpha particles induced an increase in the frequency of apoptosis and micronucleus formation (Azzam et al., 2002; Seidl et al., 2005; Zhu et al., 2005). Scoring of micronuclei can be performed relatively easily and on different cell types relevant for human biomonitoring: lymphocytes, fibroblasts and exfoliated epithelial cells, without extra in vitro cultivation step. MN observed in exfoliated cells are not induced when the cells are at the epithelial surface, but when they are in the basal layer. An ex vivo/in vitro analysis of lymphocytes in the presence of cytochalasin-B (added 44 hours after the start of cultivation), an inhibitor of actins, can distinguish easily between mononucleated cells which do not divide and binucleated cells which have completed nuclear division during in vitro culture. Indeed, in these conditions the frequencies of

mononucleated cells provide an indication of the background level of chromosome/genome mutations accumulated *in vivo* and the frequencies of binucleated cells with MN a measure of the damage accumulated before cultivation plus mutations expressed during the first *in vitro* mitosis.

1.3.4 Toxicity to normal tissue

1.3.4.1 Bone marrow

Usually, the red marrow (RM) is the first activity-limiting organ in systemic radionuclide therapy, e.g., radioimmuno-or radiopeptide therapy. The severity of myelosupreesion caused by alpha particles is in a activity dependant fashion. 17 myeloid leukemia patients treated with 10 – 37 MBq/kg of ^{213}Bi-HuM195 developed myelosuppression, with a median time to recovery of 22 days (Jurcic et al., 2002). Alpha particles produce prolonged myelosuppression requiring hematopoietic stem cell transplantation at high activity. Tissues affected in order of severity were: spleen, lymph nodes, bone marrow, gonads, thyroid, salivary glands and stomach post- treated with 61 MBq/kg of At-211 at 14 and 56 days (Cobb et al., 1988). Horak et al reported (Horak et al., 1997) that the activity-limiting acute toxicity in mice after i.v. administration of ^{212}Pb-AE1 was bone marrow suppression, which was observed at activities above 9.25 MBq. Mice treated with 46 MBq/kg of ^{211}At-81C6 have shown toxic effects in perivascular fibrosis of the intraventricular septum of the heart, bone marrow suppression, spleenic white pulp atrophy, and spermatic maturational delay (McLendon et al., 1999). However, no signs of bone marrow toxicity or body weight loss were observed in rats model treated with low activity 6– 30 kBq of bone-seeking radionuclide Ra-223. Additionally, for bone marrow, the most radiosensitive and often activity-limiting organ, no excessive toxicity for α- versus β-particle irradiation

has been found (Behr et al., 1999a; Gratz et al., 1999). Furthermore, repeated injection of a MTD of a ^{213}Bi immunoconjugate did not result in increased bone marrow toxicity (Behr et al., 1999a).

1.3.4.2 Kidneys

Another activity limiting organ is the kidney, caused by radiation nephritis(Jaggi et al., 2005). Radiation nephritis is a process of necrosis, atrophy and sclerosis that follows exposure of the kidney to ionizing radiation. Experimental studies with electron microscopy (EM) demonstrate that this process begins as degeneration of the glomerular endothelium and the tubular epithelium, and their basement membranes, leading to collapse of these structures and the development of interstitial fibrosis. Rather late and complicating events are necrosis and thrombosis of arteries and arterioles, contributing to the destruction of the renal parenchyma. The process is the same for both large (50 to 100 Gy) and medium activitys (10 to 30 Gy), the only difference being the extent and the speed with which the lesions develop and the frequency of arterial necrosis (Madrazo et al., 1975).

Some effort has been devoted to increase kidney tolerance to free Bismuth 213(Jaggi et al., 2005; Jaggi et al., 2006). They recently found that metal chelation, diuresis with furosemide or chlorothiazide, and competitive metal blockade could be used as adjuvant approaches to modify the renal accumulation of ^{225}Ac daughters (^{213}Bi, ^{221}Fr, and ^{217}At) (Jaggi et al., 2005). To date, the renal clearance system in mice has shown surprisingly high tolerance levels for clearance of $^{212/213}$Bi labeled radiopharmaceuticals, indicating an RBE value close to unity (Gratz et al., 1999). There are few studies where the processing of free bismuth or bismuth labeled radiopharmaceuticals in the kidneys has been investigated. Free bismuth is distributed very heterogeneously throughout the

whole kidney, concentrations varying by a factor of 10, with the central region containing lesser amounts of radioactivity than the periphery (cortex). Free bismuth is also incorporated into kidney cells to some extent (Zidenberg-Cherr et al., 1987). Morphological changes in monolayers of bovine aortic endothelial cells have been studies in vitro after α-particle irradiation from ^{212}Bi-DTPA in the medium (Speidel et al., 1993). Activitys up to 73 Gy were not toxic to the vascular system after administration of 212/213Bi radiopharmaceuticals in vitro.

Calcium-diethylenetriamine pentaacetate (Ca-DTPA) is a calcium salt that has been used since the 1960s to treat patients who have been internally contaminated with rare earth radioactive materials such as americium, plutonium, californium, curium, and berkelium. Ca-DTPA is capable of binding to radioactive materials and speeding up the release of these materials from the blood and into the urine, thus reducing the amount of internal contamination. Ca-DTPA can also chelate free bismuth in the blood, allowing final clearance into urine. The differences of kidney uptake with and without Ca-DTPA challenge may indicate the stability of alpha conjugates in vivo, as well as the reduction of accumulated activity.

In therapy studies using radiometal-conjugated Fab fragments, the kidney can be the activity-limiting organ. Radiation nephritis was observed for 9.25 MBq with ^{213}Bi-DOTA-biotin (Yao et al., 2004) and 10 MBq with ^{213}Bi-Fab' (Gratz et al., 1999) up to 6 months.

Recent studies indicated that the persistent localization of renal radioactivity would arise from the re-absorption of glomerularly-filtered radiolabeled antibody fragments, followed by the retention of the radiometabolites generated after degradation in the lysosomal compartment of the renal cells. Two major approaches have been performed to reduce the renal radioactivity levels of antibody fragments. One is to block the

reabsorption of radiolabeled antibody fragments themselves at the proximal tubular cells from the luminal fluid by administration of basic amino acids such as L-lysine (Mogensen & Solling, 1977). The other approach is to decrease the residence time of the radiometabolites within the lysosomal compartments of the renal cells by introducing a cleavable linkage between antibody fragments and radiometabolites for rapid urinary excretion. Yet another approach to reduce renal radioactivity levels of antibody fragments may be to release radiolabeled compound of urinary excretion from glomerularly-filtered antibody fragments before they are reabsorbed into the renal cells by the action of brush border enzymes present on the lumen of the renal proximal cells (Arano et al., 1996). Arano et al synthesized C-terminal Lys linkers for a radioiodinated hippuric acid-Fab conjugate that lowered kidney uptake by up to 50%. Administration of cationic amino acids results in a substantial increase in the MTD of such Fab fragments, and biochemical or histological evidence of renal damage has not been observed under these conditions. Thus, radiation nephrotoxicity of antibody fragments and peptides could be overcome, providing new prospects for cancer therapy with radiolabeled antibody fragments and peptides (Behr et al., 1998).

1.3.4.3 Carcinogenesis

Carcinogenesis has been observed following administration of α-particle emitters in mammalian cells (Ishikawa et al., 2001; Schwartz et al., 1991; Wu et al., 1999; Zhou et al., 2000). For therapy of non-terminal patients, the probability for induction of such late damage needs to be addressed (Kamikawa et al., 1999; Zhao et al., 2001). More accurate knowledge of late damage induction probabilities may come from microbeams (Folkard et al., 1997; Newman et al., 1997; Zhou et al., 2000).

1.4 Chelators

Bismuth-212 can be bound to MAb [anti-TAC directed to human interleukin 2 (IL-2) receptor] conjugated by a bifunctional metal ligand, the isobutylcarboxycarbonic anhydride of diethylene triamine penta-acetic acid (DTPA) (Kozak et al., 1986). All the other chelating agents developed later to bind bismuth-212 and were derived from DTPA (Brechbiel & Gansow, 1992; Macklis et al., 1992).

For in vivo stable attachment of radio-bismuth to carrier molecules, a bifunctional chelating agent is needed for forming a radiometal complex that must be exceedingly stable in vivo (Hassfjell & Brechbiel, 2001). The development of suitable bifunctional chelating agents for conjugating Bi(III) radionuclides to proteins began by abstraction of existing chelating reagents from the chemistry literature. These reagents were then modified to produce an active species derivative for protein conjugation. Acyclic DTPA was recognized very early to be an effective chelating agent with high thermodynamic stability constants for a variety of metal ions (Martell & Smith, 1974). The Bi(III) complex of this ligand was thought to be possibly adequate to meet the requirements of forming kinetically inert complexes in vivo while retaining reasonable complex formation rates, a critical consideration for the short half-life Bi isotopes. Thus, one finds the stability constant for the DTPA complexes of Bi(III) to be $10^{35.6}$, providing the impetus for the evaluation of two of the first derivatives for linking DTPA to proteins (Martell & Smith, 1974).

An early demonstration of the potential of targeting ^{212}Bi to specific cells was accomplished by using the isobutylcarbonic anhydride of DTPA reacted with mAb anti-Tac (Kozak et al., 1986). While this chelate conjugate was highly successful in vitro, and in the treatment of malignant cells in a compartmentalized animal model (Macklis

et al., 1988), the lack of acceptable stability was also readily apparent with this chelating agent.

This instability was initially attributed to inadequate denticity providing an unstable complex in vivo (Ruegg et al., 1990), and hence evaluation of bifunctional octadentate DTPA derivatives was initiated. A C-functionalized DTPA with an aryl isothiocyanate group on the carbon backbone structure for protein linkage substantially increased the in vivo stability of Bi(III) complexes. Additional C-functionalization of the DTPA ligand with a methyl group was shown to further increase in vivo stability with Bi(III), a result that was clearly indicated from the chemical literature from a combination of both inductive and steric effects (Milenic et al., 2001)

However, despite the initial very high stability constant of the DTPA[Bi(III)] complex, none of these bifunctional DTPA derivatives demonstrated acceptable in vivo stability when conjugated to mAb and radiolabeled with $^{205/206}$Bi (Brechbiel & Gansow, 1991). Further review of the chemical literature revealed that the *trans*-cyclohexyl-EDTA (Cy-EDTA) (Figure 1-3) Bi(III) complex possessed a stability constant close to that of the DTPA complex (Martell & Smith, 1974). Merging the *trans*-cyclohexyl substructure with the previously reported bifunctional DTPA provided the family of CHX-DTPA ligands) (Brechbiel & Gansow, 1991). These ligands were substantial improvements over the prior bifunctional DTPA reagents because the preorganization geometry conferred by the *trans*-cyclohexyl unit provided not only exceptional stability for the Bi(III) isotopes, but also retained the rapid complex formation kinetics. The effects of adding an alkyl group or inclusion of the *trans*-cyclohexyl ring to a bifunctional DTPA are clearly indicated by the decreased accretion of $^{205/206}$Bi in the kidneys and statistical congruency with the biodistribution of radio-iodinated monoclonal antibody. These

ligands exist in several stereochemical configurations, and while very significant differences have been reported for the in vivo stability with ^{88}Y radiolabeled immunoconjugates with these ligands (Wu et al., 1997), those differences are irrelevant to use with $^{212,213}Bi(III)$ due to half-life considerations.

Concurrent with development of an acyclic bifunctional chelating agent for Bi(III) radioisotopes, the inherent potential of macrocyclic polyaminocarboxylates ligands such as NOTA, DOTA, and TETA (Figure 1-3) were readily apparent. Their macrocyclic nature confers a high degree of preorganization and limits conformational disorder while providing a range of both denticity and cavity size.

Figure 1-3 Acyclic DTPA

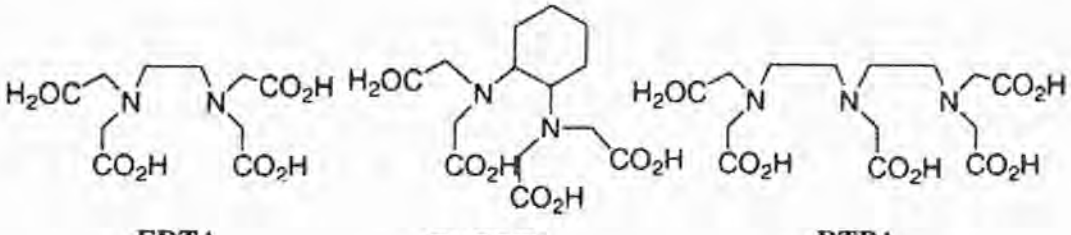

1.4.1 Chelator stability comparison in vivo

A series of bifunctional chelating agents to prepare ^{206}Bi-labeled monoclonal antibody 103 A, which is specific for gp70 expressed on Rauscher verus-infected cells, have been assessed the in vivo stability and tumor targeting of these conjugates in the Rauscher murine erythroleukemia model. The following compounds were conjugated to the monoclonal antibody 103A:

The stability in vivo of ^{206}Bi chelate-103A conjugates was first evaluated in normal mice by determining the levels of ^{206}Bi in blood and kidney, since these were the organs in which free ^{206}Bi, ^{206}Bi-cDTPA-103A, and ^{35}S-103A accumulated. The biodistribution of ^{206}Bi administered as a chelate of cDTPA-103A was virtually indistinguishable from that of free ^{206}Bi, indicating a low degree of in vivo stability of this bismuth chelate when compared to biosynthetically labeled ^{35}S-103A. There was a progressive increase in the ^{206}Bi levels observed in blood when the series of 103A conjugates prepared using SCNBzDTPA, MxDTPA, and DOTA was compared to ^{206}Bi administered free or as a cDTPA-103A chelate. At 1 h after injection into normal mice, the blood level of ^{206}Bi-DOTA-103A was 25-fold greater than that observed for ^{206}Bi-caDTPA-103A and the level in kidney was 6-fold less, values that did not differ significantly from those observed for ^{35}S-103A. Targeting to leukemic spleen was increased by 10-fold when the DOTA conjugate was used; the tumor level was 90% injected activity/g for DOTA, as compared to only 9% injected activity/g for cDTPA-103A at 1 h after injection. Use of the DOTA chelator also reduced by 7-fold the level of uptake by the kidney in the leukemic animals. The chelator DOTA is a promising reagent for the delivery of ^{212}Bi-antibody conjugates to vascularized tumors under conditions that require targeting via the circulatory system (Huneke et al., 1992; Ruegg et al., 1990).

However, the synthesis time of DOTA is excessive for use with the short lived Bi-213.

1.4.2 Chelators used in Bismuth chelation

The Memorial Sloan–Kettering Cancer team from New York pioneered RIT with bismuth-213. Murine MAb M195, its humanised HuM195 analogue (anti-CD33), and a specific anti-antigen MAb of prostate J591 have been conjugated to bismuth-213 via the

bifunctional chelating agent CHX-A"-DTPA (Ballangrud et al., 2001; Jurcic et al., 1995; Jurcic et al., 1997). The complexation of the HuM195 with CHX-A-DTPA made it possible to build functionalised antibodies with several chelating agents (up to ten) by molecule of antibody, and the radiolabelling yield with bismuth-213 was higher than 80% with specific activities of 740 MBq/mg (Jurcic et al., 1997). Using the same chelating agent, CHX-A-DTPA, rituximab (anti-CD20) was labelled with bismuth-213 (Vandenbulcke et al., 2003). Another anti-CD33 MAb (WM-53) was labelled with either bismuth-213 or terbium-149 via a cyclic anhydride of diethylene triamine penta-acetic acid (cDTPA)(Allen & Blagojevic, 1996; Allen et al., 2004). Other ligands derived from DTPA were also synthesised, such as the *p*-isothiocyanatobenzyl-DTPA (CITC-DTPA) for the radiolabelling of B-B4 and MA5 (directed against a transmembrane heparan sulphate proteoglycan, syndecan-1, and transmembrane muc-1 respectively, both of which are expressed by multiple myeloma cells) (Mishra et al., 2002).

1.5 Targeting vectors

Specific MAbs against an appropriate molecular target can potentially be employed as delivery vehicles for radioactivity, drugs, or toxins. Antibodies that recognize cancer-associated antigens and are conjugated to potent beta and alpha emitting radionuclides can provide selective systemic radiotherapy to primary and metastatic tumor sites. This approach has already achieved success in highly radiation-sensitive diseases such as lymphoma and leukaemia (DeNardo et al., 1999). Attempts are underway to develop various antibody-based reagents by modifying affinity, size, and valency for effective cancer diagnosis and treatment (Hudson, 1999).

Oncogene-associated and/or cell surface products have been proposed as cancer-associated target molecules for several cancers and can provide an opportunity for the design of novel immunotherapy and vaccine strategies. Although over 100 tumour associated antigens have been catalogued, only a handful of immunologically detected molecules described have been considered viable candidates as targets for immunotherapeutic intervention (Urban & Schreiber, 1992). The candidate molecules include altered or overexpressed oncogene products [platelet-derived growth factor (PDGF) and receptors for same (PDGFR) and epidermal growth factor receptor (EGFR)], developmentally related or cell lineage-related epitopes [neural cell adhesion molecule (NCAM), L1, gangliosides], high molecular weight glycoprotein mucins (MUC1 and MUC4), matrix metalloproteinases (MMPs), and epitopes with an extracellular matrix location (tenascin, Gp40).

1.5.1 HER2/neu -Herceptin

The c-erbB2 gene (HER2/neu) is a member of the class of oncogene associated with tyrosine protein kinase(Coussens et al., 1985). The protein encoded by c-erbB2 is a 185-

kDa transmembrane receptor (p185), show in Figure 1-4 (Rubin & Yarden, 2001); it is also a glycoprotein having intracellular, transmembrane and extracellular domains. The tyrosine kinase activity of the protein is associated with the intracelular or cytosolic domain of the receptor, whereas the extracellular domain is responsible to react with extracellular growth factors.

Figure 1-4 Structure of The HER2 and Its Transmembrane Topology.

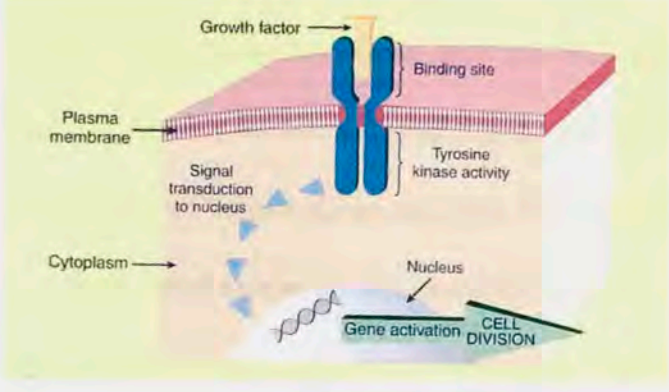

The HER2 protein shows structural and functional homology with the epidermal growth factor receptor (EGFR) (Tzahar & Yarden, 1998). The cytosolic tyrosine kinase domains of these two receptors are almost identical. They differ at the extracellular domain of the molecule, therefore, a monoclonal antibody reacting with the extracellular domain of HER2 oncoprotein would not cross-react with the EGFR (Akiyama et al., 1986; Schechter et al., 1985). This transmembrane receptor is presumably involved in the regulation of cell growth and cell transformation through signal transduction pathway (Klapper et al., 2000). HER2 expression has shown different level in normal and malignancies (Cohen et al., 1989; Zajchowski et al., 1988), with low level expression in normal tissues. Overexpression of the HER-2/*neu* protein has been shown in experimental studies to be an important determinant of malignant transformation, development of metastatic disease, and increased cell proliferation

(Kaptain et al., 2001). The high expression of erb-b2 was reported in ovarian cancer and breast cancer from 15-35 % (Bossard et al., 2005; Choi et al., 2005; Nielsen et al., 2004; Wang et al., 2005).

Monoclonal antibody directed against HER2 protein has caused growth inhibition in over-expression cells. Trastuzumab (Goldenberg, 1999), also known as Herceptin and rhuMAb HER2 is a humanized antibody derived from 4D5, a murine MAb, which recognizes an epitope on the extracellular domain of HER2 . Herceptin has been approved for therapeutic use and the first oncogene-targeted treatment with proven survival benefit in women with HER2 positive metastatic breast cancer. However, its mechanism of action of has not been fully characterized and appears to be complex. The mechanisms of action of Herceptin include HER2 protein downregulation, prevention of HER2-containing heterodimer formation, initiation of G1 arrest and induction of p27, prevention of HER2 cleavage, inhibition of angiogenesis, and induction of immune mechanisms has been reported.

The anti-ErbB2 antibody trastuzumab is used for the treatment of patients with advanced breast cancer, resulting in a response rate of 40-60%. Coupling with a cytotoxic nuclide, e.g. alpha-emitting ^{211}At, may further increase tumour response (Persson et al., 2006). The use of ^{212}Pb-Herceptin radioimmunottherapy of disseminated peritoneal disease (Milenic et al., 2005) and ^{225}Ac-labeled trastuzumab of ovarian cancer (Borchardt et al., 2003) has been shown to be effective and specific in ovarian cancer mice model.

1.5.2 MUC1: C595

MUC1 is a polymorphic, highly glycosylated, type I transmembrane protein expressed by ductal epithelial cells of many organs including pancreas, breast, gastrointestinal

tract, and airway (de The et al., 1990). MUC1 is overexpressed and differentially glycosylated by different adenocarcinomas. Previous studies demonstrated that tumor cells expressing high levels of MUC1 may have increased invasive and metastatic potential (Matsuishi et al., 1982; Osako et al., 1993). It has been proposed that MUC1 mediates anti-adhesion activity by interfering with cell-cell and/or cell-ECM (cell-extracellular matrix) interactions, and thereby facilitates detachment of tumor cells from the primary growth (Ligtenberg et al., 1992; van de Wiel-van Kemenade et al., 1993; Wesseling et al., 1995).

Mucins are large (>200 kDa) glycoproteins with a high carbohydrate content (50–90% by weight). They are expressed by a variety of normal and malignant epithelial cells (Devine & McKenzie, 1992). Although at least 21 human mucin-encoding genes have been cloned, MUC1 is unique in its cell-surface transmembrane expression (Gendler et al., 1990). MUC1 contains a polypeptide core consisting of 30–100 repeats of a 20-amino-acid sequenc (Gendler et al., 1990). The presence of large amounts of oligosaccharides attached along the length of the proline-rich polypeptide core of MUC1 enhances its rigidity, resulting in large, flexible, rod-like molecules that can extend several hundred nanometers from the apical cell surface into the lumens of ducts and glands (Bramwell et al., 1986). Cancer-associated MUC1 is incompletely glycosylated, with truncated carbohydrate chains largely made up of one to six sugar units (Hanisch et al., 1996). As a result of these truncated carbohydrate structures, cancer-associated MUC1 has exposed internal sugar units and naked peptide sequences that are cryptic in the normal mucin molecule (Figure 1-5) (Burchell et al., 1987). This reduced glycosylation permits the antibody access the peptide core of the tumour associated MUC1 antigen.

Figure 1-5 Structure of MUC1 and Tandem Repeat

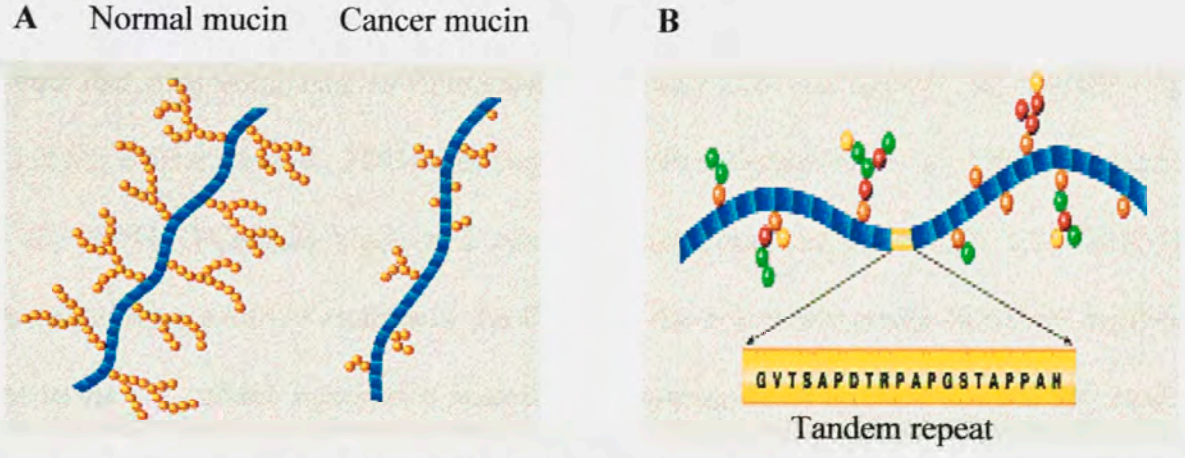

Figure 1-5 Structure of MUC1 (**A**) The glycosylation pattern of normal versus cancer-associated MUC1. The brown circles represent sugar residues of carbohydrate side-chains on MUC1. Because of defects in carbohydrate metabolism in cancer cells, cancer-associated mucins are underglycosylated. (**B**) The nature of the core peptide, which is a tandem repeat of a 20-amino-acid sequence (highlighted as the amino acid single letter representation) (Agrawal et al., 1998).

Structurally, MUC1 contains two domains believed to be of functional significance. The large extracellular tandem repeat (TR) domain of MUC1 is heavily *O*-glycosylated. Glycosylation of the TR domain varies among the different tissues, and tumor-associated MUC1 has been reported to be both less glycosylated (Gendler et al., 1991) or more glycosylated than forms expressed by normal tissues (Hanisch et al., 1996). Differential glycosylation patterns on the TR may affect adhesion properties that result in an increased ability of tumor cells to metastasize. Additional evidence suggests that MUC1 may also confer anti-adhesive properties, thereby aiding in the metastatic spread of tumor cells (McDermott et al., 2001). Another important domain of MUC1 is the cytoplasmic and transmembrane domain (CT), which is highly conserved across mammalian species and hypothesized to play a role in its post-translational processing, subcellular localization, signal transduction, and intracellular localization (Spicer et al.,

1995). Alterations to the CT may affect trafficking through the Golgi apparatus thereby influence glycosylation of the TR domain. The CT also mediates signal transduction events that may contribute to functional differences between tumors and normal cells (Li et al., 2001a; Li et al., 2001b; Pandey et al., 1995; Pemberton et al., 1996; Schroeder et al., 2001). ß-Catenin binds to a consensus site found in the MUC1 CT; GSK-3ß phosphorylates a serine residue in the CT; and there is a consensus Grb2/Sos binding site in the CT, which includes a potentially phosphorylated tyrosine residue (Li et al., 2001a; Li et al., 2001b; Schroeder et al., 2001). Tumor-associated modifications of these sites may affect the ability of tumor cells to associate with components of the extracellular matrix (ECM) or other cells (both malignant and benign).

Deletion of either the CT or TR of MUC1 resulted in an increased propensity of tumor cells to invade vessels and metastasize to lymph nodes compared with a cell line expressing full-length MUC1 (Chen et al., 1994; Schroeder et al., 2001). These results suggest a cooperative relationship between the CT and TR domain of MUC1. Deletion of the CT or TR domain produced cell lines with a more aggressive phenotype on implantation onto the cecum. On the other hand, overexpression of full-length MUC1 resulted in the other extreme: a substantially decreased invasive and metastatic character on implantation on the cecum. Results of cDNA array gene expression analysis showed differences in the gene expression profiles between the different cell lines. Among the genes differentially expressed were several encoding proteins believed to play a role in invasion and metastasis (Oosterkamp et al., 1997).

Most serous carcinomas (19/21; 90%) expressed MUC1 (Feng et al., 2002). MUC1 mucins are highly glycosylated glycoproteins expressed on the luminal surfaces of glandular epithelia. In breast and ovarian carcinomas, their expression is frequently

upregulated and they may be secreted into the circulation of cancer patients. The immunogenicity of MUC1 has now been extended to human studies and it is apparent that patients with breast and ovarian malignant disease are able to mount immune responses against MUC1. These findings provide information on the mechanisms involved in the recognition of MUC1 expressing tumours. The utilisation of MUC1 related immunogens to stimulate immune responses to tumours could lead to the improved management of patients and the development of new immunotherapeutic strategies aimed at the eradication of MUC1 mucin expressing cancers (Denton & Price, 1995).

C595 is a monoclonal antibody against the protein core of the human urinary epithelial mucin (MUC1). The C595 murine antibody (IgG3) was raised by the Cancer Research Laboratories at Nottingham University. Antibody was purified from the supernatant of in vitro cultures of the hybridoma by affinity chromatography and stored at -20°C in PH 7.2 (PBS). Viruses were inactivated by heat treatment (50°C for 30 min). Stabilization of the PPII helix by GalNAc glycosylation presents the epitope of the C595 antibody with a favourable conformation for binding. Glycosylation of the MUC1 tumor marker protein with a simple O-linked saccharide expressed in many cancers, can enhance the binding of the clinically relevant C595 antibody (Spencer et al., 1999).

The use of ^{99m}Tc-C595 immunoscintigraphy for staging bladder cancer (Simms et al., 2001), ^{188}Re-C595 for radioimmunotherapy of bladder cancer (Murray et al., 2001) and Bi-C595 for targeted alpha therapy of breast, prostate, pancreatic and ovarian cancers in mice (Allen et al., 2004) has been shown to be effective and specific.

1.5.3 uPA/uPAR: PAI2

Urokinase-type plasminogen activator (uPA) and its receptor (uPAR) can activate plasminogen at the cell surface, potentially augmenting migration of cells and exacerbating atherogenesis, restenosis, or both. Migration may be facilitated by digestion of ECM, a process that can be potentiated by plasmin (Engelholm et al., 2001). uPA is believed to be involved in remodeling of the ECM as seen with invasion of tumors (Bajou et al., 1998; Borstnar et al., 2002; Fisher et al., 2000; Konno et al., 2001). uPA was significantly associated with the malignant progression of ovarian tissues; the levels were increased going from normal tissue, via benign and borderline adenomas, to primary and metastatic adenocarcinomas (van der Burg et al., 1996). The uPA expression has shown different level in normal and malignancies (Miseljic et al., 1995), with low level expression in normal tissues.

Migration of cells into and within vessel walls and atherosclerotic plaque may depend on analogous phenomena regulated by cell-surface plasminogen activators, their receptors, and plasminogen activator inhibitors types 1 and 2 (PAI-1 and PAI-2) (Lundgren et al., 1994). Two lines of evidence have strongly suggested an important and apparently causal role for the uPA system in cancer metastasis: results from experimental model systems with animal tumor metastasis and the finding that high levels of uPA, PAI-1 and uPAR in many tumor types predict poor patient prognosis. Many findings suggest that the system does not support tumor metastasis by the unrestricted enzyme activity of uPA and plasmin. Rather, pericellular molecular and functional interactions between uPA, uPAR, PAI-1, extracellular matrix proteins, integrins, endocytosis receptors and growth factors appear to allow temporal and spatial re-organizations of the system during cell migration and a selective degradation of extracellular matrix proteins during invasion. Differential expression of components of

the system by cancer and non-cancer cells, regulated by paracrine mechanisms, appear to determine the involvement of the system in cancer cell-directed tissue remodeling. A detailed knowledge of these processes is necessary for utilization of the therapeutic potential of interfering with the action of the system in cancers.

The activity of uPA is physically regulated by plasminogen activator inhibitors type 1 and 2 (PAI1 and PAI2) PAI2 is a member of the serine protease inhibitor superfamily and forms SDS-stable 1: 1 complexes with uPA. It was suggested that cell surface-bound uPA is accessible to PAI2, and PAI2 can inhibit cancer cell invasion and metastasis. PAI-2 targets the urokinase plasminogen activator (uPA). Since uPA has high affinity and specificity for cell-surface localized receptors (ie, uPAR), where it can be inhibited by PAI-2 (Hang et al., 1998; Kruithof et al., 1995), PAI-2 is more likely involved in pericellular proteolysis in which uPA-mediated proteolysis plays an important role, such as tumour cell invasion and metastasis. The pharmacokinetics and biodistribution of exogenously administered human recombinant radioiodinated ^{125}I-PAI-2 in both control and tumour-bearing animals have been established (Hang et al., 1998). Radio-labeled PAI-2 accumulated in tumour xenografts (~1.5% of total injected activity) without an accompanying increase in major organ toxicity, and that tumour associated PAI-2 correlated with tumour mass. Thus exogenously administered PAI-2 targets uPA expressing tumour cells, particularly those that have or are likely to metastasise. Targeting uPA-overexpressing cells by its natural inhibitor remains an unexploited mode of attack for prostate and pancreatic cancer malignancy (Allen et al., 2003; Li et al., 2002; Song et al., 2006).

1.6 Preclinical in vitro and animal studies

Several studies were carried out with the human myeloid leukaemia (de The et al., 1990). The murine MAb M195 is directed against the CD33 antigen expressed by most of the cells of myeloid leukaemia and clonogenic progenitor of the leukaemia (Jurcic et al., 1995; Sgouros et al., 1993). A humanised antibody HuM195 was constructed and is directed against the same antigenic targets but without significant immunogenicity (Caron et al., 1994). HuM195 is able to modulate the response of human blood mononuclear cells, resulting in the death of the leukaemic cells (Caron et al., 1992; Co et al., 1992). Pharmacokinetic and biodistribution tests in mice showed good stability of ^{213}Bi-RIC, a lack of uptake in healthy normal tissues which did not express CD33 antigen and a lack of renal activity, a natural route of elimination of the free bismuth (McDevitt et al., 1998). Activities up to 740 MBq/kg of ^{213}Bi-HuM195 were i.v. injected without any problem of tolerance, but activities of 2,590 MBq/kg resulted in the death of two out of three mice, and leucopenia in the survivor (Nikula et al., 1999).

The MSK group also studied the MAb J591, directed against the prostate-specific membrane antigen (PSMA). This therapeutic approach appeared of particular interest because the metastatic spread of prostatic cancer is via bone marrow migration of cancer cells or clusters of cells, which are ideal targets for α-particles. In a first in vitro study on spheroids of LNCaP-LN3 prostate carcinoma cells, a decrease in the spheroid volume was observed, and this decrease was related to the initial volume and the delivered activity (Ballangrud et al., 2001). In vivo cytotoxic tests were later performed on athymic mice bearing subcutaneous xenografts of LNCaP cells. The i.v. injection of ^{213}Bi-J591 prolonged survival times significantly as compared with the i.v. injection of

non-specific MAb ^{213}Bi-HuM195 or the lack of injection of RIC. The prostate-specific antigen level was also significantly lowered in animals treated with ^{213}Bi-J591 (McDevitt et al., 2000). Similar results were reported by CERO

The effectiveness of ^{213}Bi-MAbs has also been studied in vitro using other models, with comparison to irrelevant MAbs, MAbs radiolabelled with α-emitters, free isotope, external irradiation or cold MAb. In a human epidermoid tumour cell line A431 model, cell killing with a specific murine ^{213}Bi-MAb, 2D11, about 90% cell death was caused by 30 α-particle disintegrations in monolayer cell culture versus one in multicell spheroid (Kaspersen et al., 1995). In multiple myeloma cell line models (U266, RPMI 8226 and LP1), the effectiveness of two specific ^{213}Bi-MAbs (B-B4 and MA5) was compared with that of non-specific ^{213}Bi-IgG134 and that of B-B4 radiolabelled with iodine-131. With ^{213}Bi-B-B4, excellent tumour targeting was reported, resulting in a specific mortality 20 times that observed with the irrelevant ^{213}Bi-IgG 134 or with ^{131}I-B-B4 (Supiot et al., 2002). Low D_0 values (37% cell survival) for different ^{213}Bi-RICs (specific for melanoma, colorectal cancer or pancreatic cancer cell lines) wee found compared with control RICs radiolabelled with α-emitter, control free isotope or control cold MAb (Allen et al., 2004; Allen et al., 2001). Recently, with a model of B cell chronic lymphocytic leukaemia (B-CLL), Vandenbulcke et al. showed ^{213}Bi-rituximab to be more effective than external α-irradiation. They calculated an RBE of 2 at low activitys (<10 Gy) with respect to the induction of apoptosis (expressed as percentage excess over spontaneous apoptosis in control) and an RBE of 2–5 with respect to chromosomal damage (Vandenbulcke et al., 2003). In their latest study, these authors reported cell binding of ^{213}Bi-rituximab to be significantly higher for splenic lymphoma with villous lymphocytes (SLVL) than for B-CLL, resulting in greater induction of

apoptosis in SLVL than in B-CLL (Vandenbulcke et al., 2004). An anti-colorectal cancer MAb, c30.6, radiolabelled with bismuth-213 or terbium-152 (a positron emitter), has been tested in vitro and in vivo (Rizvi et al., 2001). In vitro, only the ^{213}Bi-RIC was able to kill cancer cells, while in vivo high uptake and retention of both conjugates was seen in tumours whereas no retention was observed in the kidneys. These results demonstrated the efficiency and selectivity of the targeted α-therapy approach.

Another RIT approach consists in targeting tumour vasculture rather than a membrane MAb specific to only one type of tumour. Kennel and Mirzadeh have radiolabelled the MAb 201B with bismuth-213. This MAb is specific to murine thrombomodulin and targets lung micrometastases (Davis & Kennel, 1999; Kennel et al., 1999b). Five primitive cancer cell lines were used to generate lung micrometastases in mice: mammary carcinoma EMT-6, murine lung carcinoma Line 1, murine tracheal carcinoma IC-12, human epidermoid carcinoma A431 and human lung cancer A549 (Kennel et al., 1999a). The ^{213}Bi-RICs have also been injected by the loco-regional route, to improve access to the tumour. Intra-lesional injection of a low activity of ^{213}Bi-(9.2.27), a radiolabelled MAb directed against a surface antigen expressed on most melanomas, completely inhibited the growth of subcutaneous xenografts of melanoma in nude mice (Allen et al., 2001).

Another multiple-step biotin–streptavidin model employed a biotin MAb radiolabelled with bismuth-213 via DOTA in A431 tumour- bearing mice pretargeted with B3-streptavidin MAb (B3-SA) (Yao et al., 2004). Activitys lower than 37 MBq inhibited tumour growth and prolonged survival whereas a activity of 74 MBq was lethal in all animals.

1.7 Human studies

In 1996, the Memorial Sloan–Kettering Cancer Center team started its first human study with bismuth-213 (Jurcic et al., 2002) in patients with acute or chronic myeloid leukaemia. The antibody was the humanised MAb HuM195, specific to CD33 antigen, radiolabelled with bismuth-213 via the chelating agent CHX-A-DTPA(Nikula et al., 1999). Prior to this, a phase I trial with ten patients had shown that this MAb radiolabelled with iodine-131 was able to quickly and specifically target the leukaemia sites (Scheinberg et al., 1991). In a later study with activity escalation using the same ^{131}I-RIC, the cancer load was significantly diminished in patients with refractory myeloid leukaemia or in relapse (Schwartz et al., 1991). 18 patients with myeloid leukaemia (14 with acute myeloid leukaemia in relapse, including three who had benefited from a bone marrow transplant, three with acute myeloid leukaemia refractory to chemotherapy and one with chronic myeloid leukaemia in relapse) were included in a therapeutic phase I trial, with the aim of assessing the tolerance, pharmacokinetics and biological activity of ^{213}Bi-HuM195. Patients received 10.36–37 MBq/kg of ^{213}Bi-HuM195 in three to seven systemic injections in 2–4 days. Five activity levels were employed (10, 16, 21, 26 and 37 MBq/kg), yielding total activitys from 602 to 3,515 MBq. Treatment was well supported without any accidental acute toxicity. The delayed toxicity was limited to (1) myelosuppression in all patients, characterised by a decrease in leucocytes and blasts in peripheral blood, which lasted an average of 22 days (12–41 days) and (2) transient, mild liver function abnormalities in five patients. Sampling of blood and scintigraphic scans centered on the 440-keV photopeak were performed, thereby obtaining dosimetric and biodistribution data. Uptake of bismuth-213 in bone, liver and spleen was observed from the tenth minute after administration,

but no significant uptake was measured in other organs. The estimated activitys to the bone marrow, liver and spleen were as much as 40,000 times higher than the activitys estimated for kidneys or the whole body. The organ target/whole body ratios of absorbed activitys with ^{213}Bi-HuM195 were 1,000–10,000 times higher than the same activity ratios with α -emitters such as iodine-131 or yttrium-90 (Sgouros et al., 1999).

Another clinical trial was carried out at St George Hospital, Australia (Allen et al., 2005). 16 melanoma patients were recruited. All the patients were positive to the murine monoclonal antibody 9.2.27. Alpha conjugates activities from 5.6 – 50 GBq injected into lesions of different sizes resulted in massive cell death, as observed by the presence of tumour debris. There were no significant changes in blood proteins and electrolytes. There was no evidence of a human-antimouse-antibody reaction. Evidence of significant decline in serum marker melanoma-inhibitory-activity protein (MIA) at 2 weeks post-TAT was observed. Intralesional TAT for melanoma was found to be safe up to 50 GBq, and efficacious at a activity of 22.2 GBq. MIA, apoptosis and ki67 proliferation marker tests all indicated that TAT is a promising therapy for the control of inoperable secondary melanoma or primary ocular melanoma.

Chapter 2

Materials & Methods

2.1 Materials

2.1.1 Preparation of medium and buffers

All water used to prepare non-tissue culture solution was deionised and filtered using the Modulab Analytical laboratory Research Grade Water System. Prepared solutions and buffers were subsequently sterilised by filter sterilisation as indicated. Filter sterilisation was performed using ether a sterivex GS 0.22 μm filter system, or by o.22 μm minister filters, power suppled by a peristaltic pump (Australia Millipore). After sterilisation, all solutions were stored at 4° C, -20°C or -80°C as indicated. Medium and buffers were used in this study are listed in Table 2-1. The details of buffer preparation are attached in Appendix.I.

Table 2-1: Medium, Buffers and Reagents

Name	Company	Catalogue
Inactive fetal bovine serum (FBS)	In Vitrogen corporation, Australia	16140-071
Dulbecco's phosphate buffered saline (DPBS)	In Vitrogen corporation, Australia	21300-025
Roswell park memorial institute (RPMI - 1640) medium	In Vitrogen corporation, Australia	31800-022
McCoy's 5a Medium	In Vitrogen corporation, Australia	16600-082
DMEM	In Vitrogen corporation, Australia	12800-017
MCDB 105 medium	Sigma , Australia	M6395
Medium 109	Sigma , Australia	M5017
Cytochalasin B (Cyt B)	Sigma , Australia	#6762
Phytohaemagglutinin (PHA)	Sigma , Australia	L8754
cDTPA	Sigma , Australia	284025

2.1.2 Cell lines

Cell lines used in this study were all cancer cell lines (Table 2-2), obtained from the America Type Cell Culture (ATCC, USA).

Table 2-2: Cell Lines

Cell line	Catalogue #	Origin or Characters	Medium
OVCAR-3	HTB-161	Adenocarcinoma of ovary	RPMI-1640 modified medium, supplemented with 0.01 mg/mL bovine insulin and 20% FBS
SKOV-3	HTB-77	Ascites, papillary serous adenocarcinoma of ovary	McCoy's 5a Medium, modified with 10% FBS
OV-90	CRL-11732	Ascites, ovarian adenocarcinoma	1:1 mixture of MCDB 105 medium and Medium 199 supplemented with 15% FBS
BT-474	HTB-20	Breast ductal carcinoma	EMDE medium modified with 10% bovine serum.

2.1.3 Monoclonal antibodies and protein

2.1.3.1 Herceptin

Herceptin (Trastuzumab, provided by Roche Products Pty Ltd, Australia) is a humanized IgG1 that recognized the extracellular domain of the HER-2 /neu oncoprotein (Choi et al., 2005). The antibody was washed with 0.1 M PBS (PH7.3) using a centrifugal concentrator (Mistral 3000i) to remove formulating agent (Borchardt et al., 2003)

2.1.3.2 C595

IgG_3 monoclonal antibody C595 (also known as NCRC48) is reactive with the protein core of MUC1 mucin. The target epitope of the C595 antibody is the tetrameric motif Arg-Pro-Ala-pro that is repeated many times within the MUC1 protein core. Murine C595 MAb provided by Dr. Alan Perkins from Nottingham University, UK.

2.1.3.3 PAI2

Human recombinant PAI2 (47KD), reactive with the membrane-bound uPA, was provided by PAI2, Australia Pty Ltd.

2.1.3.4 #394

Mouse anti-human uPA IgG antibody (#394) was purchased from American Diagnostic Inc (Greenwich, CT, USA).

2.1.3.5 A2

A non-specific control IgG1 MAb (know as A2) was provided by Professor Andrew Collins, University of New South Wales, Australia.

2.1.3.6 BSA

Bovine serum albumin (BSA) was purchased from Invitrogen (Sydney, NSW, Australia).

2.1.3.7 Negative control

Mouse IgG1 negative control MAb was purchased from Dakopatts (Glostrup, Denmark).

2.1.3.8 Horse Reddish Phosphatase (HRP)

Rabbit anti-mouse IgG conjugated to HRP was purchased from Dakopatts (Glostrup, Denmark).

2.1.3.9 Monoclonal antibody -Fluorescence Isothiocyanate (FITC)

Mouse and-human isotype control IgG1 monoclonal antibody and goat anti-mouse IgG fluorescence isothiocyanate (FITC)–conjugated monoclonal antibody were purchased from Silenus (Sydney, NSW, Australia).

2.1.3.10 Mouse anti-HER2 IgG1

Monoclonal mouse anti-HER2 IgG1 (clone: TAB 250) was purchased from Zymed Laboratories INC (South San Francisco, CA, USA).

2.1.4 Bismuth-213

The Bi-213 was used to radiolabel the MAb construct (Boll et al., 2005). ^{213}Bi is a daughter product of ^{225}Ac ($t_{1/2}$ = 10 days). ^{213}Bi was eluted from the ^{225}Ac/^{213}Bi column (Apostolidis et al., 2005), supplied by the Institute for Transuranium Elements (ITU), Germany, with 250 µL of freshly prepared 0.15 M hydriodic acid (HI) as the (Bi-Iodide) $^{2-}$ anion species, neutralized to pH 4 - 4.5 with the addition of 3 M-ammonium acetate. ^{213}Bi has a short half-life ($t_{1/2}$ = 46 min), short range (80 µm) and emits a α particle with energy of 8.34 MeV. Actinium-225 decays to stable ^{209}Bi through six predominant radionuclidic daughters in a cascade, with a yield of 4 alpha emissions in its decay chain and a total energy release of approximately 28 MeV. The Ac-225 decay scheme is shown in Figure 1-1.

2.1.5 Yttrium-90

Yttrium-90 (^{90}Y) is a pure-beta emitter that decays to stable zirconium-90 with an average energy of 0.94 MeV via a half-life of 2.67 days (64.2 hours) and has a maximum path length of 11 mm in tissue. Y-90 was kindly provided by ITU.

2.1.6 Ovarian cancer patients

This study has the approval of SESAHS ethics committee (03/88). Specimen from 26 stage I ~ IIc ovarian adenocarcinoma patients were obtained from Peter McCallum Cancer Institute Tissue Bank. Both primary and metastasis sites were included for 11 patients. The expression of uPA/uPAR, MUC-1 and HER-2 were tested by immunohistochemistry to evaluate the targeting potential in the ovarian cancer population.

2.1.7 Mice

Female 6-8 weeks Balb/ C (nu/nu) athymic nude mice, male 6-8 weeks old SCID mice, and female 6-8 weeks Balb/c mice were obtained from the Animal Resources Centre (ARC), Western Australia. The mice were housed and maintained in laminar flow cabinets under specific pathogen-free conditions in facilities approved by University of New South Wales (UNSW) Animal Care and Ethics Committee (ACEC) and in accordance with state regulations and standards. All mice studies were approved by the ACEC of the UNSW (02/17; 04/39; and 04/79).

2.1.8 Rabbits

10 weeks old White New Zealand rabbits were obtained from Biological Resources Centre (BRC) of UNSW. Rabbits studies were approved by the ACEC of the UNSW with reference number (03/56).

2.2 Methods – In Vitro

2.2.1 Cancer cell culture

The details of cell culture procedure are attached in Appendix.II.

Preparation of cells for animal models

Cells were not completely covering the flask, to avoid confluence which decreases the ability to grow in the animal body. Cells covered only 60-70% of the flask.

Cells were detached using 0.125% (w/v) Trypsin 0.015% (w/v) EDTA solution, and then washed 2 times using PBS before injection to eliminate FBS.

Cytocentrifuge preparations of the cultured cells for slides

The cells were detached, washed and suspended with a concentration of 2 x 10^4 cells/ 60 μL of DPBS. Cytospin preparations (wetting filter paper with 400 μL of DPBS/dot, 800 rpm at 5 minutes) were made with a Shando Cytocentrifuge (Thermo Electron Corporations. USA). Cell cytospins were made on glass slides at 800 rpm for 5 minutes.

2.2.2 Spheroid cultures

Human tumor cell lines can be cultured in the form of multicell spheroids, which are cellular aggregates growing by division at the periphery. As in vitro multicell spheroids resemble micrometastases during the avascular phase of their development, this model has applications for evaluation of the effectiveness of radioimmunotherapy of tumor micrometastases (Ballangrud et al., 2001; Couturier et al., 1999; Devys et al., 1996; Essand et al., 1995; Rutgers et al., 1989).

OVCAR-3 and BT-474 cells in a monolayer culture were trypsinized, and 10^7 cells in 15 mL of medium supplemented with 10% FBS were transferred into 10 cm culture dish coated with 1 % agarose, incubated in 5% CO_2 and 95% air at 37°C. The half of

the medium was changed every two days. This procedure resulted in spheroids of various sizes. The size of spheroids was determined using an inverted microscope equipped with a cross-hair eyepiece. Spheroid diameter (D), determined by measuring 2 perpendicular diameters (D1 and D2), was the geometric mean of D1 and D2: $D = (D1 \times D2)^{1/2}$. Complete dissociation of the spheroids was achieved by incubation in 0.12% trypsin-0.02% EDTA and PBS (Ca- and Mg-free) at 37°C for 15 min, followed by mixing the suspension with a pipette. Cold medium was added to stop trypsin action (Couturier et al., 1999).

2.2.3 Lymphocytes Culture for CBMN

Cytokinesis block micronucleus assay (CBMN) methods were obtained from Dr Fenech's laboratory (CSIRO Health Sciences and Nutrition, South Australia, Australia) and modified according to published methods (Fenech, 2000)

2.2.3.1 Isolation of lymphocytes

1. Fresh blood was collected by venipuncture. The volume taken was dependent on the number of cell needed (currently work on 1 x 10^6 cells per 1 mL blood).
2. Dilute whole blood 1:1 with RPMI and gently inverted to mix.
3. Gently overlay diluted blood onto Ficoll-Paque using a ratio of 1:3, 2 mL ficoll: 6 mL diluted blood, being very careful not to disturb the interface.
4. Weigh and balance the centrifuge buckets before spinning the tubes at 400 g for 30 min at 18-20 °C.
5. Remove the fluffy lymphocyte layer at the interface of ficoll and diluted plasma into a fresh tube using a sterile, plugged Pasteur pipette, taking care not to remove too much ficoll.

6. Add 3 x this volume removed of RPMI at room temperature, then centrifuge at 180 g for 10 min.
7. Discard the supernatant and resuspend the cell pellet in 2 x the volume removed of RPMI, using a Pasteur pipette, then centrifuged at 100 g for 10 min.
8. Discard the supernatant and resuspended the cells in 1 mL culture medium at room temperature, using a Pasteur pipette.
9. Count cells.
10. Cells were left in medium at this point at room temperature in the dark for 1-2 hours with the tubes sealed.

2.2.3.2 Culture of lymphocytes

1. Using the above calculation, resuspend cells at 1 x 10^6 /mL. Add the calculated volume of medium to labelled 5 mL flat bottomed culture tubes then add the cells into the medium to a final volume of 750 µL.
2. Stimulate mitotic division of cells by adding PHA
    - Added 10 µL / 750 µL culture to give a final concentration of 30 µg/mL.
    - Discarded remaining PHA after use.
3. Incubate the cells at 37°C with lids loose in a humidified atmosphere containing 5% CO_2.

For standard micronucleus measurement the following timetable applies:

T = 0 hour	Set up cells at 1 x 10^6 cells/mL with 30 µg/mL PHA (10 µL/750µL)
T = 44 hours	Add Cyt B at 4.5 µg/mL (56.2µL/mL)
T = 72 hours	Harvest cells by cytospin.

Note: at T=24 hours, when lymphocytes have been successfully stimulated, cultures appeared clumpy and grainy. Unstimulated cultures appeared cloudy and silty.

2.2.3.3 Addition of Cyt B: 44 hrs after PHA stimulation.

Carry out all handling of the Cyt-B solutions in a fume hood with the base glass window down to chest level and use personal protection.

1. Thaw out vial of 100 µL @ 600 µg/mL
2. Aseptically add 900 µL of culture media equilibrated to room temperature to the vial to give 1000 µL @ 60 µg/mL.
3. Add 56.2 µL/750 µL cell culture to give a final concentration of 4.5 µg/mL.
4. Discard after single use.

2.2.3.4 Harvesting of cells: 72 hours after PHA stimulation.

1. Centrifuge the cytocard with 400 µL of PBS.
2. Remove 200 µL of the culture medium without disturbing the cells.
3. Agitate tube gently to remove cells from the bottom of the tube.
4. Add 46 µL of DMSO.
5. Thoroughly resuspend the cells in the medium and leave at room temp for 10 minutes.
6. Sample 60 µL of cells into the sampling cup and then spin 600 rpm for 5 minutes using Cytospin.
7. Remove all slides and allow air dry for 10 minutes.
8. Fix cells by dipping slides into Diff Quik fix for 10 dips or methanol for 10 minutes.
9. Transfer directly into Diff Quik stain: 10 dips orange, 6-10 dips blue.

10. Wash in tap water then distilled water, then blot dry with tissue or filter paper, taking care not to rub the slide spots.
11. Allow the slides to air-dry for 15 minunes.
12. Cover with Depex mounting medium and No.1 coverslips.
13. Allow to air-dry overnight in the fume hood, then store at room temperature in a dust free box.

2.2.4 Immunohistochemistry

uPA, MUC1, and Her2 expression on ovarian cancer tissues was detected by immunohistochemistry as described following.

1. Paraffin embedded section (5 μm) incubated in oven for 20 min at 60°C.
2. Deparaffinized in xylene for 5 min at room temp.
3. Graded alcohols (100%, 95%, 70% 3-5 dips in each)
4. Wash with distilled water 2 times.
5. Rehydrate in TBS, PH7.6.
6. Primary murine MAb (#394, C595, and anti-Her2) incubated for 1 hour at RT. (Each section normally needs 100 μL to cover it)
7. Wash with TBS 2 times.
8. Rabbit- anti-mouse –HRP (1:100 dilution) for 45 min at RT.
9. Wash with TBS 2 times.
10. Diaminobenzidine (DAB) with 1% H_2O_2 substrate for 5-10 min.
11. Wash with tap water.
12. Counterstain in Harris's haematoxylin for 30 s - 1 min.
13. Wash with water 2-3 times.
14. Mount in glycerol gelatine under glass cover slips.

The criteria for assessment are to combine staining intensity with percentage of positive cells as follows: -, <25%; + (weak), 25-50%; ++ (moderate), 50-75%; +++ (strong), >75%.

2.2.5 Immunocytochemistry

uPA, MUC1, and Her2 expression in cancer cells was detected by immunocytochemistry as described follows:

1. Prepare cells in a concentration of 2-4 x 10^4 cells/ 60 μL
2. Prepare slides using Cytospin.
3. Allow air dry for 10 minutes
4. Fix slides with 4% paraformaldehyde (PH 7.4) for 20 minutes or Acetone for 10 minutes.
5. Air-dry for 10 minutes.
6. Wash with TBS 2 times.
7. Add primary murine MAb (#394, C595, and anti-Her2) incubated for 1 hour at RT. (Each section normally needs 100μL to cover it.)
8. Wash with TBS 2 times.
9. Rabbit- anti-mouse –HRP (1:100 dilution) for 45 min at room temperature (RT).
10. Wash with TBS 2 times.
11. Diaminobenzidine (DAB) with 1% H_2O_2 substrate for 5-10 min.
12. Wash with tap water.
13. Counterstain in Harris's haematoxylin for 30 s - 1 min.
14. Wash with water 2-3 times.
15. Mount in glycerol gelatine under glass cover slips.

The criteria for assessment was to combine staining intensity with percentage of positive cells as follows: -, <25%; + (weak), 25-50%; ++ (moderate), 50-75%; +++ (strong), >75%.

2.2.6 Flow cytometry

For the detection of cell-surface expression of targeting antigen/receptors on cancer cell lines, indirect immunofluorescence staining was performed.

1. Confluent, adherent cells were harvested by rinsing flasks twice with PBS (pH 7.2).
2. Detach with 0.25% trypsin and 0.02% EDTA at 37°C for 5min.
3. Cells ($0.5 - 1.0 \times 10^6$) were washed twice with 4mL cold DPBS containing 5% FBS (200 g, 8 min).
4. Re-suspend in 80 mL of cold DPBS plus 5% FBS.
5. Incubate with either an irrelevant isotype control (A2, BSA,IgG1) and DPBS or MAb (C595, #394, Herceptin) for 30 min on ice in the dark.
6. Wash cells with PBS.
7. Cells were re-suspended and incubated in goat anti-mouse FITC monoclonal antibody for 30 min.
8. The cells were washed again, re-suspended in 0.5 ml of DPBS plus 5% FBS.
9. In all the fluorescence-based experiments, autofluorescence was subtracted. All data were analyzed using CELLQuest software (Becton-
    i. Dickinson).

2.2.7 Confocal Microscope for antigen expression.

uPA, MUC1, and Her2 expression in cancer cells were detected by immunocytochemistry using confocal microscope as described below.

1. 1 x 10^5 cultured cancer cells were grown on coverslips.
2. Cells were washed with PBS.
3. Cells on coverslips were fixed with ice cold acetone for 10 minutes.
4. Primary antibody was incubated for 12 hours at 4 °C and rinsed with PBS.
5. Second antibody (goat-anti-mouse conjugated Alexa 488 green antibody) was incubated for 1 hour at RT.
6. Slides rinsed with PBS for 10 minutes.
7. The slides were mounted with coverslips using glycerol (Sigma-Aldrich Pty, Limited, Castle Hill, NSW, Australia).
8. Examination was performed with Confocal Microscope (FV300/FV500 Olympus, Japan).

2.2.8 In vitro cytotoxicity

2.2.8.1 MTS assay

This MTS assay [3-(4,5-dimethylthiazol-2-yl)-5-(3-carboxymethoxyphenyl)-2-(4-sulfophenyl)-2H-tetrazolium, inner salt] is a colorimetric method for determining the number of viable cells in proliferation or cytotoxicity assays. The non-radioactive MTS Assay has become popular due to its simplicity and accuracy (Riss & Moravec, 2004). The method is based on the cellular conversion of tetrazolium compounds to the ultraviolet-absorbing formazan product (Promega Technical Bulletin 169, 245 and 112). This product has been demonstrated to be directly proportional to the number of viable cells for most assay procedures.

Trypsinized monolayer cancer cells in exponential growth were washed twice with DPBS and seeded into 96-well flat-bottomed plates at a density of 2 x 10^4 cells in 300 μL of medium. The activities of the ACs were measured by a radioisotope calibrator

(Atomlab 200, Australia). After this, five serial dilutions of ACs/^{90}Y-PAI2 were made to give activities of 118, 237, 474, 947 and 1180 kBq for each well in triplicate. The specific activity of the ^{213}Bi: protein conjugate was 118 kBq: 1 μg. The following control conjugates, ^{213}Bi–BSA and ^{213}Bi-Iodide with activities of 118, 237, 474, 947 and 1180 kBq and 10 μg of cDTPA-protein, were tested in triplicate in the same 96-well plate for each experiment, as well as cell and medium alone. The plates were then incubated for 12 hours in a 5 % CO_2 atmosphere at 37^0 C. The cells were washed and incubated with 100 μL phenol-red free medium (without FBS) containing 20 μL of the CellTiter 96 Aqueous One Solution reagents (MTS assay) (Promega, WI, USA). After 3 hours incubation in a 5 % CO_2 atmosphere at 37 ^{0}C, the reaction was stopped by the addition of 10 % SDS, and the absorbance in each well was recorded at 490 nm using a SPECTRO max plate reader (BIO-RAD, Hercules, CA, USA). The absorbance reflects the number of surviving cells. Blanks were subtracted from all data and results analysed using Prism software (GraphPad Software Inc, USA).

2.2.8.2 Morphological change of monolayer cells.

The cultured monolayer cells were treated with ACs, free ^{213}Bi in a concentration of 1180 kBq/10^4 cells, or with cold controls (CCs) in a MAb/protein concentration of 10 μg/10^4 at 37°C for 12 hours. After treatment, the cells were washed with DPBS and suspended in fresh medium. Cells were harvested by rinsing flasks twice with DPBS (PH 7.2) and then detached with 0.25% trypsin and 0.05% EDTA at 37°C for 10- 20 minutes after 24 and 72 hours of treatment. Slides were prepared by cytospin at 600 rpm speed for 5 min for TUNEL assay or stained with Diff Quick staining system (Lab-aid, Australia) to identify apoptotic and necrotic cells. Slides were examined at x 1000 magnification using a light microscope (Olympus, Tokyo, Japan). Cells with three or

more nuclear chromatin fragments were considered as positive apoptosis, while cells with opaque cytomembrane were considered as positive necrosis. The number of necrotic and apoptotic cells in 500 cancer cells was counted and the frequency of dead cells calculated.

2.2.8.3 Morphological change of spheroids

Spheroids with size of 80 and 150 μm in diameter with 300 μL of medium were selected in each well of 24 wells plates. The activities of the ACs were measured by a radioisotope calibrator (Atomlab 200, Australia). After this, five serial dilutions of ACs were made to give activities of 118, 237, 474, 947 and 1180 kBq for each well in triplicate. Cold antibody/protein control (CC) was performed in triplicate for each experiment as well as cell and medium alone. The plates were then incubated overnight in a 5 % CO_2 atmosphere at 37° C. Then the following procedure was followed:

1) wash wells with PBS, and then add 1 mL of complete growth medium. Change half medium every two days. Record the spheroid size by two dimensions every two days. Experiment terminated when the control spheroids reached 250μm in diameter;

2) spheroids collected and disolved using proteinkenize , then make slides by cytospin for TUNEL assay, count the percentage of apoptosis cell numbers;

3) spheroids collected and cytospin spheroids for TUNEL assay.

2.2.8.4 TUNEL assay

Cells were treated and harvested as already described (paragraph 2.2.8.2). Apoptotic cells were detected using the TUNEL method (Gavrieli et al., 1992) with TdT–fragEL™ *in situ* apoptotic detection kit according to the manufacturer's instruction (Oncogene Research Products, Boston, MA, USA). Specificity of TUNEL reactivity was confirmed

by undertaking in parallel appropriate negative (omitting TdT from the labelling mix) and positive (treated HL-60 slides) controls. The labelled cells were examined using a Leica light microscope (Leica microscope, Nussloch, Germany) at x 40 magnifications. The results were expressed as a percentage of total cells staining positive for apoptosis.

2.3 Methods – In Vivo

2.3.1 Animal model development

The purpose of animal model development is for in vivo TAT treatment efficacy study.

2.3.1.1 Subcutaneous xenograft model

Female 6-8 weeks old Balb/C (nu/nu) athymic nude mice were used to develop this model. Subcutaneous tumour was established by inoculation of 2 x 10^6 OVCAR-3 /PC-3 cells, or 1 x 10^7 SKOV3 cells, suspended in 200 μL of serum-free medium, using a 29 G needle with a 0.5 mL syringe, into the subcutanous space of the right flank region. Tumor progression was documented by measurements using vernier callipers. Tumor volumes were calculated by the following formula: length x width x height x 0.52 in millimetres (Gleave et al., 1999). If the tumor size exceeded 10 mm in any dimension, mice were euthanized by cervical dislocation while under anaesthesia. Tumor tissues were resected and stored in 4 % neutralized formalin.

2.3.1.2 Estrogen implantation for subcutaneous xenograft model

Breast cancer cell line BT474 is able to develop subcutaneous tumour in nude mice under estrogen supplementation. 17 β estradiol pellets with 60 days release were used to develop this model. Stainless steel reusable precision trochar with regular medical point needle was used to implant 3 mm pellet intradermally as shown in Figure 2-1. Six-week-old BALB/c nu/nu athymic mice were first implanted intradermally with a 0.72 mg, 60-day sustained release 17β-estradiol pellet (Innovative Research, Sarasota, Florida, USA) required for the growth of BT-474 tumours. Two days following implantation of the 17β-estradiol pellet, 1.5 x 10^7 BT-474 cells in 100μL of a 1: 1 (v/v) mixture of Matrigel (Becton-Dickinson Labware, Bedford, Massachusetts, USA) and

culture medium were injected subcutaneously in the right flank. The procedure for tumor measurements and endpoint was followed as described previously (paragraph 2.3.1.1).

Figure 2-1 Implantation trochar

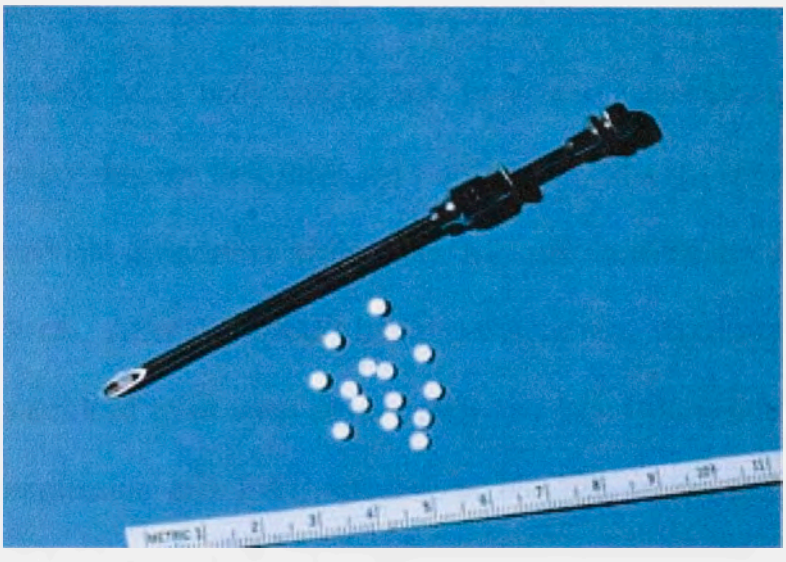

Figure 2-1 The size of pellets was 3 mm, while the size of implantation trochar was 10 cm with a medical point needle, which simplified the implantation procedure. Anaesthesia was not required for this procedure.

2.3.1.3 Ascites model

This model development was in collaboration with the Department of Surgery, St George Hospital, NSW, Australia. The OVCAR-3 cells were maintained *in vivo* by s.c. inoculation of the mice with 5 x10^6 cells in RPMI medium without supplements. Two months after inoculation, the s.c.-developed tumor was excised, mechanically dissociated, and inoculated i.p. into non-pre-inoculated nude mice. Only the ascites tumour cells were used for further experiments by harvesting the cells suspended in 50 ml of RPMI medium and centrifugation at 800 *g* for 5 min at room temperature (24–26°C). After cell washing (in RPMI as above), the cells were re-suspended in the same medium to a concentration of approximately 6 x 10^6 cells/ml, and 0.5 ml was injected i.p. into an untreated group of the mice. Mice girth was measured to evaluate the ascites volume. (Andersson et al., 2000; Avichezer et al., 1997; Hamilton TC).

2.3.2 Treatment efficacy

2.3.2.1 ^{213}Bi-C595 in a mice ascites model

Systemic injection (ip) of ^{213}Bi-C595 was performed at 9 days post-OVCAR3 intraperitoneal cell inoculation. Groups of five mice each received 355, 710, and 1065 MBq/kg, ^{213}Bi-A2 at 1065 MBq/kg or 9 mg/kg of cold control mix (unlabeled chelated C595). Mice body weight and the size of circumference of abdomen were measured every day for first three days and once per week after that. Mice were euthanized by cervical dislocation while under anaesthesia if the circumference of abdomen exceeded 9 cm. After 12 weeks, the experiment was terminated and tumour xenografts from sacrificed mice were immediately fixed in 10% neutral buffered formalin for MUC-1 expression and H&E staining in paraffin sections. Ascites cell were collected and cytospin was made for MUC-1 expression using immunocytochemistry.

2.3.2.2 ^{213}Bi-PAI2 and ^{90}Y-PAI2 in a mice ascites model

In vivo treatment efficacy studies with ^{90}Y-PAI2 and ^{213}Bi-PAI2, using RBE = 4 for alpha and assuming a range factor for beta energy loss for 100 μm spheroids at 9 days post-inoculation.

Intraperitoneal inoculation of OVCAR-3 cells was made in five groups of mice of 4 mice each. Experiments started at 9 days post cell inoculation.

Group1 mice received 710 MBq/kg of ^{213}Bi-PAI2 with one i.p injection. Group 2 mice received 355 MBq/kg of ^{90}Y-PAI2 with one i.p injection. Group 3 mice received 185 MBq/kg ^{90}Y-PAI2 and 355 MBq/kg of ^{213}Bi-PAI2 at 16 days of cell inoculation. Group 4 mice received 6 mg/kg of PAI2 cold control mix (CC). Group 5 mice received no treatment (C).

Mice body weight and the size of circumference of abdomen were measured every day for first three days and once per weeks after that. Mice were euthanased by cervical dislocation while under anaesthesia if the circumference of abdomen exceeded 9 cm. After 12 weeks, the experiment was terminated and tumour xenografts from sacrificed mice were immediately fixed in 10% neutral buffered formalin.

2.3.2.3 ^{213}Bi-Herceptin in a mice estrogens implants subcutaneous model

A systemic injection (ip) of ^{213}Bi-Herceptin was performed at 2 days post-BT474 cancer cell inoculation in an estradiol-implanted mouse as described previously (paragraph 2.3.1.2), Groups of seven mice each received 237, 355, 474 MBq/kg, or 4 mg/kg of cold control mix (unlabeled chelated Herceptin). Mice body weight and the tumour size were measured every day for the first three days and once per week after that. Mice were euthanized by cervical dislocation while under anaesthesia if the tumour size exceeded 10 mm in any dimension. After 12 weeks, the experiment was terminated and tumour xenografts from sacrificed mice were immediately fixed in 10% neutral buffered formalin for MUC-1 expression and H&E staining in paraffin sections.

2.3.3 Toxicity

2.3.3.1 Acute toxicity of ^{213}Bi-PAI2

Animals

Mice: This study is an extension of the previously published study (Allen et al., 2003), which showed the MTD for weight loss to be more than 710 MBq/kg (Barry J Allen et al., 2005)) up to 90 days. Nude mice were divided into three groups (5 mice in each). Mice were ip injected with 947 or 1180 MBq/kg of ^{213}Bi-PAI2, or cold control mix (PAI2, elution solution and buffers for adjusting pH, without Bismuth). Animals were monitored up to 15 weeks for any dramatic change in weight or distressed behaviour. If

body weight loss exceeded 20%, mice were euthanized by cervical dislocation while under anaesthesia; blood and organs collected and sent for pathologic examination. Serum was obtained and kidney and liver function tests were done.

To determine haematological toxicity, 200 μL of blood was collected under anaesthesia by cardiac puncture before the mice were sacrificed. White blood cell (WBC), lymphocytes, red blood cell (RBC), and platelet count were performed before therapy and at 2-7 days, 2 and 3 weeks post 947 – 1180 MBq/kg of ^{213}Bi-PAI2 treatment (n = 3/group).

Rabbits: Four groups of three White New Zealand rabbits were used. Rabbits received 59, 118 or 355 MBq/kg of ^{213}Bi-PAI2 via ear vein, or cold control mix. Animals were monitored up to 90 days for any dramatic change in weight or distressed behaviours. Rabbits were euthanized by ketamine (1 mL) and Iluim xylazil (0.5mL) by intramuscular injection, if body weight loss exceeded 20%. Blood and organs were collected and sent for pathologic examination.

2.3.3.2 Delayed toxicity of ^{213}Bi-PAI2 in mice

To determine the long term radiation toxicity, animals were monitored up to 40 weeks for any changes in body weight or distressed behaviour. Nude mice were divided into 3 groups for lysine application, no lysine or cold control mix respectively. Lysine was injected with i.p.injection 5 minutes before ^{213}Bi-PAI2 i.p injections. The injected activity was calculated in MBq/kg according to the weight of each mouse. ^{213}Bi-PAI2 activities were from 355 MBq/kg to 592 MBq/kg for the group without lysine, and 592 MBq/kg to 829 MBq/kg for groups with lysine applicationIf the body weight loss exceeded 20% or mice suffered severe distress, mice were euthanized by cervical

dislocation while under anaesthesia. Otherwise, the experiment terminated at 40 weeks. Blood and organs were collected and sent for pathologic examination.

2.3.3.3 Toxicity of ^{213}Bi-Herceptin

Observation up to 90 days. Animals were monitored up to 90 days for any dramatic change in weight or distressed behaviour. Nude mice were divided into three groups (5 mice in each). Mice were ip injected with 355, 710, 1065 and 1420 MBq/kg of ^{213}Bi-Herceptin, or cold control mix Herceptin, elution solution and buffers for adjusting pH, without Bismuth). If body weight loss exceeded 20%, mice were euthanized by cervical dislocation while under anaesthesia; blood and organs collected and sent for pathologic examination. Serum was obtained and kidney and liver function were tested.

Observation up to 280 days. Mice were treated with activity of 237, 355, 474 MBq/kg of ^{213}Bi-Herceptin or Cold control mix. Animals were monitored up to 280 days for any dramatic change in weight or distressed behaviour. If body weight loss exceeded 20%, mice were euthanized by cervical dislocation while under anaesthesia; blood and organs collected and sent for pathologic examination. Serum was obtained and kidney and liver function were tested.

2.3.3.4 Toxicity of ^{213}Bi-C595

Animals were monitored up to 14 weeks for any dramatic change in weight or distressed behaviour. Nude mice were divided into three groups (5 mice in each). Mice were ip injected with 710, 940 and 1180 MBq/kg of ^{213}Bi-C595, or cold control mix C595 (elution solution and buffers for adjusting pH, without Bismuth). Only 1180 MBq/kg of ^{213}Bi-C595 group were monitered up to 21 weeks. If body weight loss exceeded 20%, mice were euthanized by cervical dislocation while under anaesthesia;

blood and organs collected and sent for pathologic examination. Serum was obtained and kidney and liver function tests were done.

2.3.3.5 Toxicity of Multiple targeted alpha therapy

SCID mice were divided into seven groups (3 mice in each). Mice were ip injected with 355, 474, 592, 710 MBq/kg of cocktail of ^{213}Bi –PAI2, ^{213}Bi – C595 or cold control mix (PAI2 and C595, elution solution and buffers for adjusting pH, without Bismuth).

Animals were monitored up to 13 weeks for any dramatic change in weight or distressed behaviour. If body weight loss exceeded 20%, mice were euthanized by cervical dislocation while under anaesthesia; blood and organs collected and sent for pathologic examination. Serum was obtained and kidney and liver function tests were done.

To determine haematological toxicity, 100 μL of blood was collected via saphenous vein by Microvette (SARSTEDT, Germany). White blood cell (WBC), lymphocytes, red blood cell (RBC), and platelet count were performed before treatment and at 2 and 3 weeks post 740 MBq/kg of ^{213}Bi-conjugates treatment (n = 3/group).

2.3.4 Pharmacokinetics studies

2.3.4.1 ^{213}Bi-PAI2. The in vivo pharmacokinetics of ^{213}Bi-PAI2 were studied in female Balb/c nude mice (average weight 20 g) as follows:

Lysine protection. Mice received an ip injection of 0.8 mg/g lysine (Bernard et al., 1997) 5 minutes before the 3 MBq of ^{213}Bi-PAI2 i.p injection. The control mice received the ^{213}Bi-PAI2 only.

Chelator study. Kinetics were studied for ip administration of 3 MBq of ^{213}Bi-cDTPA-PAI2 or ^{213}Bi-CHX-A"-DTPA-PAI2. The syringe activity was measured before and

after injection. Radiation uptake of various organs was determined after injection of the ^{213}Bi-PAI2 and euthanasia at 5, 15, 30, 60, 120 and 240 minutes post-injection (4 mice in each time point). Heart, liver, lungs, kidneys, spleen, and blood were weighed and counted for activity at each time point in the gamma scintillation counter. The percentage of the injected dose per gram of tissues was calculated and compared to the standard of the injected solution. A standard injection activity was counted for normalization.

DTPA challenge. Mice received i.p. 3 MBq of ^{213}Bi-CHX-A"-DTPA-PAI2, 15 minutes before ip injection of 1.5 mg Ca-DTPA. Activity uptake of various organs was determined after euthanasia at 15, 30 and 60 minutes post-injection (4 mice in each time point). Heart, liver, lungs, kidneys, spleen, blood were weighed and counted for activity.

2.3.4.2 ^{213}Bi-C595

Kinetics were studied for ip administration of 3 MBq of ^{213}Bi-cDTPA-C595 in mice with and without ascites development. The syringe activity was measured before and after injection. Radiation uptake of various organs was determined after injection of the ^{213}Bi-C595 and euthanasia at 30, 60, 120 and 240 minutes post-injection (3 mice in each time point). Heart, liver, lungs, kidneys, spleen, and blood were weighed and counted for activity at each time point in the gamma scintillation counter. The percentage of the injected dose per gram of tissues was calculated and compared to the standard of the injected solution. A standard injection activity was counted for normalization.

2.4 Methods – Radioactive

2.4.1 Loading Ac:Bi generator

Upon arrival of the Ac generator in radiation laboratory, the activity of the top, side, and bottom of the lead sealed container (Figure 2-2) was measured using a radiation monitor and recorded for radiation safety information.

Figure 2-2 Sealed container radiation measurement (example)

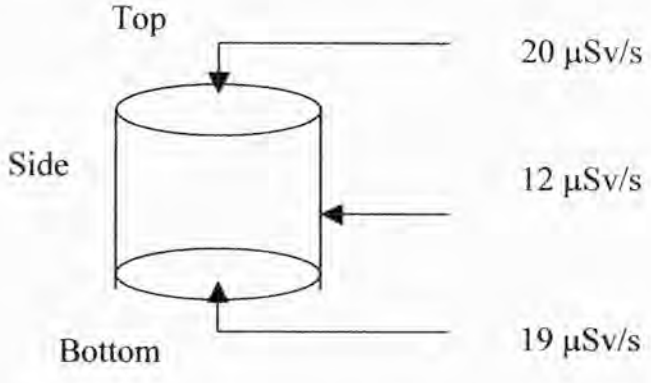

Figure 2-2 An example of shipping container and required measument.

^{225}Ac was received in the form of solid ^{225}Ac-nitrate from ITU, Germany. Actinium was loaded onto an AG50 X 4 column with a 100-200 mesh. The column was in H^+ form in H_2O. The following steps were involved in the loading of ^{225}Ac on the column, elution of ^{213}Bi and subsequent reloading of ^{225}Ac on a new column.

1. The generator was opened in the alpha hot laboratory with the ^{225}Ac being in the shipping container. Radiation dose was monitored with a Radiation Alert Monitor 4/4EC alpha, beta and gamma dosimeter.
2. The column was pre-equilibrated with 1 mL of 0.1 M HNO_3.
3. ^{225}Ac in the shipping vial was dissolved with 1 mL of 0.1 M HNO_3 and the solution was transferred to a small plastic vial (5 mL volume).

4. The procedure was repeated two more times by adding 1 mL of the 0.1 M HNO_3 and the contents were transferred to the solution in the plastic vial (from step 3). The vial was assayed for radioactivity. Radioactivity in the shipping vial was also assayed at this stage to make sure that all ^{225}Ac was recovered.
5. The ^{198}Au setting was used on the AtomLab 200 dose calibrator (the gamma ray energies are similar for both isotopes i.e. 412 keV for ^{198}Au and 440 keV for ^{213}Bi). The manufacturer recommends a factor of 3.2 to obtain the correct Bi-213 activity when using the gold setting (paragraph 2.4.3).
6. The contents of the vial were then loaded at the top of the column using a long glass pasteur pipette.

2.4.2 Elution of Bismuth-213

1. Bismuth was eluted from the generator. The three-way valve was inserted. In one of the two syringes (the washing syringe), put 2 mL of 2 mM HCl plus 1 mL of air. In the second syringe (the elution syringe), about 600 microliters of elution solution plus 1 mL of air. The elution solution was a mixture of 0.2 M NaI with 0.2 M HCl, 300 microliter of each. The activity of eluted ^{213}Bi was assayed against ^{198}Au setting. This was the first elution of ^{213}Bi and contains a large quantity of cold ^{209}Bi. The eluted Bismuth, though pure, cannot be used for labeling purposes as the stable ^{209}Bi competes with ^{213}Bi in labeling.
2. A time of 2-3 hours was allowed for ^{213}Bi to grow back within 85% activity in the generator which was then eluted again as step 1. This ^{213}Bi was suitable for labeling as the long-lived ^{209}Pb ($t_{1/2}$ 3.3 hours) has insufficient time to decay to ^{209}Bi. As a guide the activity of the ^{213}Bi should be approximately half of the total activity of the column as ^{225}Ac and ^{213}Bi should be in equilibrium by this

time. The bismuth regeneration kinetics was tested for 5 hours and results are shown in . Note that there is 75% regeneration of activity in 100 minutes, and 90% at 200 minutes.

Figure 2-3 ^{213}Bi regeneration

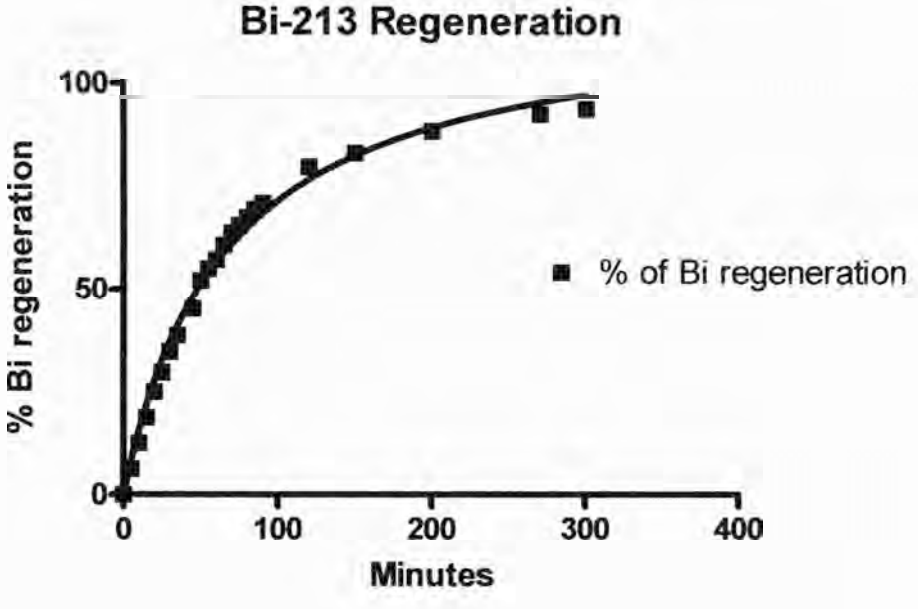

Figure 2-3 75% activity was regenerated at 100 minutes and 90% in 200 minutes.

2.4.3 Dose calibrator setting for Bismuth-213

Activity was measured using a dose calibrator (ATOMLAB 200 dose Calibrator, BIODEX, USA) on the gold setting, as the 440 keV gamma ray emitted in the Bi-213 decay has similar energy to that for Au-198 (411 keV) (Allen et al., 2005).

Tissue samples were measured for gamma activity in counts per minutes with a 1470 automatic gamma scintillation counter (Perkin Elmer, Finland). The setting of the machine was normalized relative to the dose calibrator using the Bismuth-213 gamma decay.

2.4.4 The relationship between dose calibrator and gamma counter

The dose calibrator was used to measure the activity of radioisotope in units of Ci or Bq, whereas the gamma counter gives counts per minute. To find the relationship between these two machines was not straightforward, because of dead time effects at high count rates. If the count rate is too high, then the machine presents very high percentage of errors, and the results are not accurate. To minimise these errors, the injected dose for boiodistribution studies should be in the range that is not too low to be tested by dose calibrator and not too high for the gamma counter. Activities (1 μCi-100 μCi) of eluted solution were counted in the dose calibrator and gamma counter, the reading values were recorded and plotted.

2.4.5 Protein chelation

Antibody/protein was dissolved in 2 mL of PBS. 0.45 mg of cDTPA was dissolved in 0.45 mL of chloroform. These prepared solutions were mixed together and incubated at room temperature on a slow rotated platform for 2 hours. A PD10 column (Amersham, Australia) was prepared by pre-equilibrating it with PBS, pH 7.6 buffer. Incubated solution passed through the column, collected in 2.5 mL aliquots, and then the concentration of the chelated antibody/protein is determined using a Micro BCA™ Protein Assay Reagent Kit (from Pierce – Progen, Australia. Code 0023235).

2.4.6 Labelling and Quality control

^{213}Bi conjugate labelling were performed as previously described (Abbas Rizvi et al., 2000; Ranson et al., 2002). Routine quality control of the labeled protein was performed using instant TLC (Appendix III) to estimate the radiopurity. The immunoreatitivity was tested using the method published by Mcdevitt et al (McDevitt et al., 1999). The

standard procedure of labelling ^{213}Bi with IgG antibodies (C595, 9.2.27, BLCA-38), protein PAI2, and humanized antibody Herceptin are given in Appendix III. The procedure of labelling Y-90 with PAI2 is also described in Appendix III.

To estimate the maximam bound sites on cell and affinity of the antibody

Scatchard analysis was used to determine the B_{max} (Maximum bound concentration) and K_a (affinity constant). 1 x 10^6 cancer cells in triplicated were incubated with 0.1, 0.2, 0.4, 0.6, 0.8, and 1 μg/mL of ^{213}Bi-conjugates in a total volume of 200 μL. After 30 minutes incubation at 0°C, the cells were collected by centrifugation (1000 rpm @ 5 minutes) and the supernatant was removed; the cells were washed twice with PBS, and this wash was removed. The three components (cell pellet, supernatant and wash) were then counted. The percent immunoreactivity was calculated as equal to alpha conjugates bound to cells/ total bound plus unbound activity x 100. The concentration of bound radiolabelled antibody was calculated. The number of bound radiolabelled antibody can be calculated from the Bmax value.

Assay of immunoreactive fraction

The immunoreactivity of alpha conjugates construct was determined by incubating 2 ng of radiolabelled antibody in 0.03 mL total volume with a 50 fold excess antigens. (approximatly 1 x 10^7 cancer cells). Scatchard anlysis shows that these MM138 cells express approximatly 400,000 positive-binding sites per cell (MCSP) and were in antigen excess to added antibody. After a 30-minunes inoculation on ice, cells were centrifuged and washed twice with 1 mL PBS. Radioactivity in the collected supernents and the cell pellets was quantified by gamma ray counting and the ratios between bound and total activity were calculated. The three components (cell pellet, supernent and wash) were then counted. The percent immunoreactivity was calculated as equal to

alpha conjugates bound to cells/ total bound plus unbound activity x 100. Specific binding in these assays was confirmed by testing the antibody negative cell line. To avoid nonspecific and Fc site binding, the assays were performed in the present of 2% human serum albumin. The immunoreactivity can be corrected for radiochmical purity by dividing the value for the percent immunoreacivity fraction by the fraction of pure radiolabeled antibody.

To test the quality of antibody

The antibody positive cell line was cultured and cytospin prepared for immunohistostaining. The MAb was tested in three forms (antibody alone, chelator chelated antibody, and ^{213}Bi labled antibody). A known postive antibody as a positive control, an antibody negative isotype as negative contol, were tested as the same time.

2.4.7 Absorbed Dose Calculation

The radiation dose to the kidney from ^{213}Bi-PAI2 was determined from pharmacokinetic studies. The kidney was weighed and counted in a gamma counter and activity was expressed as a percentage of the initial injected dose of radioactivity and was plotted as a function of time. The cumulative activity for dose estimation was determined as the area integrated under this curve. The absorbed dose to kidney was calculated (Loevinger & Berman, 1968) as:

$D = (A \times \sum i \, \Delta i \phi I)/m$ Gy

where A is the accumulated activity (Bq•s); m is the mean organ mass (kg); ΔI is the mean energy emitted per nuclear transition (MeV) and ϕ_i is the absorbed radiation fraction by the organ of the ith emission. ^{213}Bi is an alpha and beta emitter with $E_{\alpha max}$ = 8.35 MeV(98%) + 5.86 MeV(2%) = 8.3 MeV; $E_{\beta max}$ = 1.39 MeV + 0.64 MeV = 2.03

MeV. ϕ_i was assumed to be 1 for both alpha and beta. Gy = J/kg; 1 MeV = 1.602 x 10^{-13} J.

2.4.8 Biological dosimetry-CBMN

2.4.8.1 In vitro CBMN evaluation

A group of 3 healthy volunteers with a mean age of 48 years (range 36-64) donated 20 mL of blood for in vitro study. The blood samples from volunteers were divided into 12 fractions. One fraction served as a non-irradiated control. The other 9 fractions were irradiated in vitro at 37°C with activities of 15 – 240 kBq of ^{213}Bi-9.2.27. two fractions were irradiated with low energy phonons. One volunteer's blood samples were irradiated in vitro with ^{213}Bi alone and ^{213}Bi-9.2.27. Lymphocytes isolated from three healthy volunteers were counted using a Coulter counter and viability was measured using Trypan blue as described previously (paragraph 2.2.3.1). The lymphocytes were cultured in a concentration of 1 x 10^6 /mL in a supplemented medium (RPMI-1640, 10% Fetal bovine serum, 2 mM L-Glutamine) in a sterilized 5 mL tube. The activities of ^{213}Bi-9.2.27, and ^{213}Bi were measured using a radioisotope calibrator and neutralized to pH 7.0 via the addition of 10% (vol/vol) 1 M $NaHCO_3$ (pH 9.0). ACs was added to culture tubes containing 0.75 million cells in different concentrations. Cells incubated at 37°C for 3 hours. 10 µL of PHA was added to cultured tubes post 3 hours alpha incubation to give a final concentration of 30 mg/mL as described previously (paragraph 2.2.3.2). After that, cells were cultured at 37°C in atmosphere with 5% CO_2 for 44 hours. The addition of 56.2 µL/750 µL Cyt-B in culture medium gave a final concentration of 4.5 µg/mL (paragraph 2.2.3.3). 72 hours post-addition of PHA, cells

were harvested by cytospin and were stained using Diff Quik to count the number of MNs in 1000 cells (paragraph 2.2.3.4).

2.4.8.2 In vivo CBMN evaluation

This study comprises a total of 7 trial patients (6 females, 1 male) stage IV melanoma patients and three healthy volunteers (1 female and 2 males). A group of 5 patients, age range of 46 – 85 years, receive one injection with activity range in the range of 260-360 MBq. Another group of 2 patients with age of 40 and 50 years receive one injection with activity of 783 and 630 MBq.

5 ml of blood samples were collected in heparinized tubes at baseline (before administration of therapy), 3 hours, 2, 4, and 8 weeks post ^{213}Bi-9.2.27 therapy. Also, 4 blood samples were collected at 15, 30, 120 and 180 minutes post injection for counting against a gamma counter (paragraph 2.2.3) for absorbed dose calculation.

2.5 Statistical analysis

All numerical data were expressed as the average and standard deviation of the values obtained. For the in vivo studies, students t-test was used to compare data and results with a P value < 0.05 were considered statistically significant. Time to endpoint curves were constructed using the prism software package (Graphpad Software inc, Sabin Diego, CA) based on the method of Kaplan-Merier method.

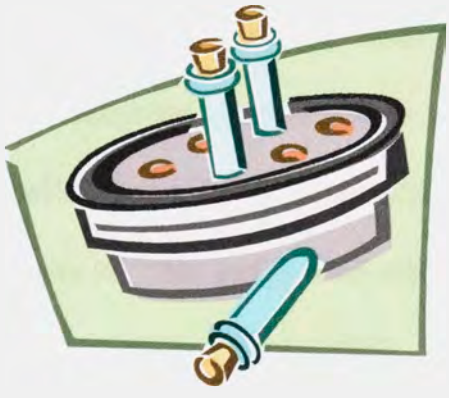

Chapter 3

Preclinical studies of ^{213}Bi-PAI2 Results & Discussion

Introduction

The targeting characteristics of ^{213}Bi-PAI2 allow the alpha radiation to deliver a large fraction of the total decay energy to the nucleus of those cancer cells with high expression of uPA/uPAR, these cells being the most malignant ovarian cancer cells, with greatly reduced irradiation of distant normal cells. Cell killing occurs after the uPA/uPAR-^{213}Bi-PAI2 complex formation with the decay of ^{213}Bi, and is most effective on endocytosis of the complex, which occurs in 40 minutes (Al-Ejeh et al., 2004).

In this chapter the new investigation of uPA/uPAR expression in ovarian cancer tissues and in three established cancer cell lines is reported. The *in vitro* cytotoxicity of ^{213}Bi-PAI2 to established primary and metastatic ovarian cancer cell lines is determined, and the efficacy of targeted alpha therapy (TAT) in inhibiting tumor growth in a metastatic ovarian cancer xenograft model (ascites model) is demonstrated.

This chapter also investigates for the first time the effect of ^{213}Bi-PAI2 on the kidneys. The more unstable the ^{213}Bi-PAI2 complex, the more kidney uptake is observed because free bismuth forms small blood protein conjugates in the blood, which are filtered by the kidney glomeruli, and then reabsorbed through proximal tubules. In this study, we compare the kinetics of ^{213}Bi-PAI2 using two different chelators, viz cyclic diethylenetriaminepentacetic acid (cDTPA) and 2-(p-isothiocyanatobenzyl)-cyclohexyl-DTPA (CHX-A"-DTPA). Further, the stability of ^{213}Bi-PAI2 on Ca-DTPA challenge in vivo and the effect of lysine on ^{213}Bi-PAI2 kidney uptake is reported. The short and long-term toxicity of ^{213}Bi-PAI2 in nude mice and rabbits is investigated to establish the maximum tolerance dose (MTD).

3.1 uPA/uPAR expression

3.1.1 Immunocytochemistry for cancer cell lines

The immunoreaction of four cancer cell lines to MAb #394 was tested and results were summarized in Table 3-1. The ovarian cancer cell lines OVCAR3 and SKOV3, and the breast cancer cell line BT474 were positive to #394 and negative to isotype control. Ovarian cancer cell line OV-90 was negative to #394 and isotype control. Representative pictures were shown in Figure 3-1.

Figure 3-1 Expression of uPA in OVCAR3 cells

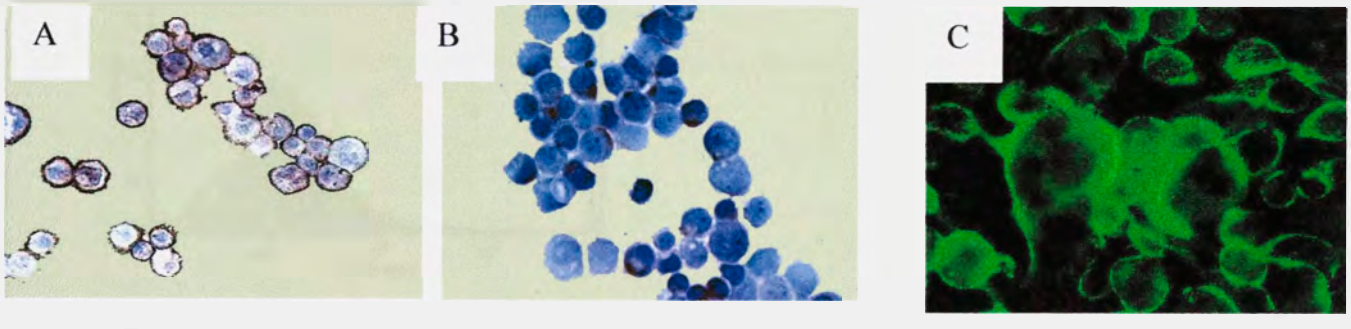

Figure 3-1 A: Moderate expression of uPA was found in OVCAR-3 monolayer cultured cells. Brown staining indicates positive cells. B: Negative control has shown blue staining only; C: Green florescence has shown the positive cells. Magnification was at x 400 for A and B and x 1000 for C.

Table 3-1 uPA expression in cancer cell lines

	OVCAR3	SKOV3	OV90	BT474
Immunocytochemistry	++	++	–	++
Flow cytometry*	64%	44%	6%	NA
Spheroids	++	NA	NA	++
Animal model	++	++	NA	++

Note: +++ strong positive, ++moderate positive, + weak positive, - negative.
*Percentage of positive cells. NA: not available.

3.1.2 Flow cytometry for cancer cell lines

Flow cytometry demonstrated distinct differences in the patterns of reactivity of the MAb #394 with OVCAR3 (Figure 3-2), SKOV3, and BT474 cancer cell lines with isotype control. There were little differences in the pattern of staining with MAb #394 and isotype control for the OV90 cell line. The results of flow cytometry are also summarized in Table 3-1.

Figure 3-2 Flow Cytometry for uPA expression

B

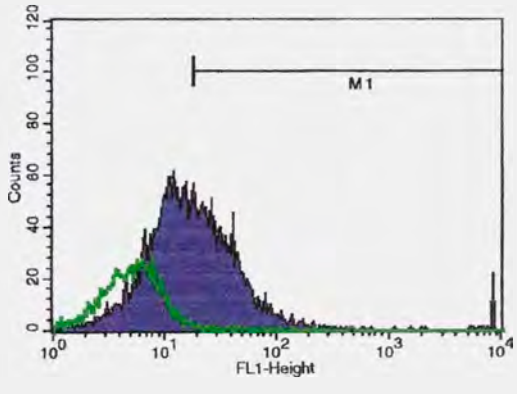

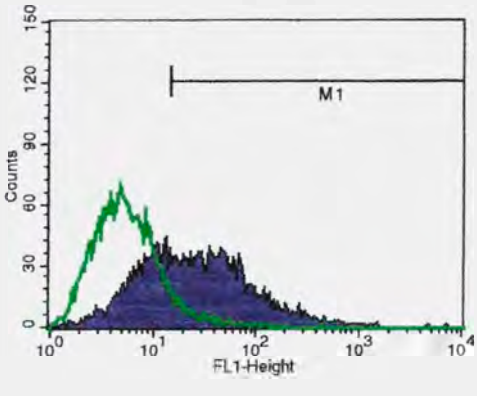

C

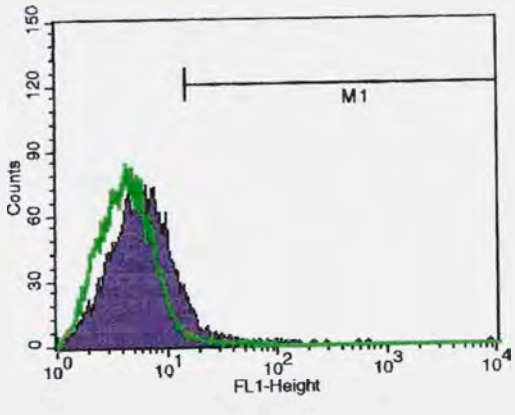

Figure 3-2 Flow cytometry confirmed viable OVCAR-3 cells (A) with 64% expression of uPA, SKOV3 (B) with 44%, OV90 (C) with 6%. Data are presented as histogram, using a mouse IgG1 isotope negative control to determine background fluorescence and to set the marker (M1).

3.1.3 Immunohistochemistry for ovarian cancer tissue

uPA expression in 26 ovarian cancer tissues (paragraph 3.1.6.1) was assessed by immunohistochemistry. Representative pictures were shown for immunostaining with MAb #394 (test) and Mouse anti-human isotype control IgG1 MAb (isotype control). uPA expression was found in 46.2% (12 / 26, n = 26) of ovarian tumor sections (Figure 3-3). In these positive tissues, 4 out of 26 were strong positive, 5 out of 26 were moderate positive, and 3 out of 26 were weak positive. 11 patients were included primary ovarian cancer site and omentum metastasis tissue. Four of them with matched metastases were negative to #394, one was positive in primary tumour (+), and omentum (+++) and the other 6 has shown positive in primary but negative in metastasis tissue. No immunoreactivity was found with isotype control and in normal ovarian tissue. The staining intensity was from positive (+) to strong positive staining (+++). Results were summarized in Table 3-2.

Figure 3-3 uPA expression in ovarian cancer tissues

A 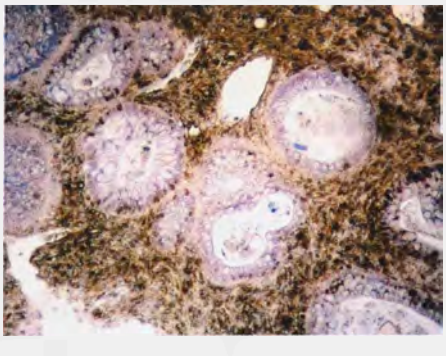 B 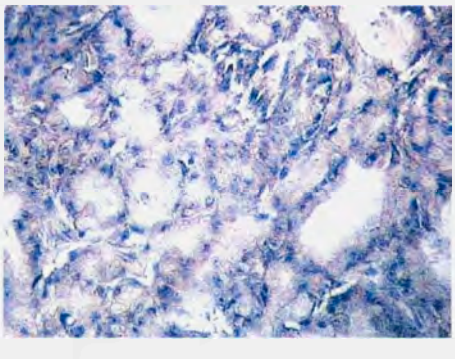

Figure 3-3 Expression of uPA. Over-expression of uPA was found in ovarian cancer tissues. Magnification x 200 in all photos. A represents positive staining, while B represents negative control.

Table 3-2 Intensity of immunohistochemical staining of ovarian cancer tissue, omentum metastases and normal ovarian tissues with #394 MAb

Tissue	Tissues staining with #394 MAb				
	+++	++	+	–	N
Tumor	4	5	3	14	26
Omentum metastases	1			10	11
Normal ovarian tissue				5	5

Note: Ovarian tumors (n = 26), matched omentum metastases (n = 11) and normal parts of the ovaries (n = 5) were collected from 26 ovarian cancer patients.
– Negative staining; + weak staining; ++ moderate staining; +++ strong staining.

3.1.4 Immunocytochemistry in spheroids

The immunoreactivity of OVCAR3 and BT474 cell clusters to MAb #394 was tested on cytospin and shown in Figure 3-4. Strong uPA expression was found in OVCAR3 and BT474 cell clusters. The isotype control was negative to the matched cell line. Results are summarized in Table 3-1.

Figure 3-4 Expression of uPA/uPAR in spheroids

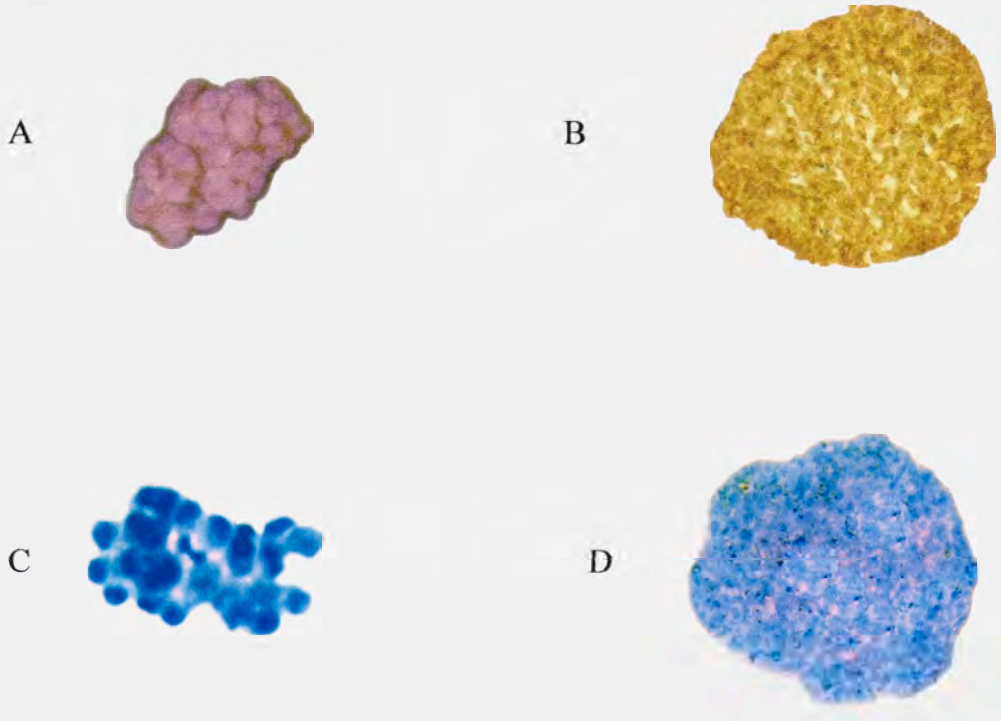

Figure 3-4 Moderate expression of uPA/uPAR was found in OVCAR-3 cell 40 μm (A) diameter clusters. A similar staining pattern was found in cultured spheroids (150 μm B). C and D were shown matched sized spheroids negative control. Magnification was at x 100.

3.1.5 Immunohistochemistry in animal models

Cancer tissues from the animal model were stored in 4% neutralized formalin. Paraffin sections and slides were prepared by Pathology Department of South East Area Laboratory Services (SEALS), St George Hospital, Australia. OVCAR3, and BT474 tumors, and OVCAR3 ascites cells were positive to C595 MAb, while negative to isotype control. Representative images are shown in Figure 3-5. Results are summarized in Table 3-1.

Figure 3-5 Animal xenograft tumors uPA/uPAR expression

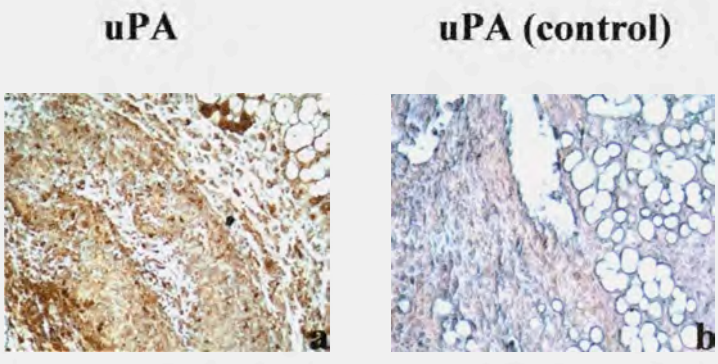

Figure 3-5 Expression of uPA. Over-expression of uPA was found at OVCAR3 xenograft tumors. Magnification x 200 in all photos.

3.2 In vitro

3.2.1 ^{213}Bi-PAI2 inhibition cancer cells proliferation – MTS assay

The effects of ^{213}Bi-PAI2 on cell growth were assessed using MTS assay in triplicate (P value relative to the free ^{213}Bi). D_0 values (activity required for 37% cell survival) for 2 x 10^4 cells in 300 μL for ^{213}Bi-PAI2 are 0. 51 ± 0.05 MBq (A), 0.36 MBq (B), 5.3 MBq and 0.53 MBq for OVCAR3, SKOV3, and OV90 (Figure 3-6 A, B, C), whereas the D_0 values of ^{213}Bi-BSA and ^{213}Bi-Iodide were 7.9 ± 1.2 MBq, being 12-16 times greater than uPA/uPAR positive expression cells with ^{213}Bi-PAI2 (P <0.001). Cell survival for antibody/protein alone group was the same as for untreated cells.

Figure 3-6 MTS assay

A

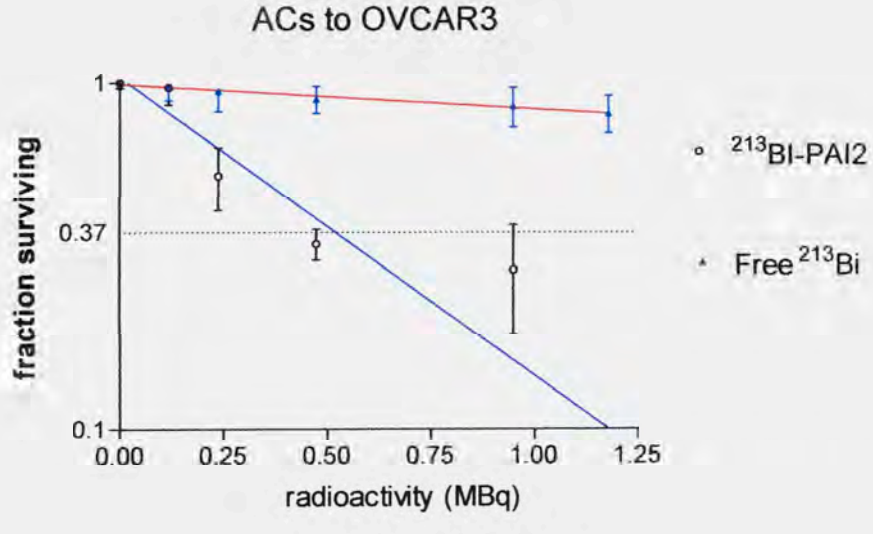

B

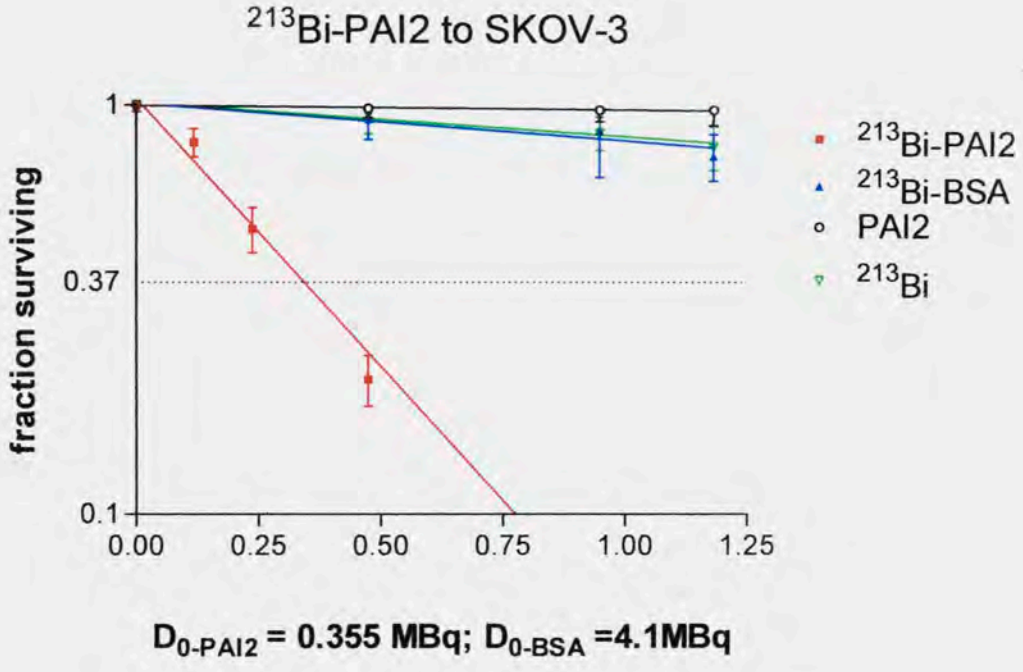

C

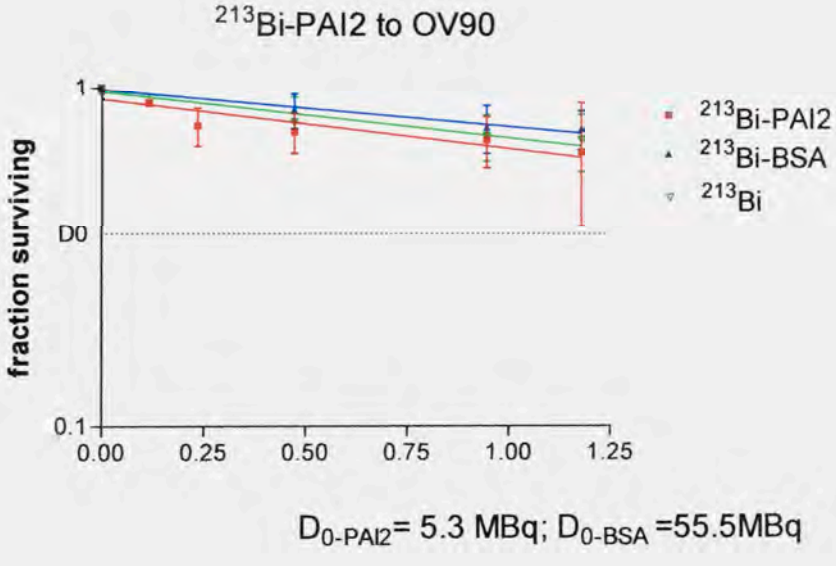

Figure 3-6 Cytotoxicity study of Cancer cell lines following incubation for 24 h with ^{213}Bi-PAI2 and free ^{213}Bi (A-C). Ovarian cells were treated with varying concentrations of ACs, and cell survival measured by MTS assay and expressed as a percentage of cell survival of control cells. Each experiment was performed in triplicate, and each point represents the mean of three experiments. Graphs A and B were OVCAR3 and SKOV3 cell lines with strong expression of uPA/uPAR, whereas graph C is OV90 with weak expression of uPA/uPAR.

3.2.2 ^{90}Y-PAI2 inhibition of cancer cell proliferation in vitro

The effects of ^{90}Y-PAI2 on OVCAR3 cell growth were assessed using MTS assay in triplicate. D_0 values (activity required for 37% cell survival) for 2 x 10^4 cells in 300 μL for ^{90}Y-PAI2 are 0.74 ± 0.08 MBq for OVCAR3 cell line (Figure 3-7), whereas the D_0 values of the non-specific control ^{90}Y-BSA were 4.4 ± 0.8 MBq, being 6 times greater than uPA/uPAR positive expression cells with ^{90}Y-PAI2 ($P < 0.001$).

Figure 3-7 ^{90}Y-PAI2 MTS

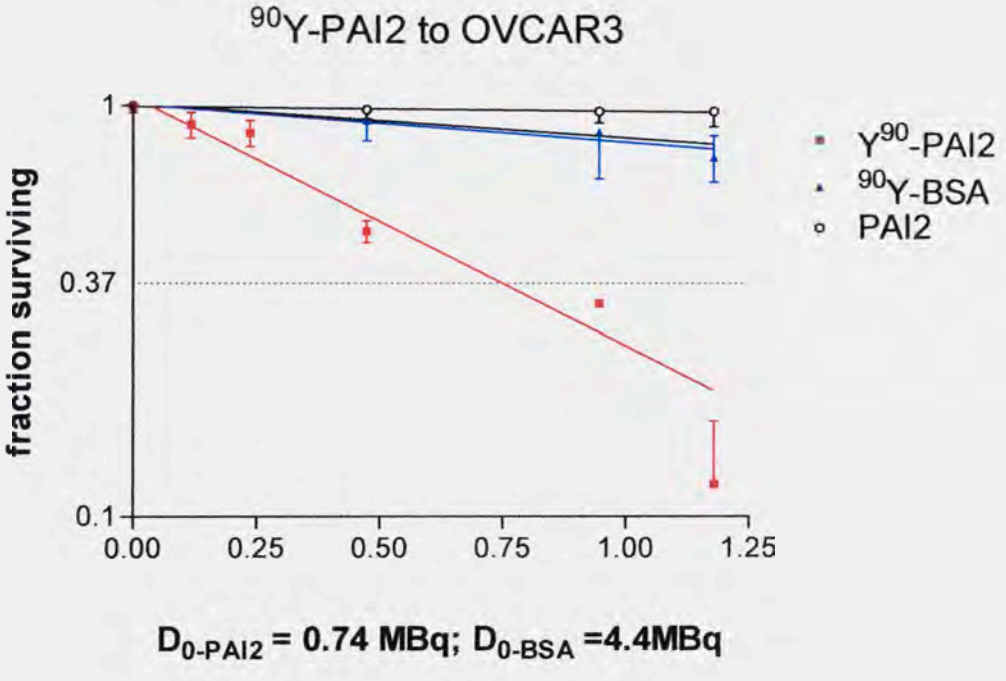

Figure 3-7 Cytotoxicity study of OVCAR3 cells following incubation for 24 h with ^{90}Y-PAI2. D_0 value is 0.74 MBq (the activity 37% cell surviving)

3.2.3 Morphological changes: Monolayer cells

After treatment with ^{213}Bi-PAI2, the treated cells in 24 well plates showed typical apoptotic morphology, *i.e.*, cells became rounded, shrunken and detached, whereas cells incubated with CCs (Cold control mix), free ^{213}Bi showed similar morphological patterns with untreated cells. Representative morphological changes are shown in Figure 3-8. ^{213}Bi-PAI2 incubation of monolayer cells at 24 h gave 30 ± 4% of apoptosis cells and ~10% necrosis cells by Diff-Quik staining (Figure 3-8). After 72 h of treatment, the percentage of apoptosis cells increased to 68 ± 7% for ^{213}Bi-PAI2.

Figure 3-8 Morphological changes after ACs treatment

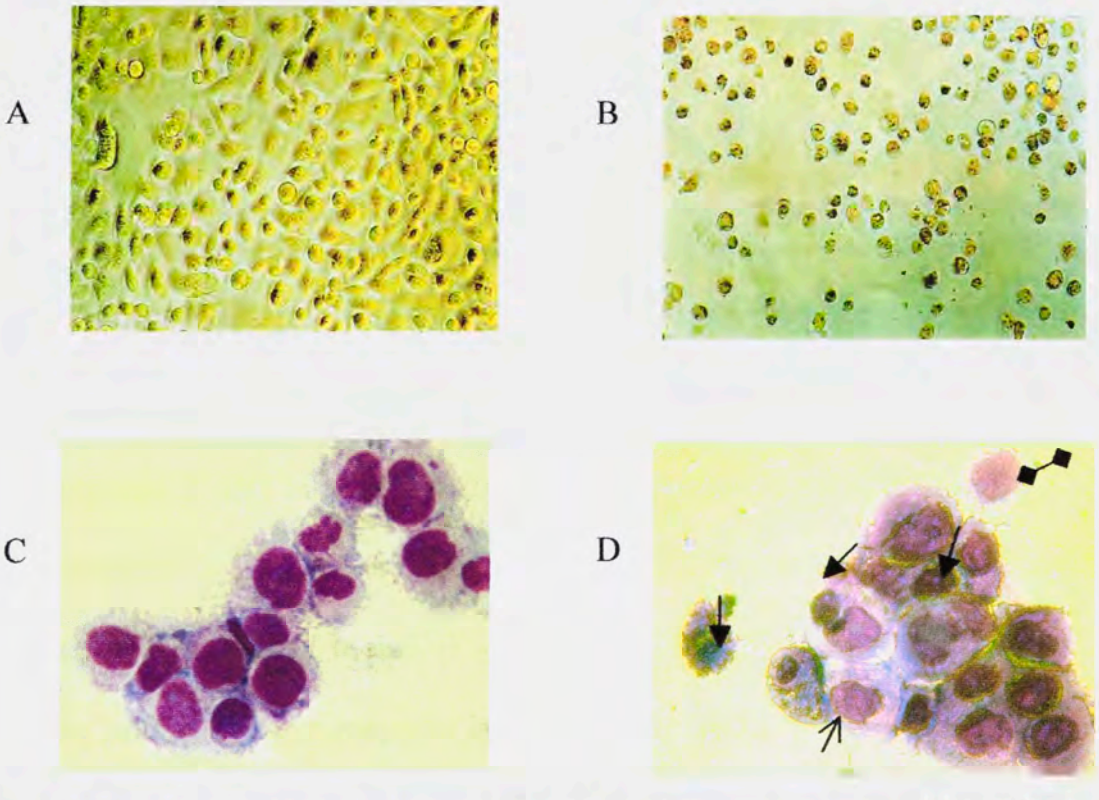

Figure 3-8 Morphological changes in OVCAR-3 monolayer treated with ^{213}Bi-PAI2(B) and untreated (A). Photographs were at x 400 magnification. Morphological changes of treated (D) and untreated (C) cells were confirmed using Diff- Quik staining. (▲)Arrow indicates apoptosis cells; (↑) Arrow indicates necrosis cells; (↔) Arrow indicates living cells. Photographs were at x 1000 magnification.

3.2.4 Morphological changes: Spheroids

The 80 and 150 μm spheroids of OVCAR3 partially disaggregated post-treatment with ^{213}Bi-PAI2 (Figure 3-9). There were no significant differences in the percentage of apoptosis cells (80 ± 7% and 11 ± 10%) between 80 and 150 μm spheroids. Cell colony formation was not observed for ^{213}Bi-PAI2 incubation, while many cell colonies formed in all other plates after 2 weeks. Thus complete cell kill was observed for the targeted ACs.

Figure 3-9 Spheroids morphological changes after ACs treatment

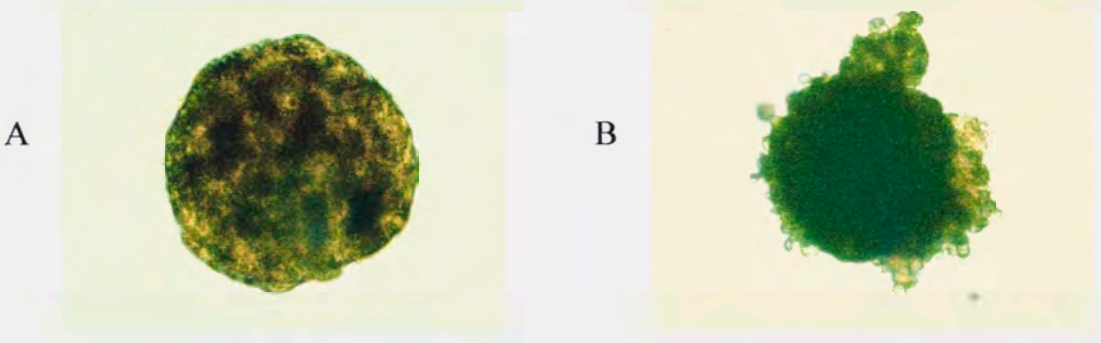

Figure 3-9 Morphological changes in OVCAR-3 cell spheroids (150 μm) before treated with ^{213}Bi-PAI2 (A) and after treated (B). Photographs were at x 100 magnification.

3.2.5 TUNEL assay

The exposed 3'-OH ends of DNA fragments generated by apoptotic DNA cleavage were detected by TUNEL assay, in which the non-apoptotic cells stained green while apoptotic cells stained brown (Figure 3-10). The results confirmed the Quik-Diff staining results. The percentage of apoptosis (68 ± 7%) and necrosis cells (11 ± 10%) at 72 hours post treatment were counted.

Figure 3-10 TUNEL assay

A

B

Figure 3-10 Picture A represented the positive blown staining cells, while picture B represented the negative control cells. Magnification was at x100.

3.3 Animal model development

3.3.1 Subcutaneous model

After 2 x 10^6 OVCAR3 cells inoculation (paragraph 3.3.2.1), the tumor uptake rate was 100% after 2 weeks. Once tumor size reached 10 mm in diameter, tumor was excited and prepared for ascites model development.

After 1 x 10^7 SKOV3 cells inoculation, the tumor uptake rate was only 50% after 4 weeks.

Figure 3-11 Subcutaneous model

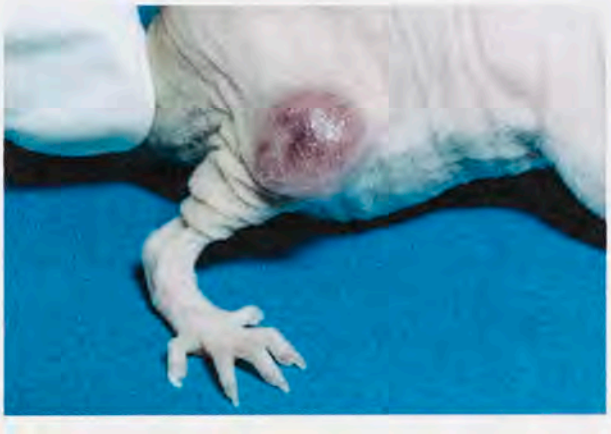

Figure 3-11 SKOV3 cell line subcutaneous models developed in nude mouse frank.

3.3.2 Ascites model

Balb/c nude mice all developed ascites after 9 days of i.p cell inoculation. To evaluate the size of cell clusters at day 9, 0.9% saline was used to wash the peritoneal cavity, and cell cluster collected and observed under microscopy. The cells in cluster were loose contact, and the size of clusters was less than 80 μm in diameter. This is an ideal model for targeted alpha therapy. In this model, cancer cells presented in forms of isolated or small clusters. ACs can be directed delivered to the cancer cell sites without penetration problems encountered in solid tumors. A represented picture is shown in Figure 3-12.

Figure 3-12 Ascites model

Figure 3-12 The upper mouse is normal, while the lower mouse has the developed ascites.

3.4 In vivo

3.4.1 Treatment efficacy

The median survival was 50, 40, 41.5, 24, and 25 days for 710 MBq/kg of ^{213}Bi-PAI2, 355 MBq/kg of ^{90}Y-PAI2, 355 MBq/kg of ^{213}Bi-PAI2 followed by 185 MBq/kg of of ^{90}Y-PAI2, cold control and control groups (paragraph 3.3.3.2), respectively. There was no significant difference between mice that received 710 MBq/kg of ^{213}Bi-PAI2, 355 MBq/kg of ^{90}Y-PAI2, and 355 MBq/kg of ^{213}Bi-PAI2 followed by 185 MBq/kg of of ^{90}Y-PAI2 ($P > 0.05$). There was no significant difference between two control groups ($P = 0.67$). However, significant differences were found between ^{213}Bi-PAI2 with control groups ($P< 0.01$). No significant differences were found between ^{90}Y-PAI2 and control groups ($P > 0.05$). Detailed P values were listed in Table 3-3.

Table 3-3 Significance table

	^{90}Y	^{213}Bi+^{90}Y	CC	C
P related to ^{213}Bi (95% CI of ration)	0.25 (1.05-1.45) ns	0.27 (0.98-1.43) ns	0.007 (1.86-2.3) **	0.007 (1.76- 2.24) **
P related to ^{90}Y(95% CI of ration)	-	0.8 (0.74-1.18) ns	0.08 (1.44-1.9) ns	0.05 (1.36-1.8) ns
P related to ^{213}Bi + ^{90}Y(95% CI of ration)	-	-	0.03 (1.48-2.0) *	0.02 (1.4 -2.0) *
P related to CC(95% CI of ration(95% CI of ration)	-	-	-	0.67 (0.69-1.23) ns

Note: CC cold control mix; C: without any treatment. CI: confidence interval. P value summary: * statistic difference; ** significant difference; ns: no significant difference.

Figure 3-13 Treatment efficacy of ^{90}Y-PAI2 and ^{213}Bi-PAI2

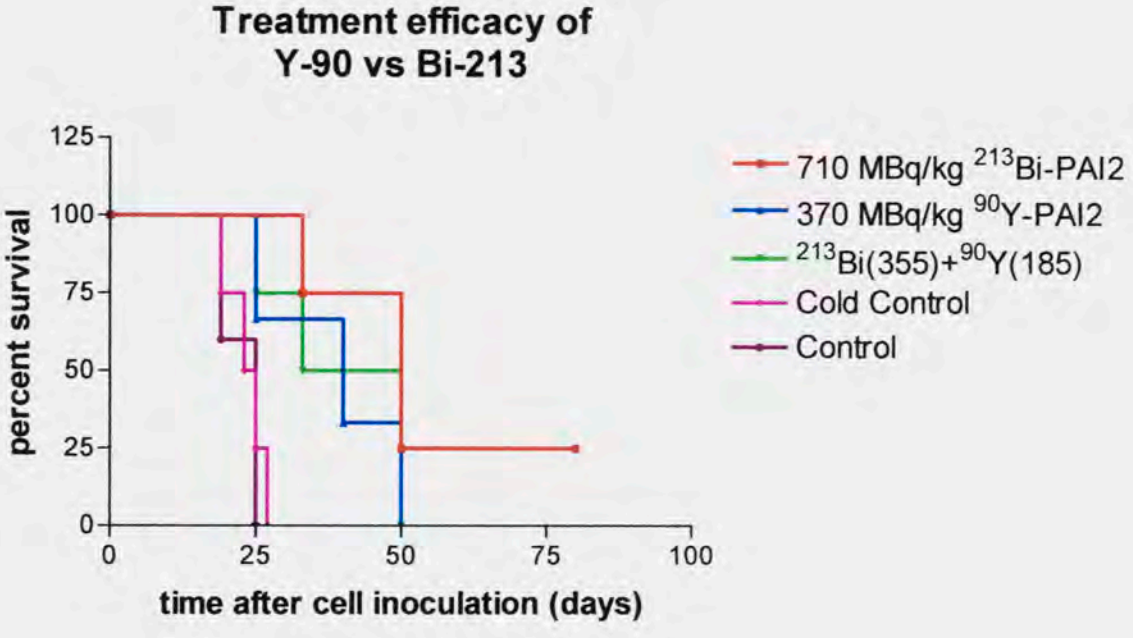

Figure 3-13 Kaplan-Meier survival curve indicate the percentage of survival.

3.4.2 Acute toxicity of ^{213}Bi-PAI2 in animal

Mice: Toxicity after i.p injection of 947 - 1420 MBq/kg ^{213}Bi-PAI2 (CHX-A"-DTPA as a chelator) was measured as leukocyte depression in peripheral blood at 2 (mean 2.6 ± 0.6 x 10^9 /L) and 7 days (mean 5 ± 0.4 x 10^9/L) post-injection, with leukocyte recovery occurring at 2 weeks (normal range 6-15 x10^9/L). Those mice found to be well after the injection experienced increasing body weight to 100 days (Figure 4). Haematology was normal at 100 days, but dose-dependent reduction in renal function was found, manifesting as mild to moderate increase in blood urea nitrogen (mean 7.8 mmol/L SD 2.2 mmol/L; normal range 1.7-5.3 mmol/L). The histopathologic changes corresponded with the decline in renal function. The kidneys showed patchy tubular nephrosis. Affected tubules are lined by a markedly attenuated epithelium with occasional

regenerative megaloblastic cells present. The affected tubules contain proteinaceous fluid.

Figure 3-14 Mice body weight changes post ^{213}Bi-PAI2 treatment

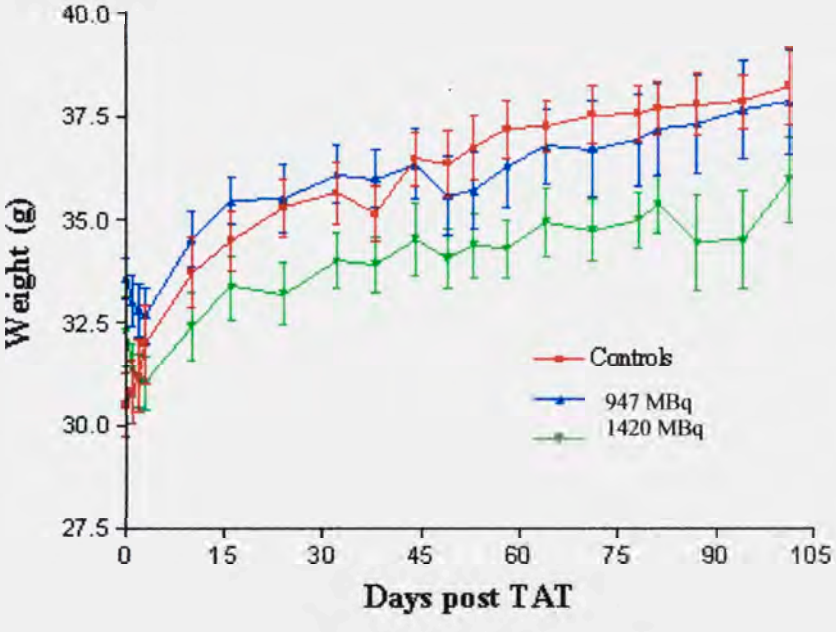

Figure 3-14 All mice in control and treated groups experienced body weight losses at first week of treatment, while mice were well up to 100 days.

Rabbits: The animals were monitored for 90 days post-^{213}Bi-PAI2 administration to observe any changes in weight, behaviour and eating/drinking abnormalities. Rabbits that received the lowest activity of 60 MBq/kg experienced weight gain similar to the controls, whereas weight gain was the slowest in the rabbits that received the highest activity of 355 MBq/kg (Figure 3-15). Histopathology revealed that all organs in all rabbits, except for the kidneys, were free of any radiation damage. The kidneys showed mild and patchy tubular necrosis for 60 and 120 MBq/kg rabbits, while for 355 MBq/kg rabbits moderate to severe and widespread renal tubular necrosis with a compensatory expansion of interstitial tissue, which appeared to be largely due to oedema rather than true fibrosis, although there was an apparent increase in fibrous tissue due to loss and

collapse of tubules (Figure 3-16). The activity of 355 MBq/kg was thus considered toxic as it was certainly at or above the MTD. Since 120 MBq/kg is safe and 355 MBq/kg is toxic, the toxic activity low (TDL) is ≥ 120 MBq/kg in rabbits.

Figure 3-15 Rabbits body weight change after TAT

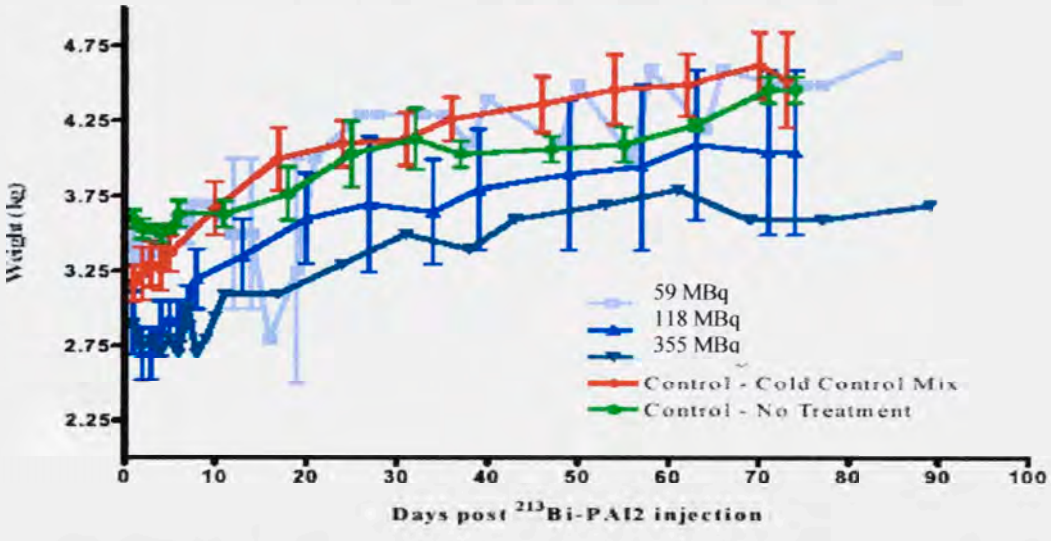

Figure 3-15 Rabbits that received the lowest activity of 60 MBq/kg experienced weight gain similar to the controls, whereas weight gain was the slowest in the rabbits that received the highest activity of 355 MBq/kg.

Figure 3-16 Kidney acute pathological changes

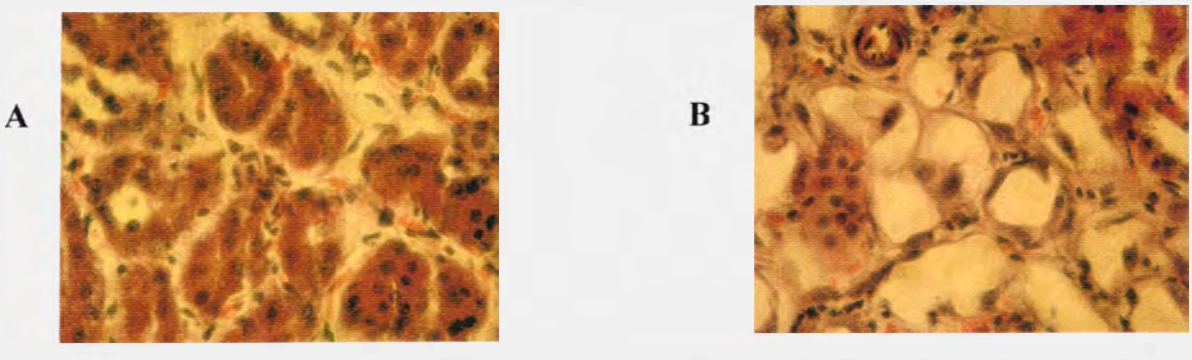

Figure 3-16 Evidence of severe and widespread renal tubular necrosis in rabbit. The normal renal structure (A) can be compared with radiation necrosis (B) caused by 350 MBq/kg of ^{213}Bi-PAI2 at 13 weeks post-injection. HE staining with magnification of x 1000.

Haematology and biochemistry revealed that all rabbits, except for 355 MBq/kg, were free of any radiation damage. One rabbit at 355 MBq/kg showed anaemia, with haemoglobin 95 g/L (103-155 g/L), and kidney function disorder with urea 11.4 mmol/L (3.3-8.1 mmol/L) at 90 days.

3.4.3 Delayed toxicity of ^{213}Bi-PAI2 in mice

Mice were monitored over a period of 40 weeks. Delayed radiation damage at 20 weeks post-treatment was found to affect those mice that received 350 to 830 MBq/kg, regardless of lysine application. All mice lost body weight in a gradual and continuous manner up to 30 weeks and reached the endpoint, except for 350 MBq/kg group of mice which recovered from weight loss, and started to gain body weight at 32 weeks (Figure 3-17). The maximum tolerance dose (MTD) was 350 MBq/kg using body weight loss as the parameter to assess MTD. The body weight changes were significantly different between control mice and all treated mice ($P < 0.001$). There was no significant difference in body weight between the "with" and "without" lysine groups at 590 MBq/kg ($P > 0.05$).

Figure 3-17 Bi-PAI2 long term toxicity

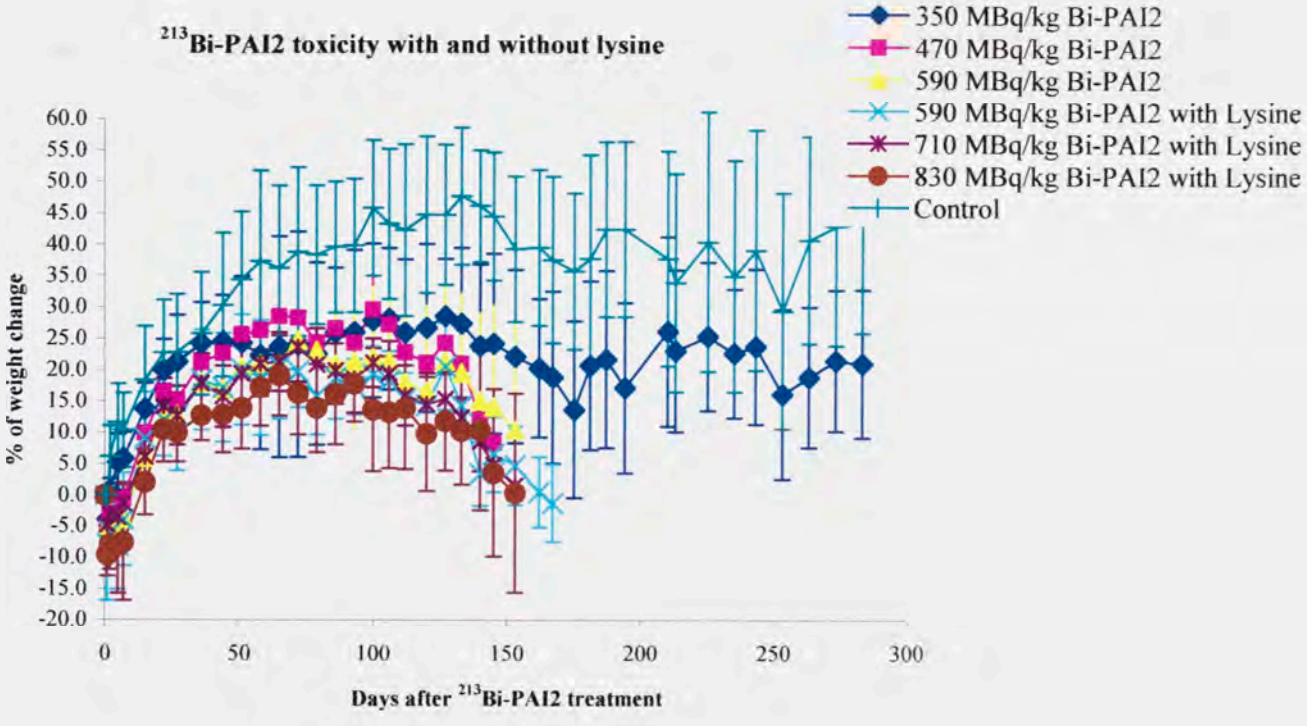

Figure 3-17 Delayed toxicity in mice. Only the 350 MBq/kg group continued to grow; all mice at higher activities showed weight loss at 20-25 weeks up to termination.

The survival rates of experimental mice in different groups are shown in Figure 3-18. The median time to end point after ^{213}Bi-PAI2 injection was 175 days for the 470 MBq/kg group without lysine, 590 MBq/kg and 710 MBq/kg with lysine groups, and 162 days for 590 MBq/kg without lysine group and 830 MBq/kg with lysine group ($P > 0.05$). One mouse was withdrawn in the 350 MBq/kg group and one in the control group due to reasons unrelated to treatment.

Figure 3-18 Mice survival- ^{213}Bi-PAI2

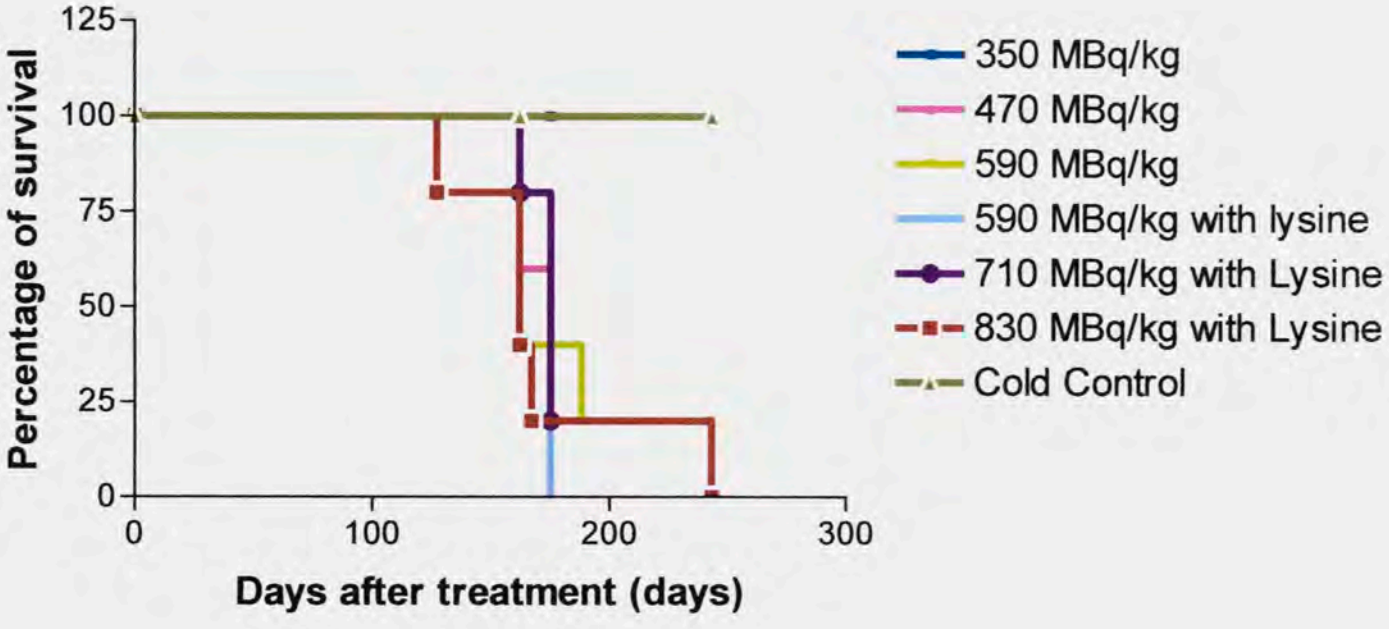

Time to endpoint for mice treated with and w/o lysine. No significant difference was found for survival for 590 MBq/kg of ^{213}Bi-PAI2 with and w/o lysine.

While haematology was normal at the end-point, reduction in renal function was found, manifested by a major increase in blood urea nitrogen (45 –80 mmol/L, normal range 2.1-3.5 mmol/L).

Histopathological examination revealed kidney damage in these mice. Evidence of radiation nephropathy was found in all treated mice (Figure 3-19). Graph **A** shows a typical stain for normal kidneys, whereas graph **B** shows radiation nephropathy at 20-30 weeks post-injection. Mice in all irradiated groups had radiation nephropathy with characteristic degeneration and regenerative changes in tubular epithelium at 20- 30 weeks. There was ionising radiation injury to tubules, glomeruli and blood vessels. The severity ratings of the radiation nephropathy were mild for 350 MBq/kg and 470

MBq/kg, moderate for 590 MBq/kg with and w/o lysine; and for 710 MBq/kg and 830 MBq/kg group with lysine.

Figure 3-19 Mouse kidney pathology changes- ^{213}Bi-PAI2

A

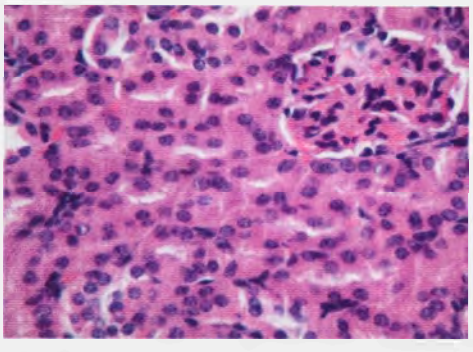

B

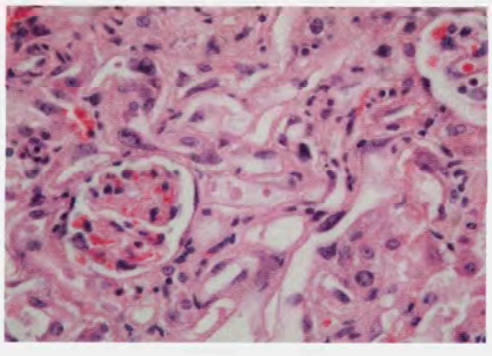

Figure 3-19 Evidence of delayed renal nephritis in mice at 590 MBq/kg. Normal renal structure (A) is compared with radiation nephrosis (B) caused by ^{213}Bi-PAI2 at 25 weeks post-therapy. HE staining with magnification of x1000.

The renal changes were concentrated in the cortex, proximal convoluted tubules being most severely affected. There was a significant glomerular component and slow evidence of vascular injury. There was multifocal necrosis, sloughing and mineralization of tubular epithelium associated with neutrophilic infiltration together with intraluminal haemorrhage, proteinaceous and cellular casts, and cystic tubular dilation. Tubular epithelium also had distinctive dysplastic regenerative activity featuring karyomegaly. The tubular lesions were most severe in subcapsular locations with tubular loss, mixed leucocytic infiltration, fibrous scarring and irregular capture contraction. There were also distinctive glomerular lesions. Glomerular tufts had cellular karyomegaly, hypercellular, sequestration of neutrophils, tuft swelling with capsular adhesions, hypertrophy of Bowman's capsular epithelium and crescent

formation. Cystic dilation of Bowman's spaces was evident. More severe glomerular changes were represented by tufts with reduced cellularity, separation of cells from basement membranes, haemorrhage and leucocytic infiltration with progression to collapse. Hypertrophy of glomerular afferent arterioles and fibrinoid necrosis of larger cortical arterioles were also observed.

3.4.4 Pharmacokinetics studies

3.4.4.1 Gamma counter vs dose calibrator

The eluent was diluted and counted in the dose calibrator and gamma counter to obtain activity in μCi and CPM. Plot CPM in function of dose activity. The results in Figure 3-20 shows the non-linear regression relationship of data (A), and the linear relationship for activities below 0.5 MBq (Figure 3-20A and B).

Figure 3-20 Normalisation of dose calibrator and gamma counter

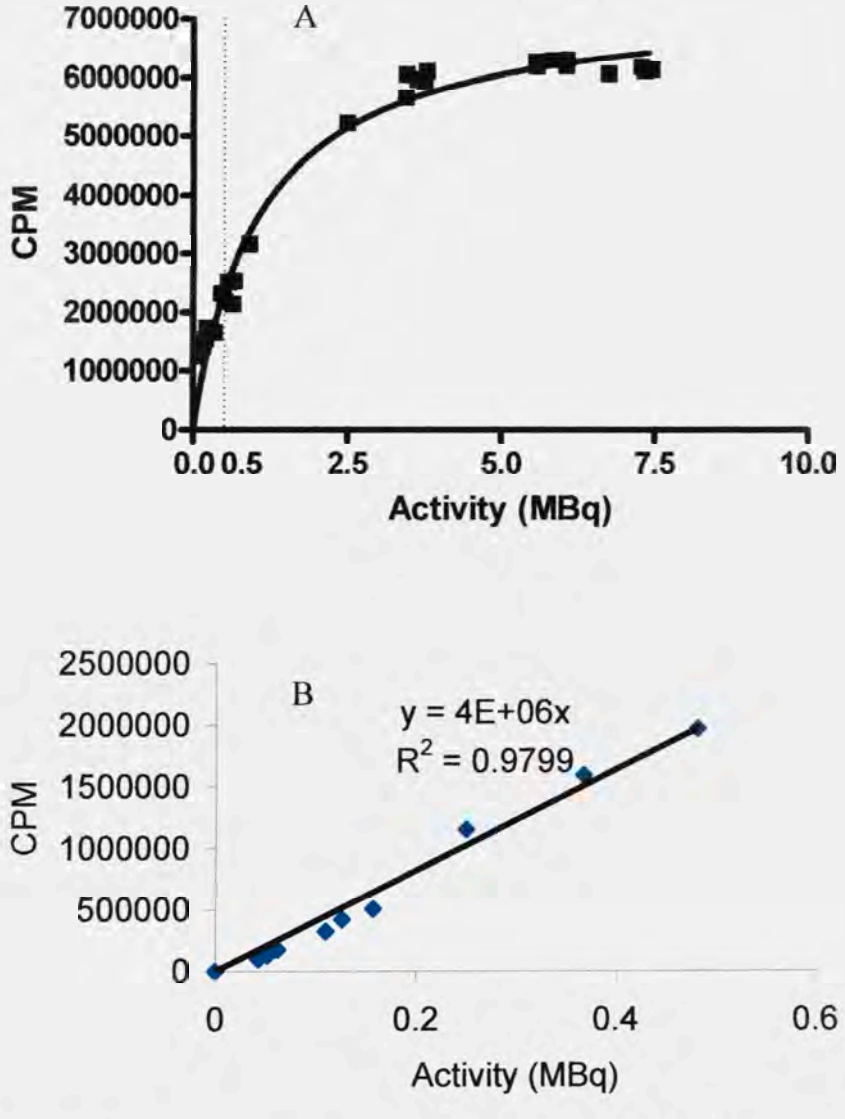

Figure 3-20 Non-linear regression relationship of CPM and activity (A), while liner relationship under 0.5 MBq.

3.4.4.2 Pharmacokinetic studies with pre-injected lysine

The concentration of ^{213}Bi-cDTPA-PAI2 in blood, spleen, liver, lung, heart, bone and kidney was similar with and without lysine application ($P>0.05$). Blood clearance, kidney uptake and accumulation at 4 hours post injection of ^{213}Bi-PAI2 are shown in Figure 3-21. The kidney was the major organ for activity uptake (Graphs A and B). The average kidney uptake with lysine application was reduced by ~50% up to 4 hours, but was not significantly different to the control data because of the large standard deviations ($P > 0.15$ for all time points). Graph C indicates the comparison of the kidney uptake with and without lysine.

Figure 3-21 Pharmacokinetic studies w/o lysine

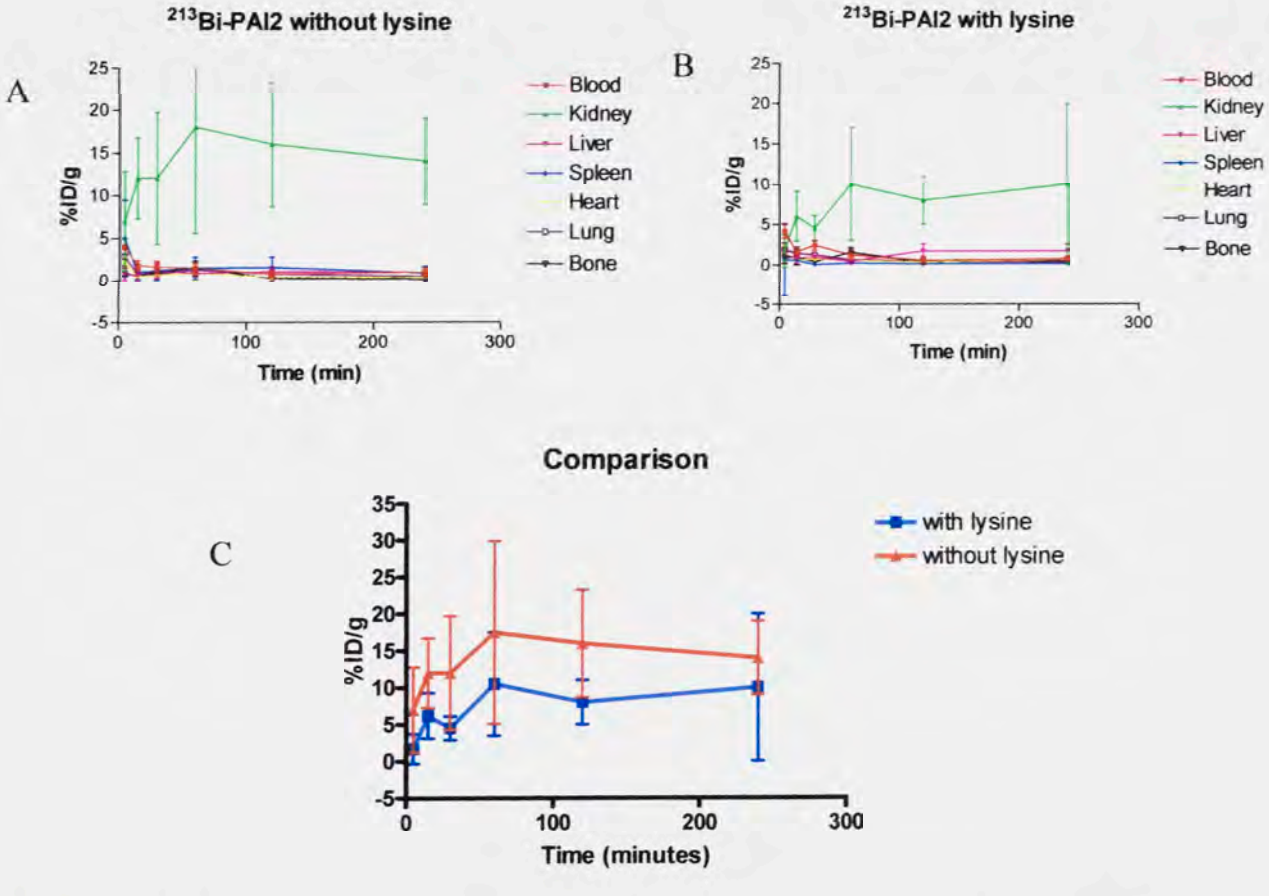

Figure 3-21 Pharmacokinetics of ^{213}Bi-PAI2 in nude mice w/o (A) and with (B) lysine application of 0.8mg/g lysine 15 minutes before i.p. injection of 3 MBq of ^{213}Bi-PAI2.

Values represent the mean %ID/g; bars, the SD. The comparison of the mean %ID/g of kidney uptake with and w/o lysine is shown in C.

3.4.4.3 Pharmacokinetic studies with chelators cDTPA and CHX-A"-DTPA

The activity of ^{213}Bi-cDTPA-PAI2 and ^{213}Bi-CHX-A"-DTPA-PAI2 ACs in the kidney was similar, with respective concentrations of 14.2 ± 2.8 and 15 ± 6.8 %ID/g at 2 hours (P = 0.85) and 11.7 ± 2.9 and 9.9 ± 4.1 %ID/g at 4 hours (P = 0.55) and. However, the activities in the liver were significantly different at 1 and 2 hours with activities of 2.7 ± 0.04 vs. 1.3 ± 0.3 (P = 0.046) and 1.9 ± 0.7 vs. 0.7 ± 0.2 (P = 0.001), respectively. There were no significant differences in lung, heart and spleen for the two chelators (P > 0.05). Figure 3-22 (A-D) shows the comparison of ^{213}Bi-cDTPA-PAI2 and ^{213}Bi-CHX-A"-DTPA-PAI2 activities in kidney, heart, lung, liver and spleen, respectively.

Figure 3-22 Chelators comparison

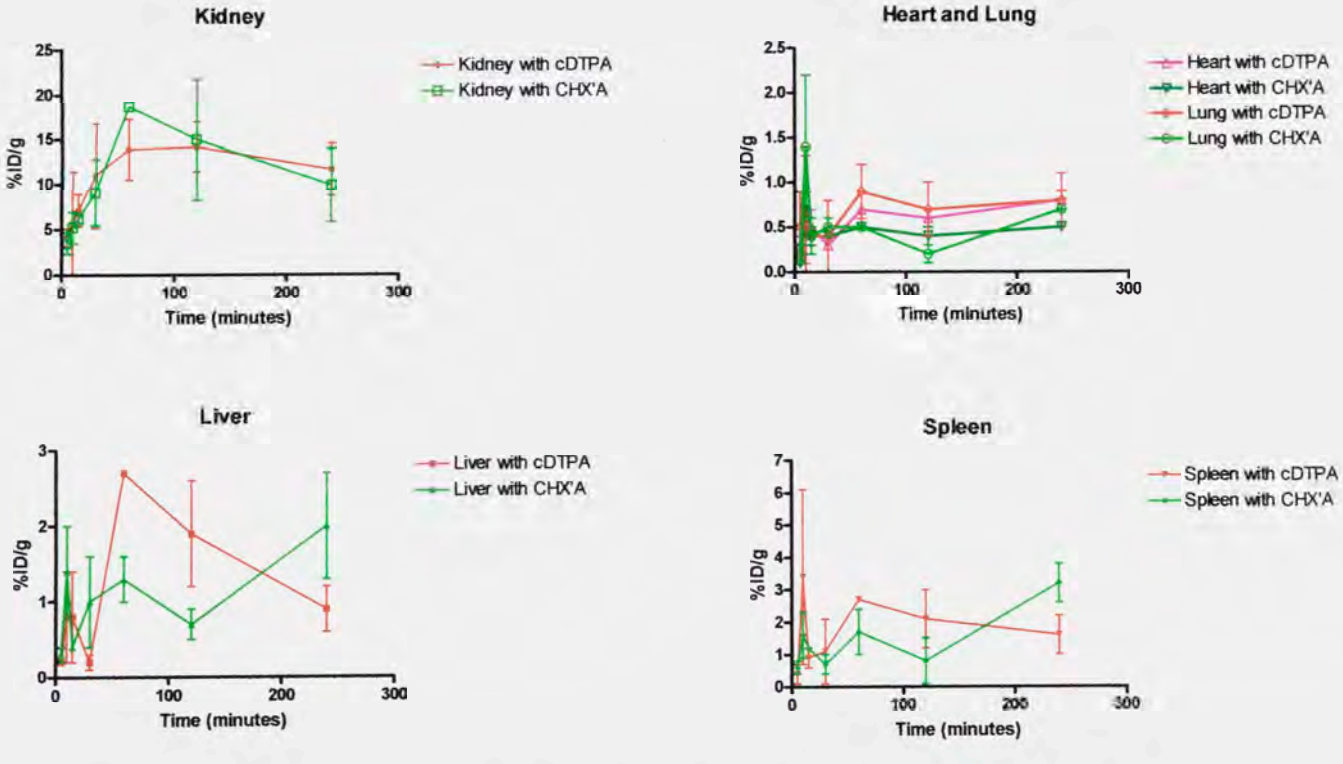

Figure 3-22 Pharmacokinetics of ^{213}Bi-PAI2 using the cDTPA or CHX-A"-DTPA chelaters in nude mice that received 3 MBq of ^{213}Bi-PAI2. Values represent the mean

%ID/g; bars, ±SD. The results show the kidney (A), heart and lung (B), liver (C) and spleen (D).

3.4.4.4 DTPA challenge

The activity of ^{213}Bi-CHX-A"-DTPA-PAI2 in the kidney with and without prior Ca-DTPA injection was similar, with respective concentrations of 12.7 ± 1.9 and 15.4 ± 5.1 at 30 minutes (P = 0.53), 22.6 ± 3 and 29.7 ± 5.8 (P = 0.62) at 60 minutes. However, the concentrations were significantly different at 15 minutes, with concentrations of 12.8 ± 0.2 and 21.3 ± 4.9 (P = 0.043) respectively. Ca-DTPA pre-treatment significantly prevented the renal accumulation of ^{213}Bi at 15 minutes. Activities of all other organs were not significantly different (P > 0.05). 40% of free Bismuth was cleared in urine at 15 minutes, and 80% at 60 minutes. Figure 3-23 (A-C) shows the %ID/g for different organs at 15, 30 and 60 minutes respectively.

Figure 3-23 DTPA challenge

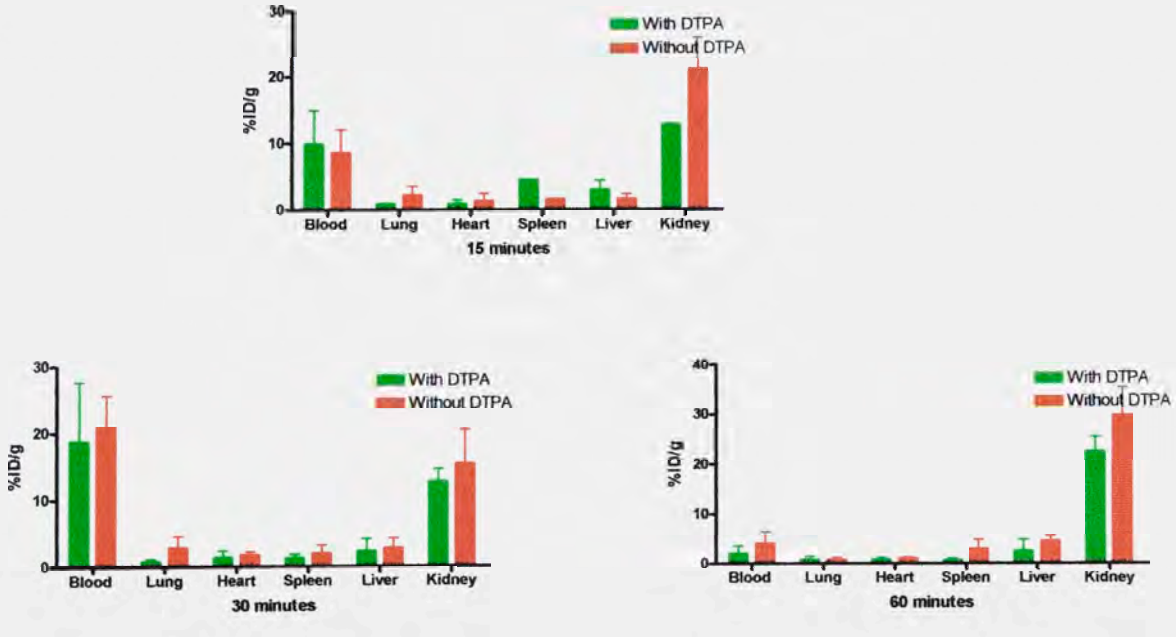

Figure 3-23 Pharmacokinetics of ^{213}Bi-PAI2 with and w/o Ca-DTPA challenge in nude mice prior to injection of 3 MBq of ^{213}Bi-PAI2. Values represent the mean %ID/g; bars, ±SD. The comparion of the mean %ID/g of kidney uptake is shown at post injection time 15 (A), 30 (B), and 60 minutes (C).

3.4.4.5 Kidney Dose

The radiation dose to the kidney was determined in mice injected i.p with ^{213}Bi-PAI2. Data are presented as mean kidney activity per gram (Bq/g) versus time (Figure 3-24). The kidney activity per gram was calculated from the percent initial injected dose per gram (data obtained from pharmacokinetic study without decay correction) multiply by injected activity. The kidney activities and absorbed doses are listed in Table 3-4.

Figure 3-24 Kidney dose

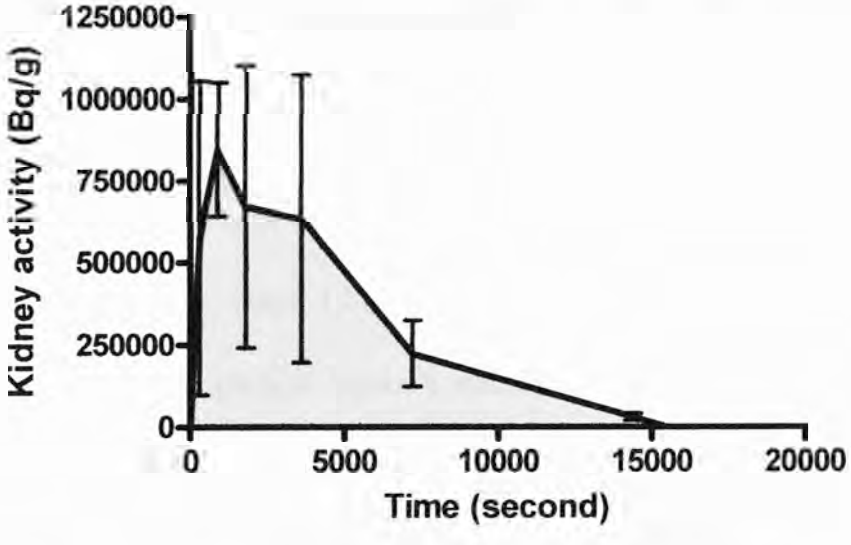

Figure 3-24 Kidney dose in nude mice after injection of ^{123}Bi-PAI2.

3.4.5 Discussion

Alpha particle based radioimmunotherapy has several advantages over β emitters. Alpha particles has higher linear energy transfer, shorter path length, and less non-specific cytotoxicity to bone marrow (Allen et al., 2004; Bethge et al., 2003). Elevated levels of the serine protease uPA, its receptor (uPAR), and inhibitor (PAI2), in tumour tissue emphasize their fundamental role in tumor invasion and metastasis and provide the rationale for this novel therapeutic strategy. The present system relies on the highly cytotoxic alpha emitting radioisotope ^{213}Bi coupled to PAI2 to kill uPA/uPAR positive cancer cells. PAI2 is a recombinant, human and internalizing protein, which can form stable complexes with uPA/uPAR. ^{213}Bi-PAI2 has shown cytotoxicity toward targeted cells (Allen et al., 2003; Li et al., 2002; Qu et al., 2005; Song et al., 2006). The high LET of the alpha particle means a much greater fraction of the total energy is deposited in cells and very few nuclear hits are required to kill a cell. Immunohistochemical and *in situ* hybridization studies have localised uPA and uPAR to various tumour and associated stromal cells [24]. The strongest and most consistent expression universally occurs in primary carcinoma tissue with high tumour grade, and in some cases has been further localised to cells at the invasive margins. For example, 79–90% (Dublin et al., 2000), and 100% (Christensen et al., 1996; Fisher et al., 2000) of invasive ductal carcinomas were positive for uPA antigen or mRNA, compared to 28–100% of non invasive cases (Christensen et al., 1996; Dublin et al., 2000; Fisher et al., 2000). In contrast, benign lesions such as fibroadenoma and normal breast tissue were either negative or with some occasional weak/diffuse staining for all markers in the majority

of studies that included such tissue for comparison. Clinical data from multiple, independent groups measuring activity and/or antigen levels in tumour extracts confirm a relationship between high levels of uPA in primary breast tumour (e.g.,>10 fold more than in normal breast (Schmitt et al., 1992), and a poor relapse-free, and/or overall survival (Andreasen et al., 1997; Ranson et al., 2002).

Our results have shown that uPA/uPAR has medium expression (++) in the OVCAR3, SKOV3 and BT474 cell lines, whereas OV90 cell has shown negative expression of uPA/uPAR. SKOV3 is metastatic ovarian cancer cell lines while OVCAR3 is a primary ovarian cancer cell line.

Ovarian cancer tissues in this study are obtained from stage I-II ovarian epithelial cancer patients which is in early stage. Only 47% of ovarian cancer positive for uPA antigen was in this study. This results is lower than other reports for advanced ovarian cancer (Kuhn et al., 1994).

OVCAR3, SKOV3 and BT474 mice tumor xenografts express uPA, indicating that cancer cells do not lose uPA expression from in vitro cell culture to in vivo animal model. uPA expression on OVCAR3 spheroids has also shown positive staining. Using Flow Cytometry and Confocal Microscopy, uPA/uPAR expressed on the surface of three cancer cell lines were confirmed, indicating that membrane-bound uPA is an effective tumor surface marker for targeting ovarian carcinoma.

The cytotoxicity of ^{213}Bi-PAI2 for ovarian cancer cells in vitro proved to be receptor-specific, receptor-intensity and activity dependent. Compared with the non-specific control, ^{213}Bi-PAI2 exhibits high levels of receptor-selective cytotoxicity, requiring very low activity (D_0 = 0.36-0.53 MBq/300mL) to kill high cell concentrations (2 x10^4 cells/300 μL) for three cell lines, whereas the D_0 value for the non-specific control (^{213}Bi-BSA) and Free ^{213}Bi was found to be12 - 16 times higher for uPA positive cells.

SKOV3 cells were found to have the lowest D_0 value, compared to OVCAR3 and BT474. ^{213}Bi-PAI2 caused the morphological changes of OVCAR3 spheroids, as well as reduced the cell apoptosis. Therefore, it is clear that ^{213}Bi-PAI2 is an effective and specific radiolabeled agent for monolayer and spheroid cultured cells in vitro.

The predominant mechanism by which radiation kills mammalian cells is the reproductive (or clonogenic) death pathway. DNA is the target, and double-stranded breaks in the DNA are regarded as the specific lesions that initiate this lethal response (Harms-Ringdahl et al., 1996; Pluschke et al., 1996). Because of very high LET (~100 keV μm^{-1}) of α-particles, cells have a limited ability to repair the damage to DNA (Nikula et al., 1999), or repair incorrectly induces cell death pathway (Friedberg et al., 1995). Macklis *et al* (Macklis et al., 1992) reported that α-particles might kill cells by apoptotic mechanisms, a result that has been confirmed by this group for several different cancers (Allen et al., 2004). In the present study, we demonstrated that ^{213}Bi-PAI2 induces a high fraction of TUNEL positive cancer cells compared with control cells. These results indicate that the lethal pathway of ovarian cancer cells *in vitro* after α-PAI2 treatment is predominantly through apoptosis.

The therapy experiments carried out *in vivo* were designed to evaluate the anticancer activity of ^{213}Bi-PAI2 after administration at 9 days post-cell inoculation (ascites model) and to optimise the dosage regimen. The ascites animal model can mimic the clinical condition because ovarian cancer metastasises via peritoneal spread.

Our findings indicate that a single i.p injection of ^{213}Bi-PAI2 at a activity of 710 MBq/kg can prolong survival by 25 days compare to untreated group. Growth inhibition of tumours and metastases was found to be similar with an activity of 710 MBq/kg of ^{213}Bi-PAI2, 355 MBq/kg of ^{90}Y-PAI2 and the combination of these two vectors. There was no significant difference between single radiation treatment and combination

treatment. Non- synergic effect was observed with the combination of two different radioisotopes for ascites model. ^{213}Bi-PAI2 can control tumorigenesis through intraperitoneal administration of ^{213}Bi-PAI2.

These preclinical studies with ^{213}Bi-PAI2 have generated optimism for their potential human clinical use (Qu et al., 2005). Kidneys were found to be the n limiting organ in our studies, as ^{213}Bi (Slikkerveer et al., 1992) and small molecules such as PAI2 tend to accumulate preferentially in the kidneys.

CDTPA (Li et al., 2004) and CHX-A"-DTPA(Seidl et al., 2005) are the chelators mostly used in bismuth-based radioimmunotherapy. The CHX-A"-DTPA conjugate has been reported to be more suitable when radio-metallo-nuclides are coupled to a MAb (Milenic et al., 2001; Roselli et al., 1999). Both cDTPA and CHXA"-DTPA, coupled to PAI2, were investigated in this study. We found that there was no significant difference up to 4 hours (5 half-lives of ^{213}Bi) in terms of kidney accumulation between the two chelators. However, CHX-A"-DTPA gave a lower liver uptake up to 2.5 half-lives, and could be the better choice for patients with liver disease. We conclude that cDTPA-PAI2 and CHX-A"-DTPA-PAI2 have similar renal pharmacokinetics.

Meso-2,3-dimercaptosuccinic acid (DMSA) and D,L-2,3-dimercapto-propane-I-sulfonic acid (DMPS) are known to chelate and enhance the urinary excretion of bismuth, having been tested for bismuth poisoning and kidney protection (Jaggi et al., 2005a; Slikkerveer et al., 1992). We tested two pharmacologic approaches in preventing the renal accumulation of ^{213}Bi. Ca-DTPA has been used worldwide as a standard chelating agent for plutonium and other transuranic elements involved in internal contamination. No significant difference was found at 30 and 60 minutes after Ca-DTPA injection, possibly because of the high stability of ^{213}Bi-PAI2 conjugates, producing limited

numbers of free ^{213}Bi atoms at 30 and 60 minutes. DTPA challenge tests at 6, 24 and 72 hours showed a reduction in renal ^{213}Bi after injection of the parent ^{225}Ac by reacting with free ^{213}Bi and thus increasing renal clearance (Jaggi et al., 2005a). The differences of %ID/g of kidney uptake may reflect the stability of ^{213}Bi-PAI2 in vivo as well. In a previous study we have shown that the *in vitro* serum stability of ^{213}Bi-PAI2 was more than 90% at one half-life (Ranson et al., 2002). The findings from this study suggest that the *in vivo* stability of ^{213}Bi-PAI2 at 60 minutes was 76%.

Administration of cationic amino acids results in a substantial increase in the MTD of Fab fragments, and biochemical or histological evidence of renal damage has not been observed under these conditions (Mogensen & Solling, 1977). Substances with a positively charged group located terminally in the molecule (ornithine, lysine, arginine, and the almost not metabolized epsilon-amino-caproic acid, and cyclocaprone) proved to instantaneously inhibit the tubular protein re-absorption. Lysine was found to be the most effective molecule tested (Mogensen & Solling, 1977). Bismuth is both filtered as well as secreted (Russ et al., 1975). It is believed that ionized bismuth (Bi^{3+}) is bound to the plasma proteins and forms a slow-clearing compartment. We attempted to reduce the reabsorption of ^{213}Bi-PAI2 on tubular sites by the use of lysine. While there was a 50% average reduction of kidney activity, this was not significant because of the large standard deviation. The absence of a significant enhancement of ^{213}Bi excretion may be due to the small sample size (4 mice in each group) and lysine application being insufficient. To confirm this result, a long-term toxicity study with and without lysine application was performed. However, mice that received 0.8 mg/g lysine 5 minutes prior to ^{213}Bi-PAI2 injection did not show any improvement in survival at 590 MBq/kg compared to control mice. Thus the effect of lysine in this study did not translate into an increased survival. This is in contrast to the results of other investigators (Behr &

Boerman, 1999), where the MTD increased significantly for bismuth labelled antibody fragments after lysine application.

The 13 week short term toxicity study showed that the MTD for weight loss was up to 1420 MBq/kg for nude mice and 120 MBq/kg for rabbits (Rizvi et al., 2006). Analysis of haematological parameters in mice did not show any abnormalities at 1420 MBq/kg. Dose-dependent reduction in renal function was manifested as mild to moderate increase in blood urea nitrogen. The histopathological changes were consistent with the decline in renal function as the kidneys showed patchy tubular nephrosis. These results suggest that the damage to the kidneys was insufficient to reduce function, so symptoms and signs of renal failure did not occur as the mice continued to grow normally by this stage. However, mild to severe renal tubular necrosis was found in treated rabbits in a dose-dependent fashion. One rabbit with an activity of 350 MBq/kg at 13 weeks post-treatment experienced renal function disorder and severe renal tubular necrosis accompanied by anaemia, which may have resulted from renal function failure.

The long-term toxicity studies showed that the mice that were asymptomatic at 13 weeks became symptomatic after 20 weeks and this was manifested by a gradual and continued reduction in their body weight. Most mice reached the end point by 30 weeks, except for mice in the 350 MBq/kg group which recovered after 32 weeks. MTD was 355 MBq/kg. These findings suggest that the ^{213}Bi induced loss of tubular epithelial cells triggers a chain of adaptive changes that results in progressive renal parenchymal damage accompanied by a loss of renal function. There was a linear progression in severity of the renal lesions with increasing radiation activity. The renal changes were concentrated in the cortex, proximal convoluted tubules being most severely affected.

The kidneys can filter ~50% of 30 kD proteins, decreasing to 0.5% for 69 kD proteins (Guyton, 1991). Consequently, free bismuth and about 20 % of ^{213}Bi-PAI2 (47 kD) can be filtered through glomeruli into Bowman's capsule. Protein is completely or almost completely reabsorbed by active processes through the brush boarder of the proximal tubular epithelium by pinocytosis, which means that the protein attaches itself to the membrane, and this portion of membrane then invaginates to the interior of the cell.

Lysine did not cause any significant change with respect to long-term radiation damage in kidneys. Dose-dependent reduction in renal function was observed and was manifested by increased blood urea nitrogen. Once the kidneys lacked an innate ability to maintain function, mice started to rapidly lose body weight, taking 1-2 weeks to reach the end-time point for the 470 MBq/kg and 830 MBq/kg groups. However, mice in 350 MBq/kg group experienced only a slight body weight loss, and then started to regain body weight, suggesting that mice recovered by tubular epithelium regeneration. These findings are consistent with Jaggi et al (Jaggi et al., 2005b).

Measured thresholds for radiation nephrosis are summarised in Table 3-4, ranging from 470 to 590 MBq/kg for different targeting vectors. Our results show that ^{213}Bi-PAI2 has a low threshold of 470 MBq/kg, which is compatible to ^{213}Bi alpha conjugates for small molecular weight proteins. The absorbed dose is calculated to be 11.5 Gy (MIRD), the corresponding RBE dose is 37 Gy, based on the following assumptions: RBE = 4 for alpha radiation (Back et al., 2005), and absorbed radiation fraction by the kidney for alpha and beta radiation is 1 (100%) This threshold dose is substantially lower than the doses for the beta-emitters Y-90 and In-111. ^{90}Y-Fab induced chronic nephropathy occurs at ≥80 Gy (Behr et al., 1997).

Table 3-4 Thresholds for chronic radiation nephropathy

	Radiation nephropathy activity (MBq/kg)	Kidney absorbed dose (Gy)	RBE.Gy **
^{213}Bi-PAI2	470	11.5	37
^{213}Bi-DOTA-biotin[1]	460*	-	-
^{213}Bi-Fab'[2]	500*	-	-
^{213}Bi-DOTATOC[3]	570*	-	-
^{90}Y-Fab'[4]	462.5*	80-100	80-100
External beam[5]		23	23

[1] (Yao et al., 2004); [2] (Behr & Boerman, 1999); [3] (Norenberg et al., 2006); [4](Behr et al., 1997); [5] (Pearse, 1994). *assuming 20 g mice. **RBE = 4 assumed for ^{213}Bi.

If the inter-species scaling between mice, rabbits and man applies (Boxenbaum, 1984; Sparks, 1999), then the mouse MTD of 350 MBq/kg translates to ~120 MBq/kg for rabbits and ~40 MBq/kg for man.

3.4.6 Conclusion

The *in vitro* conclusions support our *in vivo* results. All of these findings indicate that ^{213}Bi-PAI2 can target and kill cancer cells at the micrometastatic stage, i.e. cells in transit or at the pre-angiogenic stage. The activity limiting toxicity for ^{213}Bi-PAI2 was nephropathy caused by Bismuth accumulation in the kidney. However, the kidney dose limit for ^{213}Bi-PAI2 was not higher than other small molecular weight targeting vectors.

Chapter 4

Preclinical studies of ^{213}Bi-C595 Results & Discussion

Introduction

Radiolabeled antibodies have been used with some success in different cancers.(Behr et al., 2002) Alpha-particle therapy (TAT) has been proposed for use in single-cell disorders such as leukemia and micrometastases of carcinomas, in which rapid targeting to cancer cells is possible (Allen & Blagojevic, 1997; Allen, 1999; Jurcic et al., 2002; Kennel et al., 1999; Li et al., 2002; McDevitt et al., 1998). TAT offers the potential to inhibit the growth of micrometastases by selectively targeting markers and killing isolated and preangiogenic clusters of cancer cells.

MUC1 is a well-documented example of marker that influences pathophysiological behaviour. High molecular weight glycoproteins, described as mucins or mucin-like glycoproteins, are frequently found associated with breast carcinoma and other epithelial cell adenocarcinomas (Zotter et al., 1988). Cancer associated MUC1 is structurally different from normal MUC1 in that the former has shorter and less dense *O*-glycan chains, exposing novel regions of the protein core. MAb C595 (also known as NCRC48) is reactive with the protein core of MUC1 mucin. ^{213}Bi is chelated to the monoclonal antibody (MAb) C595 to form the alpha conjugate. Epithelial cancers often overexpress MUC1, and the overexpression is associated with poor survival (Baruch et al., 1999).

In this chapter, MUC1 expression on human primary and metastasis ovarian tumours and ovarian cancer cell lines using MAb C595 is demonstrated. An anti-cancer effect of ^{213}Bi-C595 against human ovarian cells *in vitro* is also evaluated. Multiple cell spheroids are used as an in vitro model of micrometastases of ovarian cancer, and the MUC1 expression in spheroids is evaluated. Furthermore, the efficacy of ^{213}Bi-C595 in preangiogenic cancer cell clusters grown in vitro and in the control of subcutaneous

(s.c) xenografts in a nude mouse model is also tested. The pharmacokinetics and short term toxicity studies are investigated in this chapter.

4.1 MUC1 expression

4.1.1 Immunocytochemistry for cancer cell lines

The immunoreaction of four cancer cell lines to MAb C595 was tested and results are summarized in Table 4-1. The ovarian cancer cell lines OVCAR3, SKOV3 and OV-90, breast cancer cell line BT474, positive to C595 and negative to isotype control. Representative pictures were shown in Figure4-1.

Table 4-1 C595 expression in cancer cell lines

	OVCAR3	SKOV3	OV90	BT474
Immunocytochemistry	+++	++	+	++
Flow cytometry	98%	72%	41%	NA
Spheroids	+++	NA	NA	++
Animal model	+++	++	NA	++

Note: +++ strong positive, ++moderate positive, + weak positive, - negative.
* percentage of positive cells. NA; not available.

Figure4-1 Expression of MUC1 in OVCAR3 cells

A

B

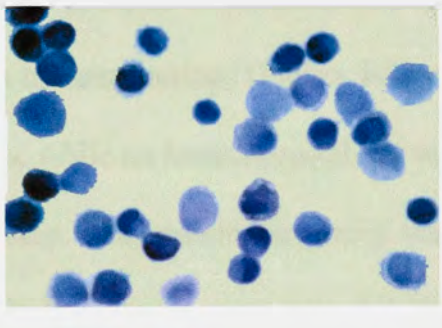

C

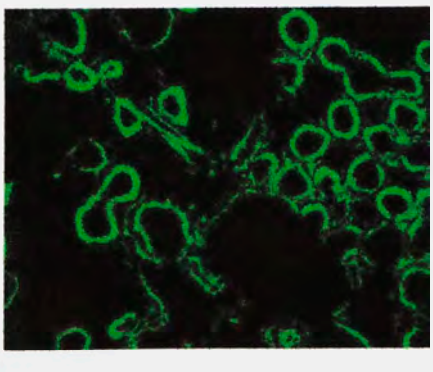

Figure4-1 A: Strong expression of MUC1 was found in OVCAR-3 monolayer cultured cells. Brown staining indicates positive cells. B: Negative control has shown blue staining only. C: Green florescence has shown the positive cells. Magnification was at x 400.

4.1.2 Flow cytometry for cancer cell lines

Flow cytometry demonstrated distinct differences in the patterns of reactivity of the MAb C595 with OVCAR3, SKOV3, OV90 and BT474 cancer cell lines with isotype control (Figure 4-2). The results of flow cytometry are also summarized in Table 4-1.

Figure 4-2 Flow cytometry for MUC1 expression in OVCAR3 cells

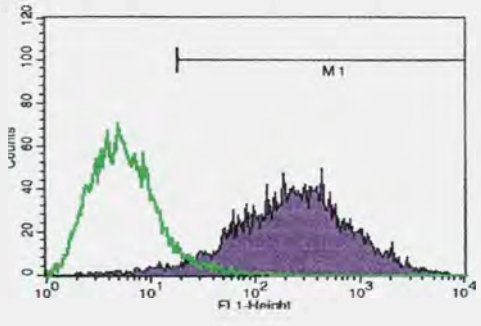

Figure 4-2 Flow cytometry confirmed viable OVCAR-3 cells with 98% expression of MUC1. Data are presented as histogram, using a mouse IgG1 isotope negative control to determine background fluorescence and to set the marker (M1).

4.1.3 Immunohistochemistry for ovarian cancer tissue

MUC1 expression in 26 ovarian cancer tissue was assessed by immunohistochemistry. Representative pictures were shown for immunostaining with MAbs C595 (test) and Mouse anti-human isotype control IgG1 MAb (isotype control). MUC1 expression was found in 73.1% (24 / 26, n = 26) of ovarian tumour sections (Figure 4-3) and 45.5% (5 / 11, n = 11) of matched omentum metastases, while no immunoreactivity was found with isotype control and in normal ovarian tissues. The staining intensity was from weak positive (+) to strong positive staining (+++). Results are summarized in Table 4-2.

Figure 4-3 MUC1 expression in ovarian cancer tissue

A 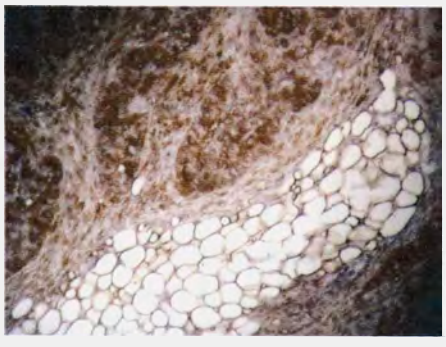 B 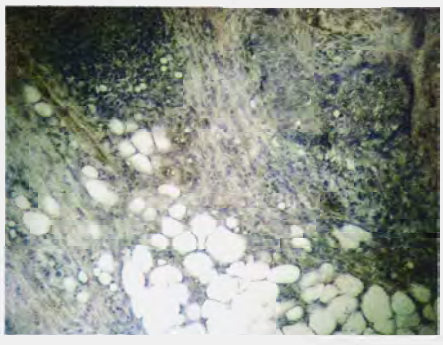

Figure 4-3 Expression of MUC1. Over-expression of MUC1 was found for ovarian cancer tissues. Magnification x 200 in all photos. A represents positive staining, while B represents a negative control.

Table 4-2 Tissue staining with C595 MAb

Tissue	Tissues staining with C595 MAb				
	+++	++	+	-	N
Tumor	7	10	2	7	26
Omentum metastases	1	3	1	6	11
Normal ovarian tissues				5	5

Table 4-2 Intensity of immunohistochemical staining of ovarian cancer tissue, omentum metastases and normal ovarian tissues with C595 MAb.

4.1.4 Immunocytochemistry in spheroids

The immunoreactivity of OVCAR3 and BT474 cell clusters to MAb C595 was tested on cytospin (data not shown). Strong MUC1 expression was found in OVCAR3 and BT474 cell clusters. The isotype control was negative to the matched cell line. Results are summarized in Table 4-1.

4.1.5 Immunohistochemistry in animal models

Animal developed cancer tissues were stored in 4% neutralized formalin. Paraffin sections and slides were prepared by Pathology Department of SEALS. OVCAR3, PC3 and BT474 tumors, and OVCAR3 ascites cells were shown positive to C595 MAb, while negative to isotype control. Representative images are shown in Figure4-4.

Figure4-4 MUC1 expression of animal xenograft tumors

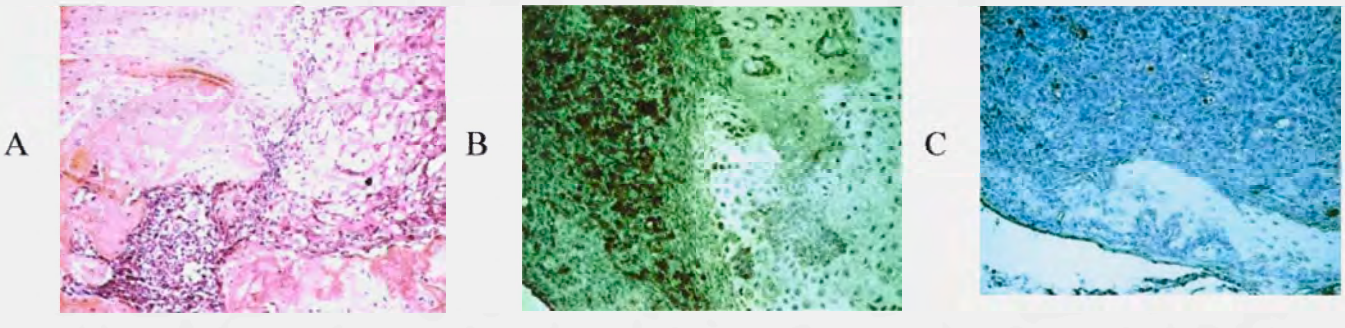

Figure4-4 Expression of MUC1 in xenograft tumours. A represented HE staining, while B represented positive staining and C for negative control. Brown colour indicates positive cancer cells. Magnification x 200.

4.2 In vitro studies

4.2.1 Bi-C595 inhibition cancer cells proliferation –MTS assay

The effects of ^{213}Bi-C595 on cell growth were assessed using MTS assay in triplicate (P value relative to the $^{213}BiI_3$). D_0 values (activity required for 37% cell survival) for 2 x 10^4 cells in 300 μL for ^{213}Bi-C595 are 0.31 ± 0.03 MBq, 0.3 ± 0.05 MBq, 1.3 ± 0.2 and 0.5 ± 0.1 MBq for OVCAR3, SKOV3, OV90, and BT474 (Figure 4-5), whereas the D_0 values for both ^{213}Bi-A2 and ^{213}Bi-Iodide were 4.4 ± 1.2 MBq, being 12-16 times greater than MUC1 positive expression cells with ^{213}Bi-C595 ($P < 0.001$). Cell survival for antibody/protein alone group was the same as for untreated cells.

Figure 4-5 MTS assay of ^{213}Bi-C595

A

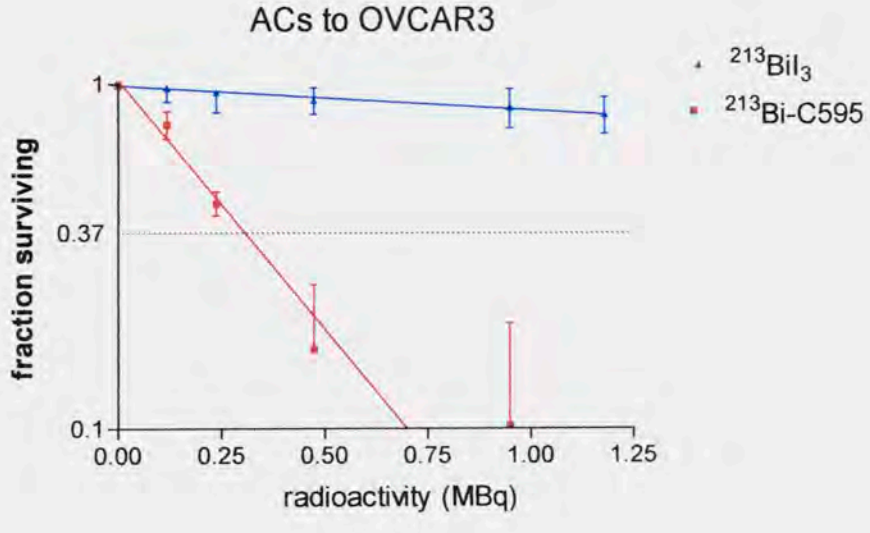

B

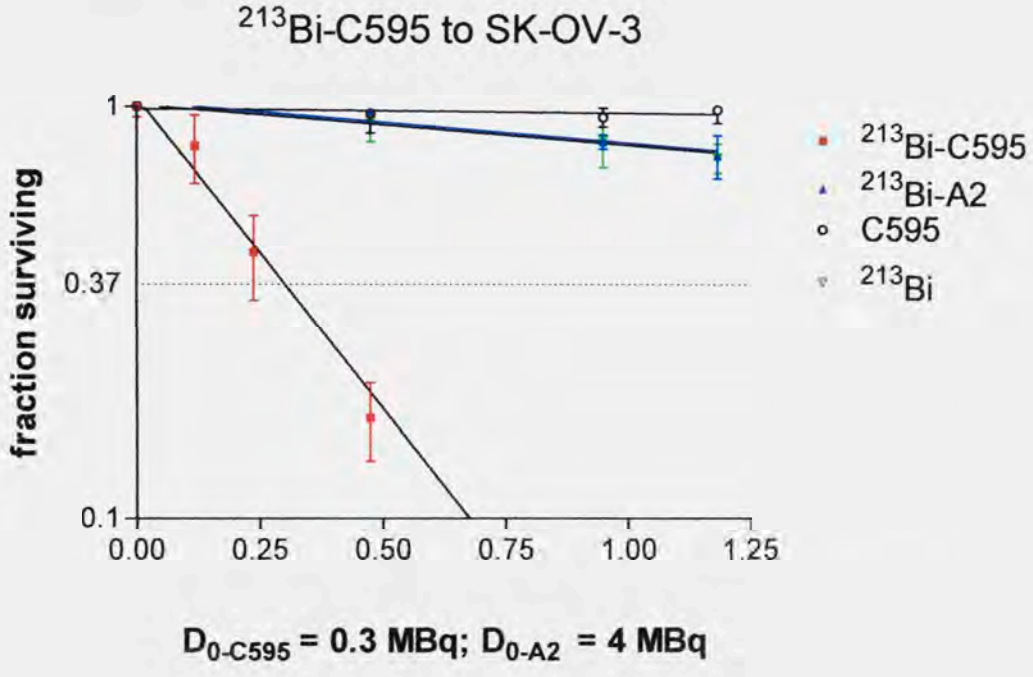

C

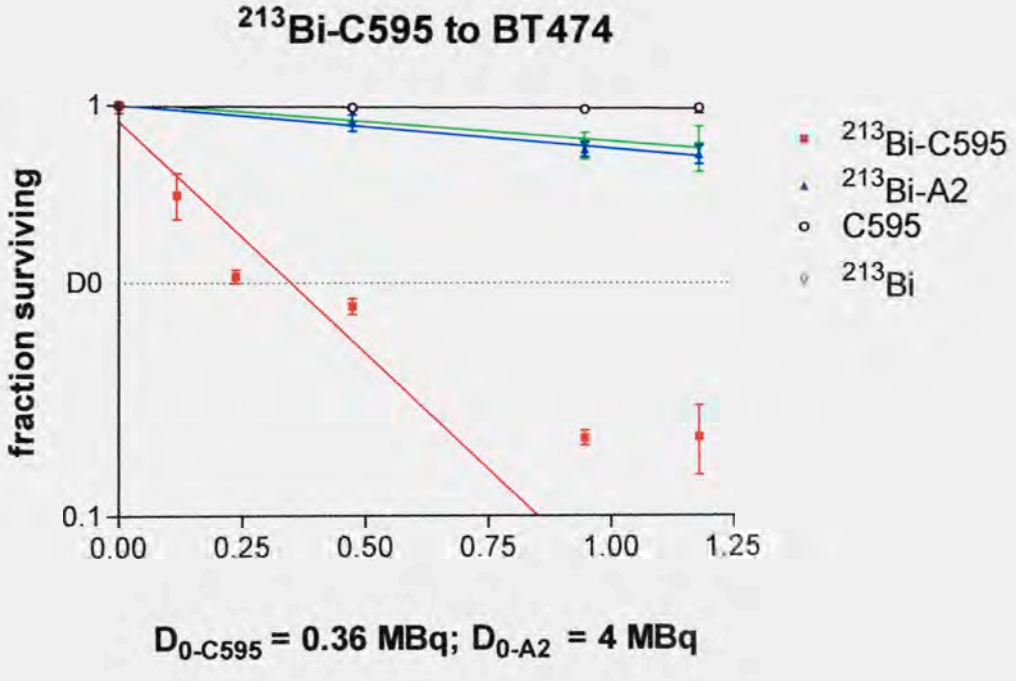

Figure 4-5 Cytotoxicity study of ovarian cancer cell lines following incubation for 24 h with ^{213}Bi-C595 and free ^{213}Bi (A-C). Cells were treated with varying concentrations of ACs, and cell survival measured by MTS assay and expressed as a percentage of cell survival of control cells. Each experiment was performed in triplicate, and each point represents the mean of three experiments. Graphs A – C are for OVCAR3, SKOV3 and BT474 cell lines with strong expression of MUC1. In contrast, C595, ^{213}Bi and ^{213}Bi-A2 have low toxicity.

4.2.2 Morphological changes -- Monolayer cells

After treatment with ^{213}Bi-C595, the treated cells in 24 well plates showed typical apoptotic morphology, *i.e.*, cells became rounded, shrunken and detached, whereas cells incubated with cold control mix, free ^{213}Bi, ^{213}Bi-A2 showed similar morphological patterns to untreated cells. ^{213}Bi-C595 incubation of monolayer cells at 24 h gave 41 ± 4% of apoptosis cells and ~10% necrosis cells by Diff-Quik staining. After 72 h of treatment, the percentage of apoptosis cells increased to 80 ± 6 % for ^{213}Bi-C595.

4.2.3 Morphological changes -- Spheroids---OVCAR3

The 80 and 150 μm spheroids of OVCAR3 partially disaggregated post-treatment with ^{213}Bi-C595. There were no significant differences in the percentage of apoptosis cells (80 ± 6%) and necrosis cells (10 ± 8%) between the 80 and 150 μm spheroids, using Quik-Diff staining. Cell colony formation was not observed for ^{213}Bi-C595 plates, while many cell colonies formed in all other plates after 2 weeks. Thus complete cell kill was observed for the targeted ACs.

4.2.4 TUNEL assay

The exposed 3'-OH ends of DNA fragments generated by apoptotic DNA cleavage were detected by TUNEL assay, in which the non-apoptotic cells stained green while apoptotic cells stained brown. The results confirmed the Quik-Diff staining results. The percentage of apoptosis (80 ± 6%) and necrosis cells (10 ± 8%) at 72 hours post treatment were counted.

4.3 In vivo

4.3.1 Treatment efficacy in a mice ascites model

The median survival was 49, 52, 69 and 25 days for 355, 710, 1065 MBq/kg of ^{213}Bi-C595 and cold control groups, respectively (Figure 4-6). There were no significant differences between different acitvity treatment groups ($P > 0.05$). However, statistical differences were found in mice that received 355 to 1065 MBq/kg of ^{213}Bi-C595 compared to control mice ($P< 0.05$)(Table 4-3).

Table 4-3 groups comparison

	710 MBq/kg	1065 MBq/kg	Cold control
P related to 355 MBq/kg (95% CI of ratio)	0.66 (0.65-1.23) ns	0.23 (0.47-0.9) ns	0.03 (1.67-2.25) *
P related to 710 MBq/kg (95% CI of ratio)	-	0.1 (0.5-1) ns	0.049 (1.79-2.4) *
P related to 1065 MBq/kg (95% CI of ratio)	-	-	0.02 (2.5-3) *

Note: CC cold control mix. CI: confidence interval. P value summary: * $P < 0.05$; ** $P < 0.01$; ns: no significant difference.

Figure 4-6 Treatment efficacy of ^{213}Bi-C595

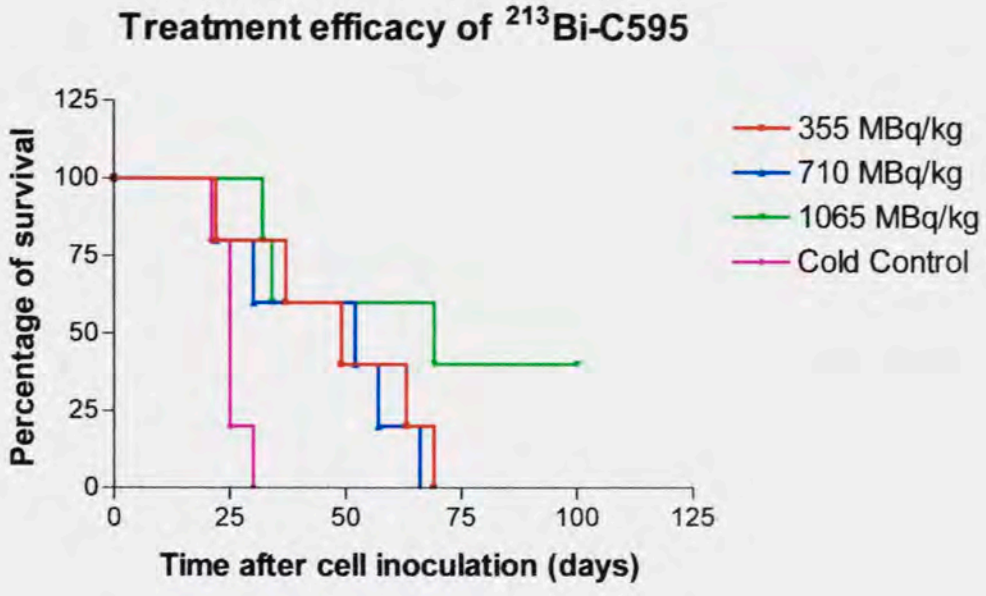

Figure 4-6 Kaplan-Meier survival curves indicate the percentage of survival.

4.3.2 Toxicity

4.3.2.1 Toxicity of ^{213}Bi-C595 in mice

Mice in the 710, 947 and 1180 MBq/kg groups were found to be well after the injection and experienced increasing body weight up to 90 days (experiment terminated). 710 MBq/kg group was observed for 26 weeks, while 1180 MBq/kg group mice were observed for 21 weeks. Only one mouse in 1180 MBq/kg group showed loss body weight more than 20% at 21 weeks. Organs resected and examined by IDEXX Laboratories. The reason of weight loss for this mouse was histiocytic sarcoma, which developed in nude mice, unrelated to ^{213}Bi-C595 treatment. There were no abnormalities found in 710 MBq/kg group. The kidney of 1180 MBq/kg group has shown dysplastic megalocytic change in cortical tubular epithelium, the radiation nephropathy was defined as mild.

Figure 4-7 Toxicity of ^{213}Bi-C595

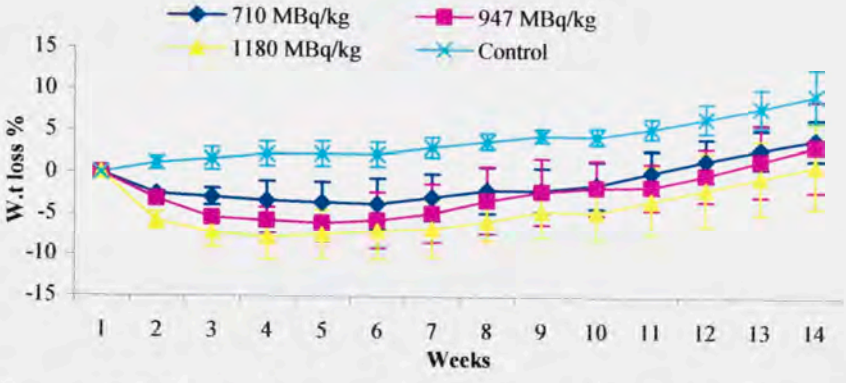

Figure 4-7 Mice in all treated groups have shown body weight increase up to 14 weeks.

4.3.2.2 Toxicity of multiple targeted alpha therapy in mice

Toxicity after i.p injection of 355-710 MBq/kg of cocktail of ^{213}Bi-C595 and ^{213}Bi-PAI2 conjugates was measured as leukocyte depression in peripheral blood at 2 weeks post injection, with leukocyte recovery occurring at 3 weeks. Mice found to be well after the injection experienced increasing body weight to 96 days (Figure 4-8). The comparison p values between different groups are listed in Table 4-4. There were significant differences between treated and cold control mice ($P < 0.001$), and between treated groups. Dose dependent toxicity in term of body weight change was found in Table 4-4. Kaplan-Meier survival curves were used to analyse survival percentage (Figure 4-9). There were significant differences between treated and cold control groups ($P<0.001$). Haematology was normal at 96 days, but dose-dependent reduction in renal function was found, manifesting as mild to moderate increase in blood urea nitrogen. The histopathologic examination showed that mild radiation nephropathy from 355-710 MBq/kg and for the hot control groups.

Figure 4-8 MTAT mice body weight changes

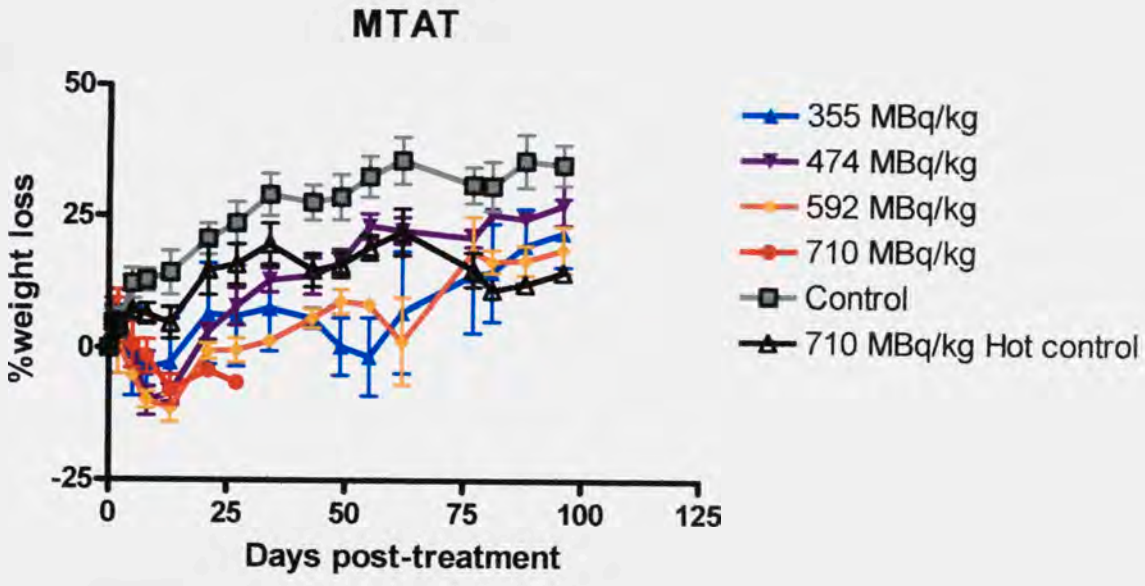

Figure 4-8 Mice in 355 –592 MBq/kg and cold control groups shows increasing body weight and good tolerance to the treatment. However, mice in 710 MBq/kg treatment group showed a decrease of body weight and all mice died or were culled at 25 days post-treatment. Mice in 710 MBq/kg hot control group experienced body weight decrease at 80 days post -treatment.

Table 4-4 P values between different groups

	474 MBq/kg	592 MBq/kg	710 MBq/kg	Cold Control	710 MBq/kg hot control
P related to 355MBq/kg	0.1; ns	0.02;*	0.019;*	0.008;**	0.024;*
P related to 474MBq/kg	-	0.15;ns	0.019;*	<0.0001 ***	0.69; ns
P related to 592MBq/kg	-	-	0.14;ns	<0.0001; ***	0.009;**
P related to 710 MBq/kg	-	-	-	<0.0001; ***	<0.0001; ***
P related to Cold control	-	-	-	-	0.0034;**

Note: ns no significant difference; * P<0.05; ** P <0.01; ***P < 0.001.

Figure 4-9 MTAT mice survival

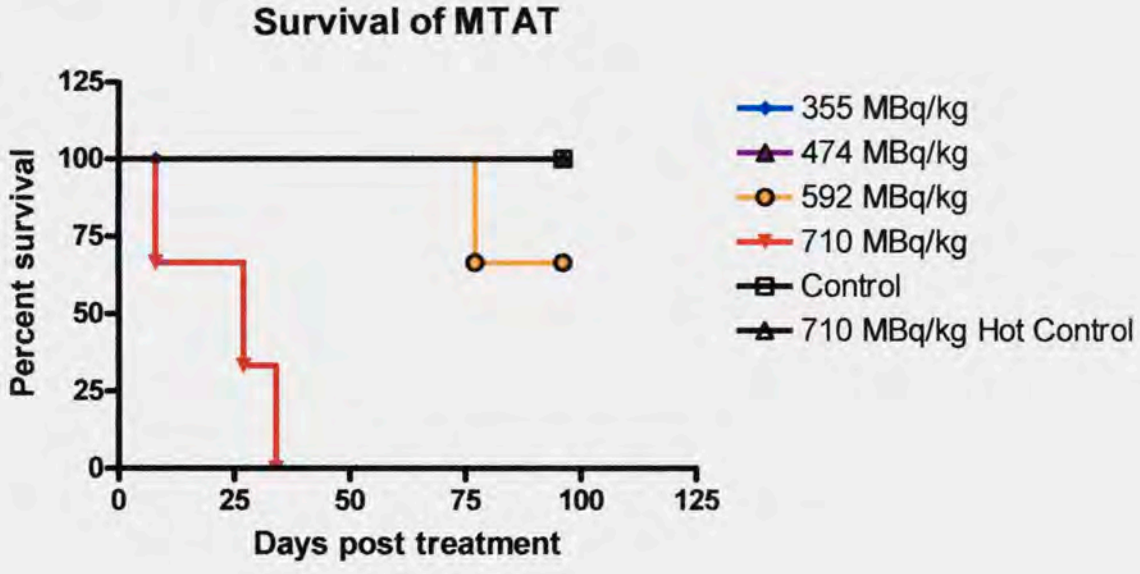

Figure 4-9 The medium survival of 355 – 592 MBq/kg and control groups were not determined, while the medium survival of 710 MBq/kg group was 27 days only ($P < 0.0001$ ***). There was significant difference between all groups.

4.3.3 Pharmacokinetics studies

The concentration of ^{213}Bi-cDTPA-C595 in blood, spleen, liver, lung, heart, bone and kidney was similar with and without lysine application ($P>0.05$) and results are shown in Figure 4-10. Blood clearance, kidney uptake and accumulation at 4 hours post injection of ^{213}Bi-C595 are shown in Figure 4-11. The kidney was the major organ for activity uptake. The activity in ascites and blood was stable up to 4 hours as shown in Figure 4-11. It has shown the stability of this conjugates up to 4 hours, which is more than 5 half-lives of ^{213}Bi. Uptake of C595 in the ascites was higher than in the other organs (except for kidney at 60 and 120 minutes time points), including the liver, heart, spleen, brain and bone marrow. The ascites: blood ratio for C595 was 5.8, which clearly indicated tumor-specific uptake.

Figure 4-10 Comparison w/o lysine application

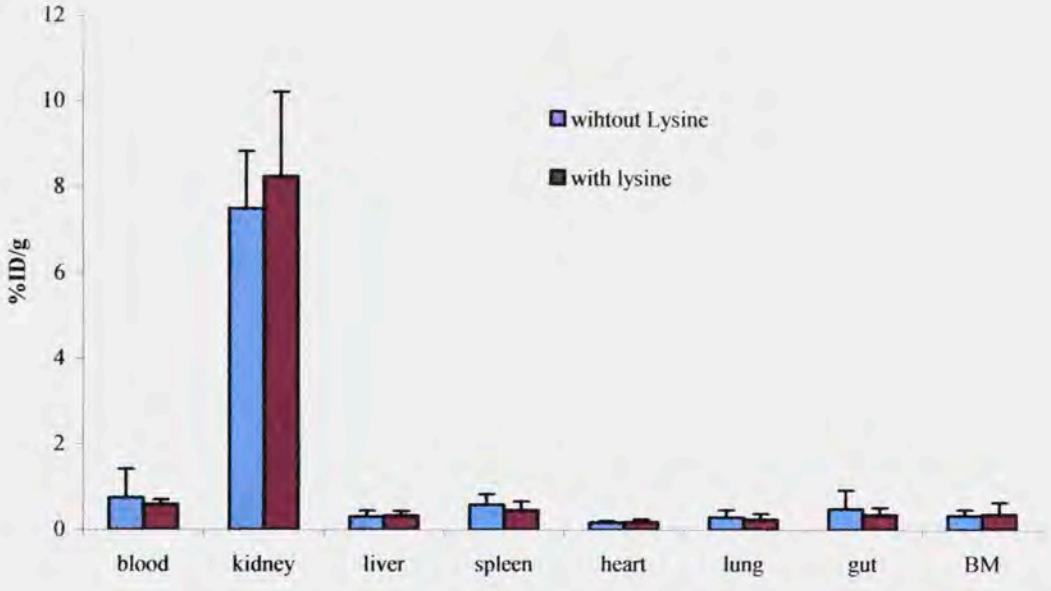

Figure 4-10 Kidney was the major uptake organ. There was no significant difference between with and w/o lysine application.

Figure 4-11 Biodistribution of ^{213}Bi-C595 in OVCAR-3 model

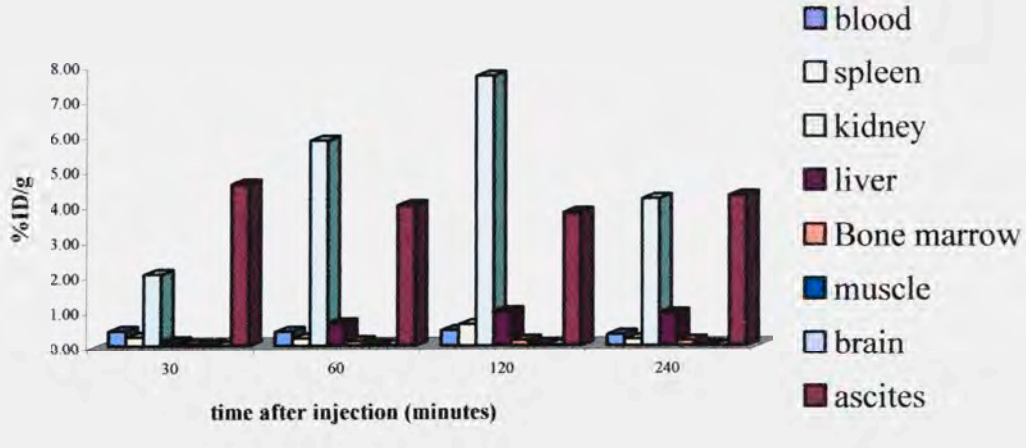

Figure 4-11 Kidney was the major activity taken organ, whereas liver is the second uptake organ. The ascites and blood level of ^{213}Bi-C595 was stable up to 4 hours.

4.3.4 Kidney absorbed dose

The radiation dose to the kidney was determined in mice injected i.p with ^{213}Bi-C595. Data are presented as mean activity per gram versus time. Area under curve was 1.5 x 10^9 (Bq.s/g); the kidney absorbed dose was 0.5 Gy (1.5 x 10^9 Bq.s/g x 2.03 MeV x 1.602 x 10^{-13} J/MeV x 10^3g/kg).

Figure 4-12 Kidney dose

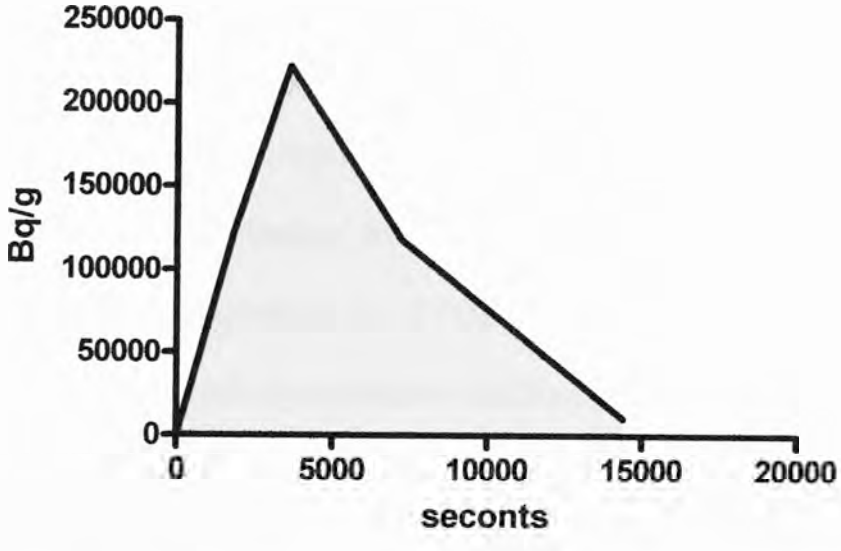

Figure 4-12 Mean activity (obtained from percent injected dose multiply by injected activity) versus time

4.4 Discussion

MAb-based therapeutics are an important option to control metastases and improve survival rate of ovarian cancer. These strategies include MAb combination with cytotoxic drugs, conjugation with radionuclides, or immunological effector cells. High specification and affinity to targeted cancer tissue are essential for the selection of targeted antigens and targeting vectors. The present system relies on the targeting of ^{213}Bi to MUC1 tumour cells. MUC1 is a mucin, high MW glycoprotein. The biological function of MUC1 may be in part due to its large size and the extended rigid structure. The expression of MUC1 in tumours may function as an anti-adhesion molecule, which inhibits cell-cell adhesion, inducing a release of cells from tumour nests and causing micrometastases (Feng et al., 2002). Over-expression of MUC1 in cancer cells may effect efficient lysis by cytotoxic lymphocytes and therefore contribute to escape from immune surveillance (van de Wiel-van Kemenade et al., 1993). It has been proposed that enhanced levels of MUC1 expression by cancer cells may mask extracellular domains from immune surveillance, confer a survival advantage on malignant cells and plays an important role in the ability of tumours to invade and metastasize (Hughes et al., 2000; Mommers et al., 1999). It was also reported that increased MUC-1 expression correlates with the stage and grade of ovarian cancer. MUC1 upregulation was significantly correlated to the depth of invasion, lymph node metastasis, and peritoneal dissemination (Satoh et al., 2000).

MAb C595 (also known as NCRC48) is reactive with the protein core of MUC1 mucin. The target epitope of the MAb C595 is the tetrameric motif Arg-Pro-Ala-Pro that is repeated many times within the MUC1 protein core (Gendler et al., 1988; Price et al., 1990).

Using the MAb C595, we found MUC1 expression on the surface of OVCAR3, SKOV3 and BT474 cancer cells by flow cytometric analysis and confocal microscopy. MUC1 was strongly expressed on the surface of viable OVCAR3 cells in monolayer, spheroids, and ascites in a animal model. Our findings indicate that the OVCAR3 ascites model is an appropriate model for investigating the efficacy of ^{213}Bi-C595.

The expression of the MUC1 antigen on human ovarian cancer specimens and human ovarian cancer cell lines using MAb C595 was investigated in this chapter. In this study, we found that around 80% of primary ovarian tumours expressed MUC1 while normal ovarian tissues did not. MUC1 is therefore an effective tumour surface marker for targeting ovarian carcinoma.

Cytotoxicity of ^{213}Bi-C595 to two ovarian cancer cell lines and one breast cancer cells proved to be specific and concentration-dependent. These cell lines demonstrated a similar pattern of cell killing because the expression of MUC1 on three cell lines is similar. These results suggest ^{213}Bi-C595 can target and kill 63% of ovarian cells (monolayer) *in vitro* using a low acitvity (0.3-0.5 MBq). Using 1.2 MBq/300 μL of ^{213}Bi-C595, only <10% cancer cells can survive after treatment while using the same activity of ^{213}Bi-A2, >90% cancer cells can survive. There was a 12-16 fold difference in the 37% survival (D_0) values *in vitro* for the test ^{213}Bi-C595 compared with a non-specific control ^{213}Bi-A2. There was no cell killing for C595 alone. These results suggest only specific ^{213}Bi-C595 can effectively target MUC1-positive cancer cells.

Additional data demonstrated that ^{213}Bi-C595 did not specifically kill the MUC1-negative OV90 ovarian cancer cell line, supporting the fact that the ^{213}Bi-C595 conjugate does not target or destroy tissue that does not express MUC1. Therefore, it is clear that ^{213}Bi-MUC1 is an effective and specific radiolabelled agent for ablation of

individual OVCAR3 ovarian cancer cells in vitro whereas non-targeted cells are spared from the radiotoxicity arising from the alpha radiation.

The exact mechanism of cell killing using ^{213}Bi-C595 is still not clear. One explanation is that after binding the surface MUC1 antigen, ^{213}Bi-C595 may form ^{213}Bi-C595-MUC1 complexes at the cell membrane, emitting alpha particles that kill ovarian cancer cells by causing double-DNA strand breaks. Another possibility is that the surface-bound ^{213}Bi-C595-MUC1 complexes may be internalised, resulting in increased cell killing efficiency. Clearly, many factors including antigen affinity and antigen density will also play an important role in the killing of targeted antigen positive cells, since those with high density will attract more AIC and those with higher antigen affinity may "hold on" to increased levels of radioactivity for a longer time period. The relative importance of these factors (antigen density, antigen affinity and internalisation) in the killing process has not yet been determined.

The most effective radiation treatments are those that not only hit the intended target but also cause the greatest amount of lethal or non-repairable damage to DNA. Therefore, alpha particles are most effective in this respect (Hall, 1994). A large number of *in vitro* and *in vivo* experiments with alpha-immunotherapy have shown dramatic superiority over beta-immunotherapy as only a few alpha hits of the nucleus are needed to kill cells (Allen, 1999; Kennel et al., 1999; McDevitt et al., 2000; Scheinberg et al., 1982; Vaughan et al., 1982). Using electron micrographs in studies of murine lymphoma, Macklis (Macklis et al., 1992) have demonstrated bizarre blebbing patterns, condensation of chromosomal material, and inter-nucleosomal DNA fragmentation pattens characteristic of programmed cell death (apoptosis) after treatment with AIC, and suggested that alpha-particles may kill cells by apoptotic mechanisms. In this study, we found typical morphologic changes and a high percentage of TUNEL-positive cells

in three ovarian cancer cell lines after treatment using ^{213}Bi-C595 *in vitro*. These data suggests that the lethal pathway for the three cell lines *in vitro* after TAT involves apoptosis. The in vitro monolayer cell model yielded valuable information regarding the mechanisms of malignant growth, but is unsuitable in representing in vivo tumors, because the solid tumors grow in a three dimensional spatial array and the cells in these tumors are exposed to non-uniform distribution of oxygen and nutrients as well as other physical and chemical stresses. Because of the microenvironmental variations present, significant cellular heterogeneity may result. Tumour spheroids represent more realistically the three-dimensional growth and organization of preangiogenic solid tumors and, consequently, simulate much more precisely the cell-cell interactions and microenvironmental conditions found in these tumors (Marian Teresa Santini & Rainaldi, 1999). ^{213}Bi-C595 can target surface cancer cells, but killing internal cells may be different, because of the short half-life of Bi-213 and penetration of the antibody. ^{213}Bi-C595 is effective for OVCAR3 spheroids with 150 μm. It causes a morphological change in the spheroids, and no colonies formed in treated plates, where control spheroids form colonies. High percentage TUNEL positive cells were evaluated. These data indicate that the lethal pathway after TAT involves apoptosis.

The in vivo therapeutic experiment was designed to evaluate the anticancer activity of ^{213}Bi-C595 after administration at 9 days-post cell inoculation (ascites model) and to optimise the dosage regimen. Our findings indicate that a single i.p injection of ^{213}Bi-C595 at a acitvity of 355 to 1065 MBq/kg can prolong survive by 24 to 34 days. The ascites growth inhibition and metastases was dose-dependent. This means that ^{213}Bi-C595 can inhibit tumourigenesis by i.p administration.

The pharmacokinetics study indicated the stability of ^{213}Bi-C595 in blood up to 4 hours, which is more than 5 half- lives of bismuth –213. Uptake of C595 in the ascites was

higher than in other organs (except for kidney at 60 – 120 minutes). The high tumor: blood ratio clearly indicates tumor specific uptake. The reason for relative high renal uptake may result from ^{213}Bi-C595 leaching in the first 2 hours post injection. The kidney uptake decreased at 4 hours. Although the biodistribution data indicated that kidney may be the acitvity limiting organ for ^{213}Bi-C595 treatment, severe radiation nephropathy was not observed for longer term and the calculated kidney absorbed dose was 0.5 Gy only.

The 90 days short term toxicity study showed that the MTD for weight loss was up to 1180 MBq/kg for nude mice. Leukocyte depression in peripheral blood was not observed at 90 days. The long-term toxicity studies (140 – 180 days) for 710 MBq/kg and 1180 MBq/kg groups showed that the mice were asymptomatic up to the endpoint. One mice suffered from histocytic sarcoma, which is often seen in nude mice and unrelated to ^{213}Bi-C595 therapy. Pathology examination indicated that there was no radiation nephropathy in the 710 MBq/kg mice, but mild radiation nephropathy was found in 1180 MBq/kg at 21 weeks. As a result, there was no long term severe toxicity observed for ^{213}Bi-C595 up to 1180 MBq/kg.

4.5 Conclusion

We have demonstrated moderate to strong MUC1 expression on the majority of human ovarian cancer tissues and cancer cell lines using MAb C595. MUC1 is therefore an ideal targeted antigen for targeted alpha therapy using ^{213}Bi-C595. This AIC can target and selectively kill ovarian cancer cells *in vitro*. The lethal pathway involves apoptosis. ^{213}Bi-C595 can inhibit growth of ovarian cancer cell clusters and preangiogenic lesions in vivo. Furthermore, these findings indicate that ^{213}Bi-C595 can target and kill cancer micrometastases, i.e. cells in transit or at the pre-angiogenic stage. Therefore, multiple metastatic sites at the minimal residual disease stage should be considered to be the most suitable targets for ^{213}Bi-C595. Such a treatment may have a role as adjuvant therapy immediately after resection of macroscopic tumour to prevent early recurrence.

Chapter 5

Preclinical studies of ^{213}Bi-Herceptin Results & Discussion

Introduction

HER2 is normally expressed at a very low level in some human secretory epithelial cells, but is overexpressed in 30% of human breast carcinomas and in other types of human cancer. Moreover, HER2 overexpression occurs in the primary tumor as well as in metastatic sites (Niehans et al., 1993). The overexpression is associated with disease progression and poor prognosis (Slamon et al., 1989), suggesting that HER2/neu overexpression likely plays a critical role in the development of human cancer metastasis. The known oncogenic potential mediated by HER2, together with its high-level expression in tumor tissue and its cell surface localization, make this oncoprotein an ideal target for anti-tumor therapeutic approaches (Menard et al., 2000). Herceptin is a humanized antibody which recognize Her2 receptor. There is little information about Herceptin combined with a therapeutic radioisotope, e.g. with an alpha emitting.

The objectives of this chapter are to investigate whether Herceptin labeled with ^{213}Bi would be suitable to treat human ovarian and breast cancer cells which overexpress HER2. In the present study, we measured the levels of HER2 expression in ovarian and breast cancer cells. Cells incubated with 213Bi-Herceptin AC demonstrates that 213Bi-Herceptin has anti-tumor effects for human breast cancer cells in vitro. Such an approach would be particularly appropriate after surgery to reduce the growth of metastatic cancer. This chapter also investigates the toxicity and the treatment efficacy of Bi-Herceptin in a breast s.c xerograph model.

5.1 HER2 expression

5.1.1 Immunocytochemistry for cancer cell lines

The immunoreaction of five cancer cell lines to MAb HER2 was tested and results are summarized in Table 5-1. The ovarian cancer cell line SKOV3, breast cancer cell line BT474 were positive to MAb HER2 and negative to isotype control. Ovarian cancer cell lines OVCAR3, OV-90 was negative to MAb HER2 and isotype control. Representative pictures were shown in Figure 5-1.

Table 5-1 HER2 expression in cancer cell lines

	OVCAR3	SKOV3	OV90	BT474
Immunocytochemistry	-	++	-	++
Flow cytometry	6%	99.6%	43%	NA
Spheroids	-	NA	NA	++
Animal model	-	++	NA	++

Figure 5-1 HER2 expression on OVCAR3 and SKOV3 cells

A

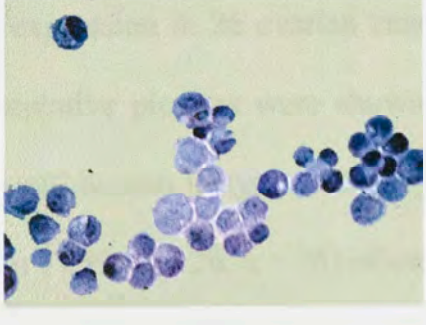

B

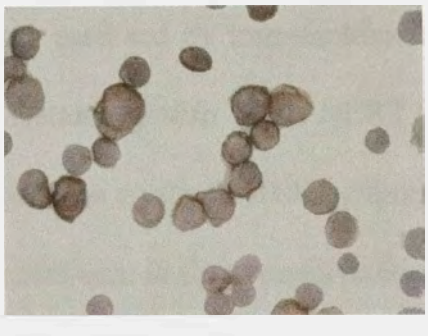

Figure 5-1 Negative expression of HER2 was found in OVCAR-3 (A) monolayer cultured cells, while moderate positive in SKOV3 (B) expression was found. Brown staining indicates positive cells. Magnification was at x 400 for A and B.

5.1.2 Flow cytometry for cancer cell lines

Flow cytometry demonstrated distinct differences in the patterns of reactivity of the MAb HER2 with SKOV3, and BT474 cancer cell lines with isotype control. There were little differences in the pattern of staining with MAb HER2 and isotype control for OVCAR3, OV90 cell lines (Figure 5-2). The results of flow cytometry are also summarized in Table 5-1.

Figure 5-2 Flow cytometry for HER2 expression in OVCAR3 cells

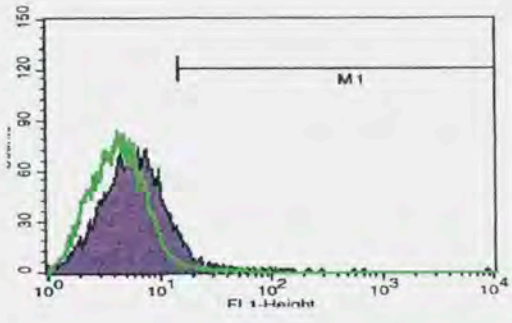

Figure 5-2 Flow cytometry confirmed viable OVCAR-3 cells with 6% expression of HER2. Data are presented as histogram, using a mouse IgG1 isotope negative control to determine background fluorescence and to set the marker (M1).

5.1.3 Immunohistochemistry for ovarian cancer tissue

HER2 expression in 26 ovarian cancer tissue was assessed by immunohistochemistry. Representative pictures were shown for immunostaining with MAb HER2 (test) and Mouse anti-human isotype control IgG1 MAb (isotype control). HER2 expression was found in 11.5% (3 / 26, n = 26) of ovarian tumor sections. In these positive tissues, 1 out of 26 were moderate positive, and 2 out of 26 were week positive. 11 patients were included primary ovarian cancer site and omentum metastasis tissue. All of them with matched metastases were negative to MAb HER2. No immunoreactivity was found with isotype control and in normal ovarian tissue. The staining intensity was from positive (+) to strong positive staining (+++). Results were summarized in Table 5-2.

Figure 5-3 Her2 expression in ovarian cancer tissue

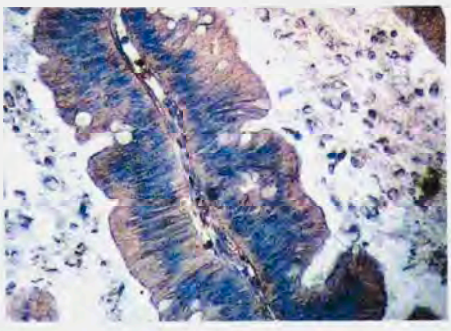

Figure 5-3 Expression of Her2. Over-expression of Her2 was found at ovarian cancer tissues. Magnification x 400.

Table 5-2 Intensity of immunohistochemical staining of ovarian cancer tissue, omentum metastases and normal ovarian tissues with MAb HER2

Tissue	Tissues staining with MAb HER2				
	+++	++	+	–	N
Tumor		1	2	23	26
Omentum metastases				11	11
Normal ovarian tissue				5	5

Note: Ovarian tumors (n = 26), matched omentum metastases (n=11) and normal parts of ovarian (n=5) were collected from 26 ovarian cancer patients.
– Negative staining; + weak staining; ++ moderate staining; +++ strong staining.

5.1.4 Immunocytochemistry in spheroids

The immunoreactivity of BT474 cell clusters to MAb HER2 was tested on cytospin and shown in Figure 5-4. Strong HER2 expression was found in BT474 cell cluster. The isotype control was negative to matched cell line. Results were summarized in Table 5-1.

Figure 5-4 Expression of HER2 in spheroids

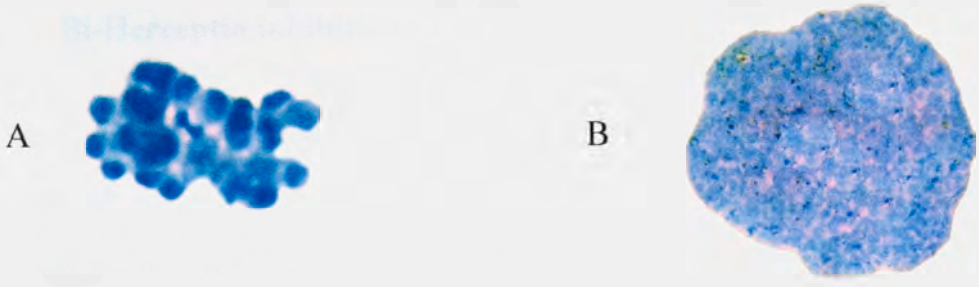

Figure 5-4 Negative expression of HER2 was found in OVCAR-3 cell 40 μm (A) diameter clusters. A similar staining pattern was found in cultured spheroids (150 μm B).

5.1.5 Immunohistochemistry in animal models

Animal developed cancer tissues were stored in 4% neutralized formalin. Paraffin sections and slides were prepared by Pathology Department of SEALS. SKOV3 and BT474 tumors cells were shown positive to HER2 MAb, while negative to isotype control. Representative pictures were shown in Figure 5-5. Results were summarized in Table 5-1.

Figure 5-5 Animal xenograft tumors HER2 expression

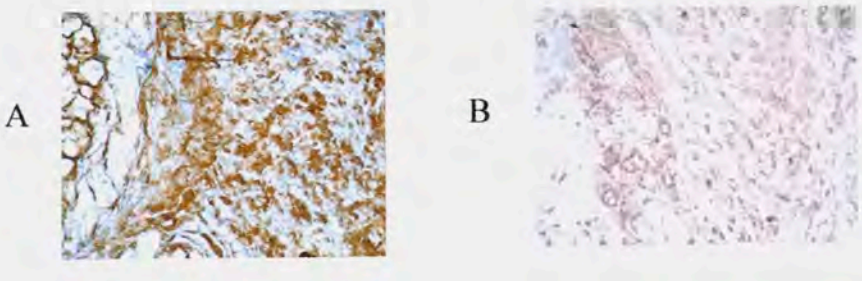

Figure 5-5 Expression of Her2. Over-expression of Her2 was found at animal xenograft tumors. Magnification x 200 in all photos. A represented a positive staining, while B represented a negative control.

5.2 In Vitro

5.2.1 Bi-Herceptin inhibition cancer cells proliferation –MTS assay

The effects of ^{213}Bi-Herceptinon cell growth were assessed using MTS assay in triplicate (P value relative to the $^{213}BiI_3$). D_0 values (activity required for 37% cell survival) for 2 x 10^4 cells in 300 μL for ^{213}Bi-Herceptin are 4.4 ± 0.5, 0.3 ± 0.05, 4.6 and 0.53 MBq for OVCAR3, SKOV3, OV90, and BT474 (Figure 5-6), whereas the D_0 values of ^{213}Bi-A_2 and ^{213}Bi-Iodide were 4 ± 0.8 MBq, being 12-16 times greater than Her2 positive expression cells with ^{213}Bi-Herceptin (P <0.001).). Cell survival for antibody/protein alone group was the same as for untreated cells.

Figure 5-6 In vitro cytotoxicity of ^{213}Bi-Herceptin

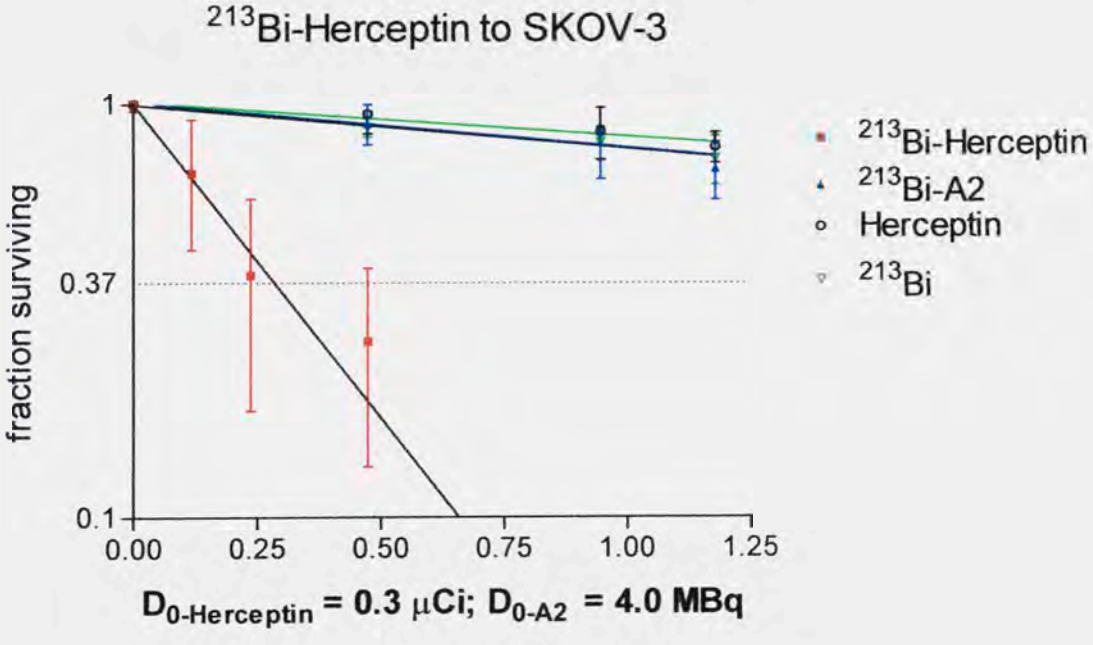

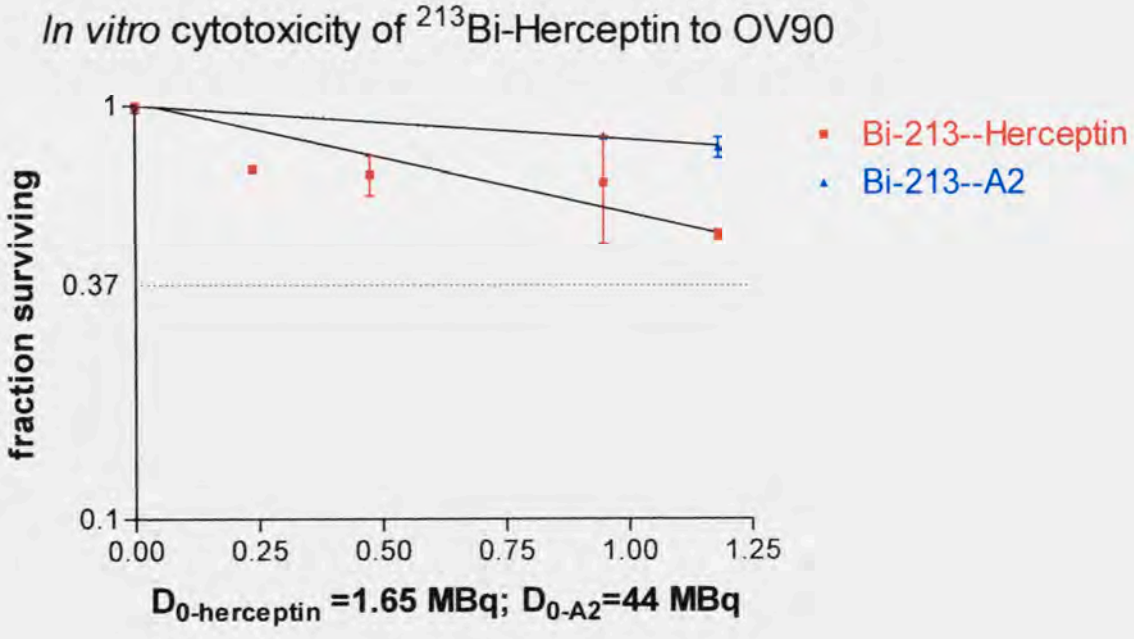

Figure 5-6 Cytotoxicity study of SKOV3 and OV90 cells following incubation for 24 h with ^{213}Bi-Herceptin and non specific control. Cells were treated with varying concentrations of ACs, and cell survival measured by MTS assay and expressed as a percentage of cell survival of control cells. Each experiment was performed in triplicate, and each point represents the mean of three experiments.

5.2.2 Morphological changes --Monolayer cells

After treatment with ^{213}Bi-Herceptin, the treated cells in 24 well plates similar morphological pattern with untreated cells. Only 12 ± 4% of cells were apoptotic. There were no significant differences for $^{213}BiI_3$, ^{213}Bi-A2, CCs and cells without any reagent incubation.

5.2.3 Morphological changes --Spheroids

The 80 and 150 μm spheroids of BT474 partially disaggregated post-treatment with ^{213}Bi-Herceptin. There were no significant differences in the percentage of apoptosis

cells between 80 and 150 μm spheroids. Cell colony formation was not observed, while many cell colonies formed in all other plates after 2 weeks.

5.2.4 TUNEL assay

The exposed 3'-OH ends of DNA fragments generated by apoptotic DNA cleavage were detected by TUNEL assay, in which the non-apoptotic cells stained green while apoptotic cells stained brown. The results confirmed the Quik-Diff staining results. The percentage of apoptosis and necrosis cells at 72 hours post treatment were listed in Table 5-3.

Table 5-3 The percentage of apoptosis and necrosis cells

	OVCAR3		SKOV3		BT474	
^{213}Bi-Herceptin	12 ± 4	10 ± 6	77 ± 18	13 ± 8	81 ± 16	14 ± 12
Hot control	18± 16	13 ± 8	-	-	-	-
Cold Control	11 ± 6	7 ± 12	12 ± 8	18 ± 12	15 ± 15	14 ± 10

Note: A: percentage of apoptosis; N: percentage of necrosis

5.3 Estrogen implantation subcutaneous model

The tumor uptake rate was 70% -90% for BT474 cells after estrogen implantation.

Figure 5-7 Estrogen implantation

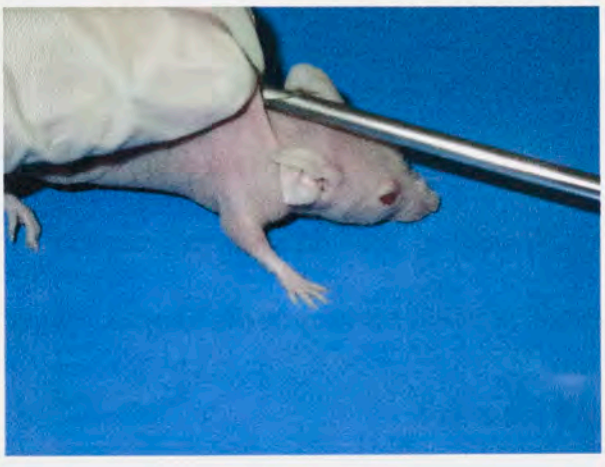

Figure 5-7 Estrogen was implanted subcutaneously via folded neck skin.

5.4 In Vivo

5.4.1 Treatment efficacy in a mice subcutaneous model

The median survival was 82.5 days for control. There were 7 out of 10 mice developed tumour in control group only. Two out of 6 mice have developed tumour in 237 MBq/kg group, whereas no tumour developed in the other treated groups. The survival medians were undefined for 237, 355, and 474 MBq/kg groups. There were significant differences between all four groups (P = 0.04) using chi square test. The every two group comparison results are listed in Table 5-4.

Table 5-4 Significance table

	355 MBq/kg	474 MBq/kg	Cold control
P related to 237 MBq/kg (95% CI of ration)	0.17 (Undefined) ns	0.17 (Undefined) ns	0.12 (0.09 to 1.3) ns
P related to 355 MBq/kg (95% CI of ration)	-	1 (0-0) ns	0.01 (0.03 to 0.6) *
P related to 474 MBq/kg (95% CI of ration)	-	-	0.01 (0.03 to 0.6) *

Note: CC cold control mix; C: without any treatment. CI: confidence interval. P value summary: * statistic difference; ** significant difference; ns: no significant difference.

Figure 5-8 Treatment efficacy of ^{213}Bi-Herceptin

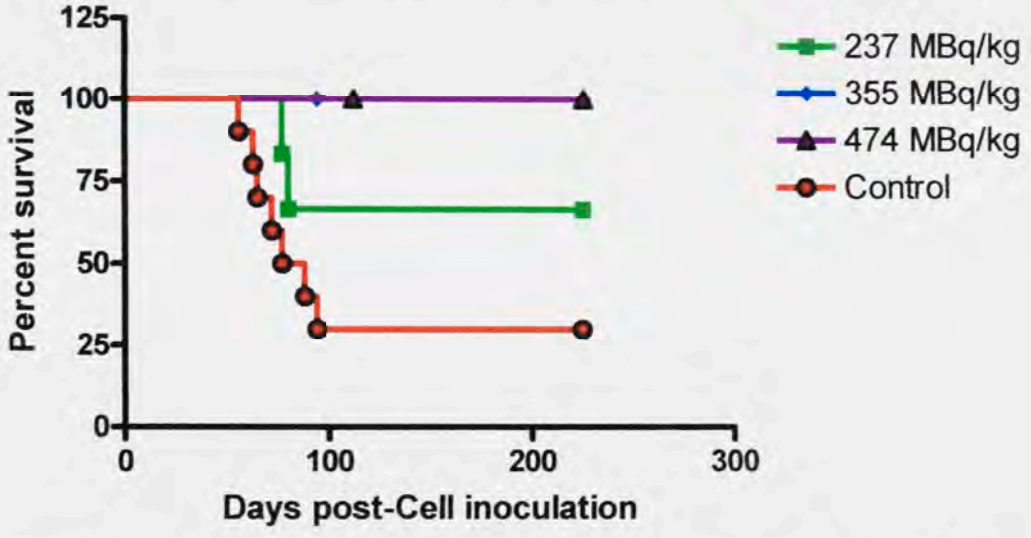

Figure 5-8 Kaplan-Meier survival curve indicate the percentage of survival.

5.4.2 Toxicity of ^{213}Bi-Herceptin in mice

Observation up to 90 days Toxicity after i.p injection of 355 - 1420 MBq/kg ^{213}Bi-Herceptin was measured as leukocyte depression in peripheral blood at 2 and 7 days post-injection, with leukocyte recovery occurring at 2 weeks. Mice in 355 MBq/kg group found to be well after the injection experienced increasing body weight to 90 days. While mice in 710 - 1420 MBq/kg groups lost the normal growth pattern. Mice lost body weight dramatically at 47 days post injection in Figure 5-9, A. Median survival for 1420 MBq/kg group was 79 days, while it was undefined for control and other tested groups ($P = 0.013$, chi square = 6.132). There were no significant differences between other tested and control groups ($P > 0.05$) (Figure 5-9, B). 4 out of 5 mice in 1420 MBq/kg group loss more than 20% body weight post treatment, while one of 5 mice in 1065 MBq/kg group and non mice died in other groups. As a such, the maximum tolerance dose could be between 710 - 1065 MBq/kg up to 90 days in relation to body weight loss. While mild patch radiation necrosis was found in 355 MBq/kg groups mice and moderate radiation necrosis was found in 710 MBq/kg.

Figure 5-9 Toxicity of ^{213}Bi-Herceptin

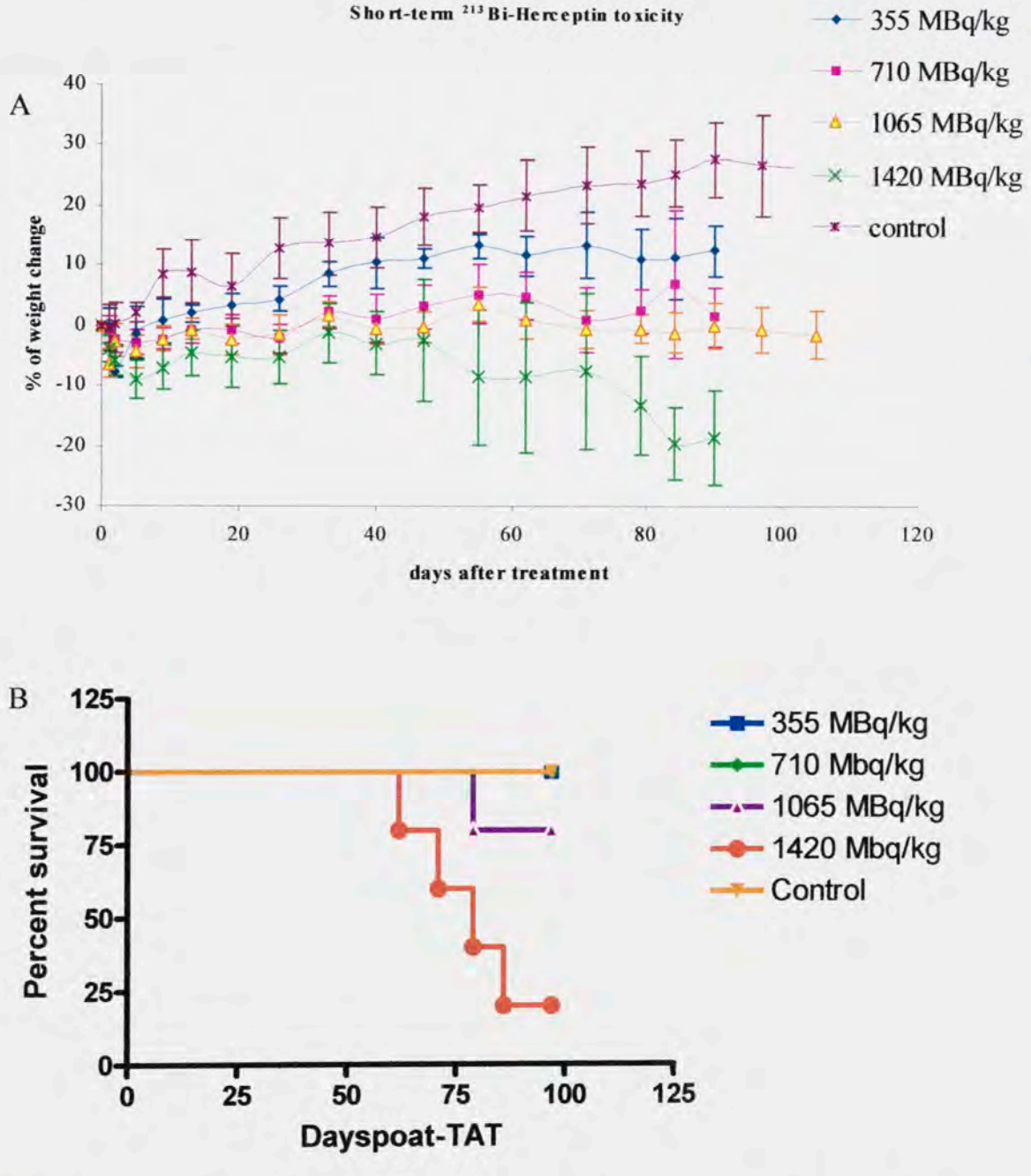

Figure 5-9 A: Mice in 355 MBq/kg group found to be well after the injection experienced increasing body weight to 90 days. While mice in 710 - 1420 MBq/kg groups lost the normal growth pattern. Mice lost body weight dramatically at 47 days post injection. B: Median survival for 1420 MBq/kg group was 79 days, while it was undefined for control and other tested groups ($P = 0.013$, chi square = 6.132). There were no significant differences between other tested and control groups ($P > 0.05$)

Observation up to 240 days. Mice in all groups found to be well after the injection and experienced increasing body weight up to 100 days, as shown in Figure 5-10. While mice in treated groups lost the normal growth patern after 100 days. Mice body weight remained stable up to 225 days for 237 and 355 MBq/kg groups, while body weight start to gradually decrease for 474 MBq/kg group at 100 days and two mice sacrificed due to body weight loss more than 20%. However, there were no mice reached end point in all other groups. Mice were sacrificed at 240 days post-treatment. Radation nephropathy was found from 237 to 474 MBq groups with severity rating of 5 – 7.

Figure 5-10 Long term ^{213}Bi-Herceptin toxicity

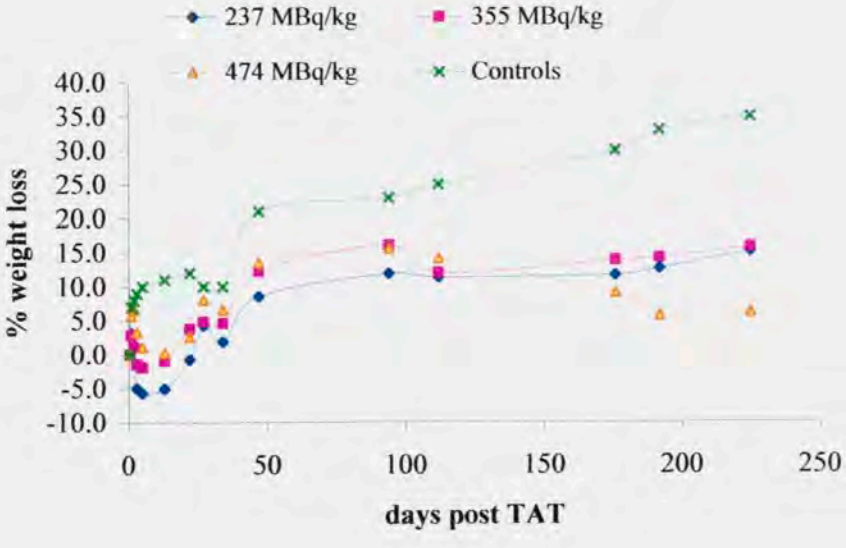

Figure 5-10 Mice in treated groups has shown different grouth patern to compare to control mice.

5.5 Discussion

HER2/neu (p185HER2) oncogene represents an attractive target for antibody-mediated immunotherapy in breast and ovarian cancer treatment. It was reported that a recombinant humanized anti-HER2 MAb such as Herceptin can inhibit the growth of HER2 overexpressing human breast and ovarian cancers (Agus et al., 2000; Baselga et al., 1998; Schaefer et al., 2006). Recently, more sensitive and specific therapeutic procedures such as radiolabeled antibodies, or radioimmunoconjugates, have been shown to be of considerable value for the clinical treatment of cancers (Allen et al., 2005; Jurcic et al., 2002; Jurcic et al., 1997).

TAT is an emerging therapeutic modality wherein labeled MAb selectively targets cancer cells and delivers a lethal payload, which can kill cancer cells in transit or pre angiogenic cell clusters. In a recent study, using ^{213}Bi-Herceptin AC, we successfully targeted breast and prostate cancer cells with HER2 overexpression in vitro (Li et al., 2004). In the present study, we have extended this research to breast in vivo and ovarian cancer in vitro treatment. As a first step, the expression of HER2 on human ovarian and breast cancer cell lines was demonstrated. We confirmed the observations of others, who have shown that HER2 is expressed by BT-474 cells in high levels (Brown, 2002). Furthermore, the target antigen (HER2) cell surface expression in viable ovarian cancer cells using flow cytometry was confirmed. The positive expression of HER2 was found in 11.5% ovarian cancer tissue only. These results indicate that overexpression in human metastatic ovarian and breast cancer cells could be a good target for using radioimmunoconjugates.

The cytotoxicity of ^{213}Bi-Herceptin to ovarian and breast cancer cell line proved to be specific and activity-dependent. Both SK-OV-3 and BT-474 cell lines demonstrated a similar pattern of cell killing because of over-expression of HER2. There was 2.5– 3.0-

fold difference in the 37% survival (D0) values in vitro for the SK-OV-3 and BT-474 cells compared with OV90 cells. Using the highest acitvity (1.2 MBq of ^{213}Bi-Herceptin), only 15–30% treated SKOV3 andBT-474 cells can survive while using the same acitvity in non-specific control (^{213}Bi-A2), 90% treated cells can survive. ^{213}Bi-Herceptin has low D_0 values in SKOV3 and BT- 474 cells and a higher D_0 value in OVCAR3 cells. SKOV3 and BT-474 cells are strongly positive to anti-HER2 MAb, so low activities would be required to kill cancer cells. OV90 cells are weakly positive to anti-HER2 MAb, so high D_0 values would therefore be expected and are observed. These results indicate that a cytotoxicity was specific to HER2 positive cells and directly correlated with the expression level of HER2 on the cancer cells.

In the clinical condition, the main metastatic sites for breast cancer are the lymph nodes and bone marrow. If metastatic cancer cells express a specific surface antigen such as HER2 as a target, TAT should have good potential to target and kill cancer cells in such conditions. In this study, ^{213}Bi-Herceptin AC can target and kill single metastatic breast and ovarian cancer cells (monolayer), and regress breast spheroid growth.

TUNEL positive wells were found in cancer cells, with overexpression of HER2 after incubation with ^{213}Bi-Herceptin. This indicates the cell death is caused by double stranded DNA breaks that initiate this lethal response by α-particles because cells have little ability to repair the damaged DNA, suggesting the cell lethal pathway may involve apoptosis.

The therapy experiments carried out *in vivo* were designed to evaluate the anticancer activity of ^{213}Bi-Herceptin after administration at 2 days post-cell inoculation (oestrogen implantation model) and to optimise the dosage regimen. This s.c animal model needs high level of oestrogen to develop, which can mimic the clinical condition because breast cancer related to estrogen expose.

Our findings indicate that a single i.p injection of ^{213}Bi-Herceptin at a acitvity of 355 MBq/kg can complete regress tumour growth up to 225 days. A acitvity of 237 MBq/kg can delay tumour growth compare to non-treated control group. In this study, the tumour uptake rate in control group was 70%, which may apply to treated groups as well. The results of treated groups may be not accurate due to this reason.

The 90 days short term toxicity study showed that the MTD for weight loss was up to 1065 MBq/kg for nude mice. Leukocyte depression in peripheral blood at 2 and 7 days post-injection was observed, with leukocyte recovery occurring at 2 weeks. Dose-dependent reduction in renal function was manifested as mild to moderate increase in blood urea nitrogen. The histopathological changes were consistent with the decline in renal function as the kidneys showed patchy tubular nephrosis.

The long-term toxicity studies showed that the mice that were asymptomatic at 100 days became symptomatic after 20 weeks and this was manifested by a gradual and continued reduction in their body weight. There were no mice reached endpoint except for two mice in 470 MBq/kg group. MTD was 355 MBq/kg in relation to delayed radiation nephropathy. Mice in 237 and 355 MBq/kg group experienced only a slight body weight loss, and then started to remain stable, suggesting that mice recovered by tubular epithelium regeneration. These findings are consistent with Jaggi et al (Jaggi et al., 2005).

5.6 Conclusion

The *in vitro* conclusions support our *in vivo* results. All of these findings indicate that ^{213}Bi-Herceptin can target and kill cancer cells at the micrometastatic stage, i.e. cells in transit or at the pre-angiogenic stage. The MTD for short term up to 90 days was more than 710 MBq/kg. The acitvity limiting toxicity of long term for ^{213}Bi-Herceptin was nephropathy caused by Bismuth accumulation in the kidney.

CHAPTER 6

Comparison of Vectors

6.1 Background

Peritoneal spread is an important feature in the natural history of ovarian cancer and failure to control disease within the peritoneal cavity is a major cause of treatment failure. Half of these patients relapse with chemo-resistant disease and cannot be rescued by additional therapy (Creemers et al., 1996). Consequently, there is an urgent need for new therapeutic approaches to control metastatic ovarian cancer.

Since the uPA/uPAR complex (Borgfeldt et al., 2003; Konecny et al., 2001), MUC1 (Giuntoli et al., 1998) and HER2 (Skirnisdottir et al., 2001) are related with tumor cell invasion, metastasis and poor prognosis, they are potentially attractive therapeutic targets for alpha particle based targeted therapy (TAT).

In previous chapters, a new loco-regional therapeutic strategy based on cancer specific vectors (C595, Herceptin and PAI2) is reported. These vectors are conjugated to high linear energy transfer alpha emitters to kill isolated cancer cells and cell clusters both in vitro and in vivo.

In this chapter, we compare the use of the two MAbs (C595 and Herceptin) and one protein (PAI2) labeled with Bi-213, to treat OVCAR3 cell line in vitro and in vivo.

6.2 In vitro

The expression of HER2, MUC1 and uPA/uPAR has been determined in the OVCAR-3 cell line and ovarian cancer tissue. uPA is expressed by OVCAR-3, whereas HER2 has low expression, and we have shown for the first time that MUC1 is overexpressed in OVCAR-3. MUC1 was observed with homogeneous expression, whereas uPA had heterogeneous expression.

The strategy of TAT is to select targeting vectors that deliver a cytotoxic reagent to the targeted cells. There was more then a 10 fold difference in the 37% survival (D_0) values *in vitro* for ^{213}Bi-C595 and ^{213}Bi-PAI2 compared with ^{213}Bi-Heceptin, which was negative in OVCAR-3, and the non-specific ^{213}Bi-A2 and $^{213}BiI_4$. These results demonstrate that alpha toxicity must be targeted to be effective. Further, receptor expression must not be negative, as is the case for HER2. ^{213}Bi-Heceptin cytotoxicity is similar to that for the non-specific controls, indicating that there must be significant HER2 expression for ^{213}Bi-Heceptin to be cytotoxic. The activity required to kill 63% of OVCAR-3 cells with ^{213}Bi-PAI2 is almost twice that required with ^{213}Bi-C595, whereas expression of receptors in OVCAR3 was higher with MUC1.

Apoptosis is the major lethal pathway of ^{213}Bi conjugates for cancer cells. However, we also found about 10% of cells undergo necrosis at 24 hours post-incubation, suggesting that the ACs can also cause cell membrane damage and induce necrosis. The percentage of necrotic cells remained stable at 24 and 72 h post-treatment, while the percentage of apoptotic cells increased by ~ 40 % from 24 h to 72 h for both ^{213}Bi-PAI2 and ^{213}Bi-C595. The apoptotic morphological change may not be observable at the early stage of apoptosis, which might be the reason for apoptosis cell number increasing at 72 h.

Many factors including antigen affinity and antigen density play an important role in cell death, since those with high density attract more ACs and those with higher antigen

affinity may "hold on" to increased levels of radioactivity for a longer time period, allowing endocytosis to occur. The relative importance of these factors (antigen density, antigen affinity and endocytosis) in the lethal process has not yet been determined. ^{213}Bi-C595 has superior lethality to ^{213}Bi-PAI2 at the same activity, because of the homogenous high expression of MUC1 compared with the moderate heterogeneous expression of uPA.

The short half life of Bi-213 (46 min) could limit cytotoxicity at depth in cell clusters. To investigate this situation, cells were grown in monolayer, 80 and 150 μm spheroids and treated with ACs. The percentage of monolayer apoptotic cells was not significantly different, indicating that penetration of the ACs into the spheroids was not a limiting factor. The percentage of monolayer apoptotic cells was significantly lower for ^{213}Bi-PAI2 than for ^{213}Bi-C595, as expected from the higher D_0.

These data show that if significant expression of the target receptor occurs, then targeted alpha therapy is completely cytotoxic to all cells in cell clusters up to 150 μm in diameter, the maximum size observed in an ascites nude mouse model (unpublished data).

The expression of MUC1 was high in 26 ovarian cancer patients, whereas only 1 patient expressed moderate HER2. Herceptin studies in vivo were not undertaken in the developed OVCAR 3 ascites model, because of the low expression in this cell line and in ovarian cancer tissue.

6.3 In vivo

The pharmacokinetic studies have shown that kidney was the major activity accumulation organ for ^{213}Bi-C595 and ^{213}Bi-PAI2. ^{213}Bi-PAI2 has higher accumulation than ^{213}Bi-C595, as PAI2, with molecular weight of 47 kD can be filtrated via kidney glomeruli and reabsorbed by tubular epithelium causing kidney accumulation of activities. ^{213}Bi-C595, with a molecular weight of 180 kD, could not be filtered via kidney glomeruli. As a result, the kidney uptake was lower for ^{213}Bi-C595. The same injected activity of ^{213}Bi-PAI2 and ^{213}Bi-C595 gives different kidney absorbed dose of 11.5 Gy for PAI2 and 0.5 Gy for C595 only. Stability of ^{213}Bi-C595 and ^{213}Bi-PAI2 in the circulation is necessary to assure effective drug delivery to the cancer cells in transit or in the organs apart from the surface of peritoneal cavity. In OVCAR3 ascites model, the majority of cancer cells should remain in peritoneal cavity, as a result the major targeting tumor site should be ascites. A high tumor: blood activity ratio was considered to be an ideal. The conjugates should not have accelerated clearance to ensure enough activity in the blood circulation to target and kill cancer cells in transit. Biodistribution studies have shown that ^{213}Bi-C595 has a stable blood concentration and high tumour: blood ratio of 5.8, whereas ^{213}Bi-PAI2 showed accelerated blood clearance and high kidney uptake. OVCAR3 cells overexpress MUC1 (+++) and uPA (++), as such, in this animal model the ascites uptake of ^{213}Bi-C595 should be higher than for ^{213}Bi-PAI2.

In summary, there was no significant difference in toxicity between the three vectors in the short term, all being tolerated well up to 1180 MBq/kg. The long term toxicity of ^{213}Bi-C595 was more than 1180 MBq/kg. This was much higher than for ^{213}Bi-Herceptin (MW 180 kD) and PAI2 (47 kD), each with 355 MBq/kg as the MTD.

The properties of the three vectors are compared in Table 6-1.

6.4 Conclusion

C595 is a specific targeting vector for ovarian cancer, which shows a high percentage of expression. MUC1 in ^{213}Bi-C595 can effectively target and kill ovarian cancer cells in a dose dependent fashion in vitro and in vivo. The pharmacokinetics studies indicate that ^{213}Bi-C595 has higher tumour specific uptake with more stable blood concentration then ^{213}Bi-PAI2, and shows less toxicity. Therefore, ^{213}Bi-C595 is the to be strongly recommended for Phase I clinical trail out of three tested conjugates for ovarian cancer. The application of Lysine can reduce renal uptake by three fold, thus the pre-lysine administration may be considered in clinical investigations.

Table 6-1 Comparison of targeting vectors

In vitro cancer cell lines												
	uPA-PAI2				**MUC1-C595**				**HER2-Herceptin**			
Cell lines	OVCAR3	SKOV3	OV90	BT474	OVCAR3	SKOV3	OV90	BT474	OVCAR3	SKOV3	OV90	BT474
Immunocytochemistry	++	++	-	++	+++	++	+	++	-	+++	-	++
Flow cytometry	64%	57%	12%	NA	98%	72%	41%	NA	6%	99.6%	43%	NA
Xenograft model	++	++	NA	++	+++	++	NA	++	-	+++	NA	++
Cytotoxicity (D_0)	0.51	0.36	5.3	0.53	0.31± 0.03	0.3± 0.05	1.3±0.2	0.5±0.1	4.4±0.5	0.3±0.05	4.6±0.4	0.53±0.1
Apoptosis cells (%)	68±7	NA	NA	NA	80±6	NA	NA	NA	12±4	77±18	NA	81±16
Ovarian cancer patient tissues												
	uPA-PAI2				**MUC1-C595**				**HER2-Herceptin**			
Staining intensity	+++	++	+	-	+++	++	+	-	+++	++	+	-
Ovarian cancer tissue	4	5	3	14	7	10	2	7	0	1	2	23
Omentum	1	0	0	10	1	3	1	6	0	0	0	11

In vivo studies									
	uPA-PAI2				**MUC1-C595**		**HER2-Herceptin**		
	Toxicity (MBq/kg)								
MTD by Body weight loss (90 d)	More than 1420 MBq/kg				More than 1180 MBq/kg		710 MBq/kg < MTD < 1065 MBq/kg		
MTD by radiation nephropathy (210 d)	355 MBq/kg				More than 1180 MBq/kg		355 MBq/kg		
Severity of radiation nephropathy (710 Mbq/kg)	355 MBq/kg	470 MBq/kg	590 MBq/kg	710 MBq/kg	710 MBq/kg	1180 MBq/kg	237 Mbq/kg	355 MBq/kg	470 MBq/kg
	Mild	Mild	Moderate	Severe	No	Mild	Moderate	Moderate	Severe
	Treatment efficacy in aOVCAR3 ascites model								
Treatment activity	355 MBq/kg	710 MBq/kg	1065 MBq/kg	355 MBq/kg	710 MBq/kg	1065 MBq/kg	NA		
Median survival	41.5 days	50 days	NA	49 days	52 days	69 days	NA		
	Pharmacokinetics studies								
Tumour: blood ratio	NA				5.8:1		NA		
Kidney uptake (470 MBq/kg)	15%ID/g				7%ID/g		NA		
Kidney absorbed dose (470 MBq/kg)	11.5 Gy				0.5 Gy		NA		

Chapter 7

Dosimetry

Introduction

As ^{213}Bi based radioimmunotherapy is in clinical trial and as the therapy has the potential to be used in the clinical trial for ovarian cancer, it is important to have the estimation of the radiation dose to the patient should be determined. Although some dose estimation studies have been performed, cytological evaluation of radiation reduced cytogenetic damage to non-targeted lymphocytes in vivo after therapy with bismuth conjugates has not yet been performed.

This is another method, which provides the estimation of dose. Models for inhomogeneous radionuclide distribution in tumors have also been proposed (Goddu et al., 1994). The MIRD model and a Monte Carlo transport code for electrons and photons have been used in *in vivo* experiments for dose determination after α-particle irradiation (Behr et al., 1999; Gratz et al., 1999; Kennel et al., 1999).

For common radionuclide therapies, such as ^{131}I therapy for thyroid disease and ^{89}Sr therapy for pain palliation of bone metastases, examination of the radiation dose to lymphocytes has been performed using the cytokinesis blocked micronucleus assay (Grawe et al., 2005; Monsieurs et al., 2003; Monsieurs et al., 2001; Watanabe et al., 1998).

Cytological evaluation of radiation induced cytogenetic damage to lymphocytes in vivo after therapy with ^{213}Bi-RIC has not yet been performed.

The purpose of this study was primarily an evaluation of the degree of cytological radiation induced damage to lymphocytes in vivo after ^{213}Bi-RIC therapy for melanoma using the cytokinesis blocked micronucleus assay. Secondly, the genetic damage to the lymphocytes was correlated with the total body dose calculated according to the Medical Internal Radiation Dosimetry (MIRD) formalism.

7.1 In vitro

Methods: Described in chapter 2.2.9.

Results: An average 18 MN (SD 10) per thousand BNC was found in 3 healthy volunteers. There were no significant differences in micronucleus yields in vitro for blood samples treated with 10-240 kBq of ^{213}Bi and ^{213}Bi-9.2.27, shown in Figure 7-1, as the 9.2.27 MAb is not specific for lymphocytes. After blood incubation with ^{213}Bi, the number of micronuclei increases with radiation activity. A dose response curve with linear dose relationship was observed up to 125 kBq/mL, and sublinear at higher doses, as shown in Figure 7-2. Figure 7-3 showed typical micronucleus images. The results indicate that this method can be used for the ovarian cancer trial.

Figure 7-1 The number of CBMN yield in vitro after ^{213}Bi-9.2.27 and ^{213}Bi treatment

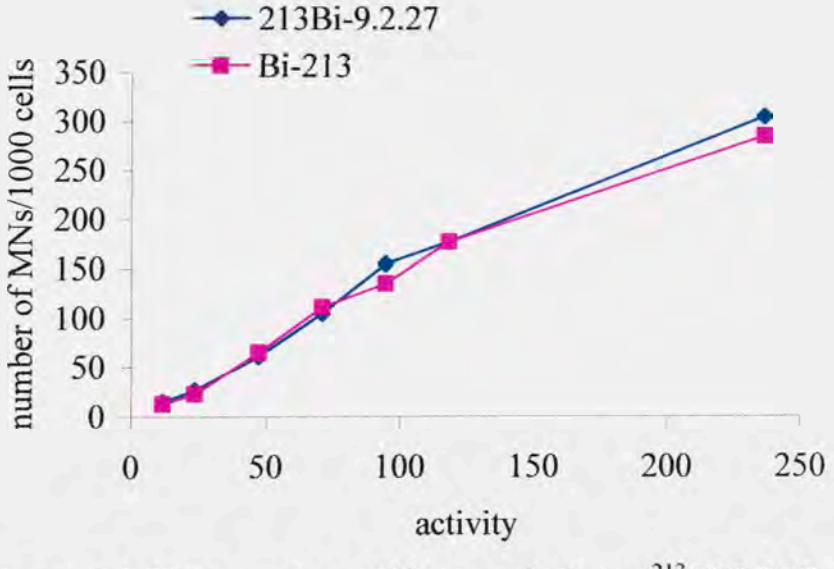

Figure 7-1 There were no differences between ^{213}Bi-9.2.27 and ^{213}Bi, as both of them are non-specific for lymphocytes.

Figure 7-2 The frequency of MN in vitro

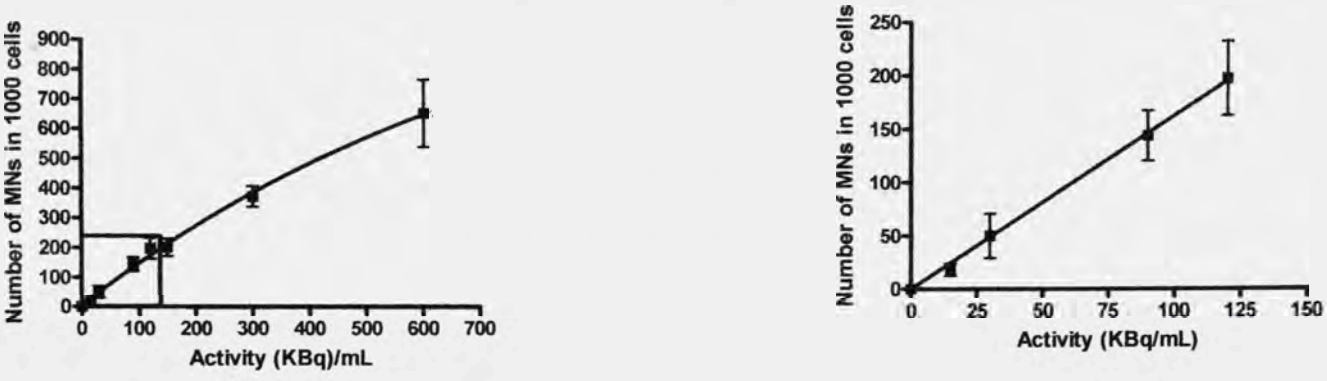

Figure 7-2 A dose response curve with linear dose relationship was observed up to 125 kBq/mL, with sublinear response at higher doses.

Figure 7-3 Cells with MN

A

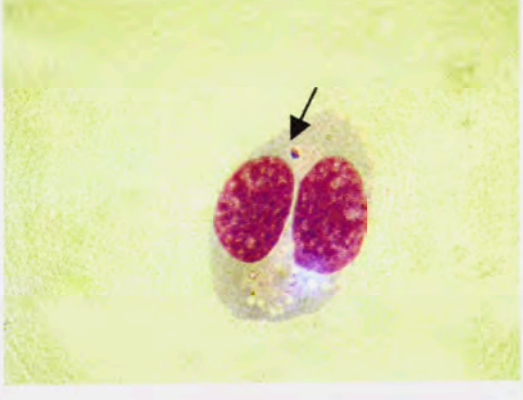

B

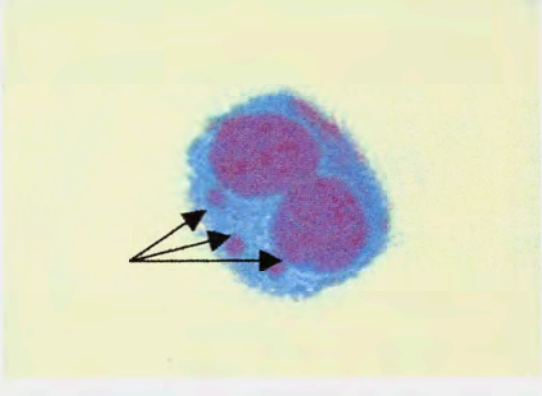

Figure 7-3 Cell A with one micronuclei, cell B with three micronucleus, ▲ points to MNs.

Table 7-1 The frequency of MNs after ^{213}Bi inoculation

	Activities of ^{213}Bi (kBq/mL)									
	0	15	30	60	90	120	150	300	600	1200
Subject 1	15	30	42	72	120	170	192	320	805	1090
Subject 2	34	44	65	-	221	-	199	422	546	-
Subject 3	10	40	102	66	150	250	270	430	-	-
Average	20	38	70	69	164	210	220	391	676	
Average increase	0	18	50	49	144	190	200	371	656	
SD	12.7	7.2	30.3		51.9		43.2	61.3		

7.2 In TAT patients

Methods: Described in chapter 2.3.1.

Results: Five patients received doses of ^{213}Bi-9.2.27 injection (Table 7-2). The micronucleus yields before and after therapy are plotted against time in Figure 7-4. As can be seen in Figure 7-4, the increase in micronucleus yield at 3 hours after administration of the therapeutic activity has reached at the peak. The number of micronuclei decreased at 2 weeks time and fully recovered to baseline at 4 weeks time after administration of ^{213}Bi-9.2.27.

As can been seen from Figure 7-4, the micronucleus yield in 5 patients was significantly ($P < 0.001$) increased after ^{213}Bi-9.2.27 therapy. The mean increase was 33.6 micronuclei (SD = 8) for patients. The relationship between the number of MNs and the injected activities is shown in Figure 7-5. A dose response was observed as shown in Table 7-2, and Figure 7-5.

Figure 7-4 MNs yield in trial patients

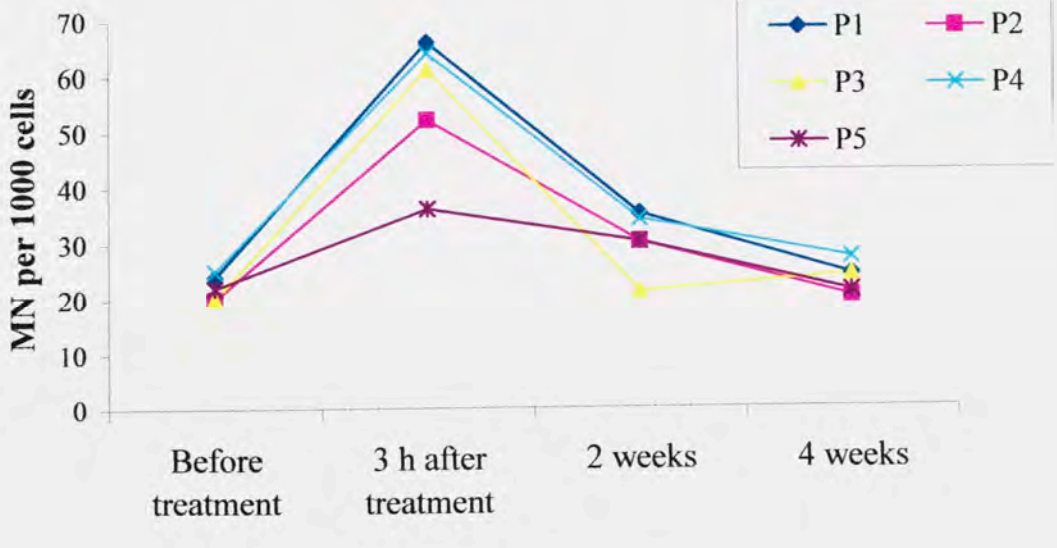

Table 7-2 Overview of the demographic data and results

Patients	Age (years)	Gender	Activity (MBq)	MN		
				Before treatment	3h post-treatment	Increase
1	74	F	276	24	66	44
2	82	F	258	20	52	32
3	45	F	350	20	61	41
4	47	F	363	25	64	39
5	84	F	263	22	36	14
Average			300	22	56	34 (SD12)

Figure 7-5 The relationship of activities and number of MNs

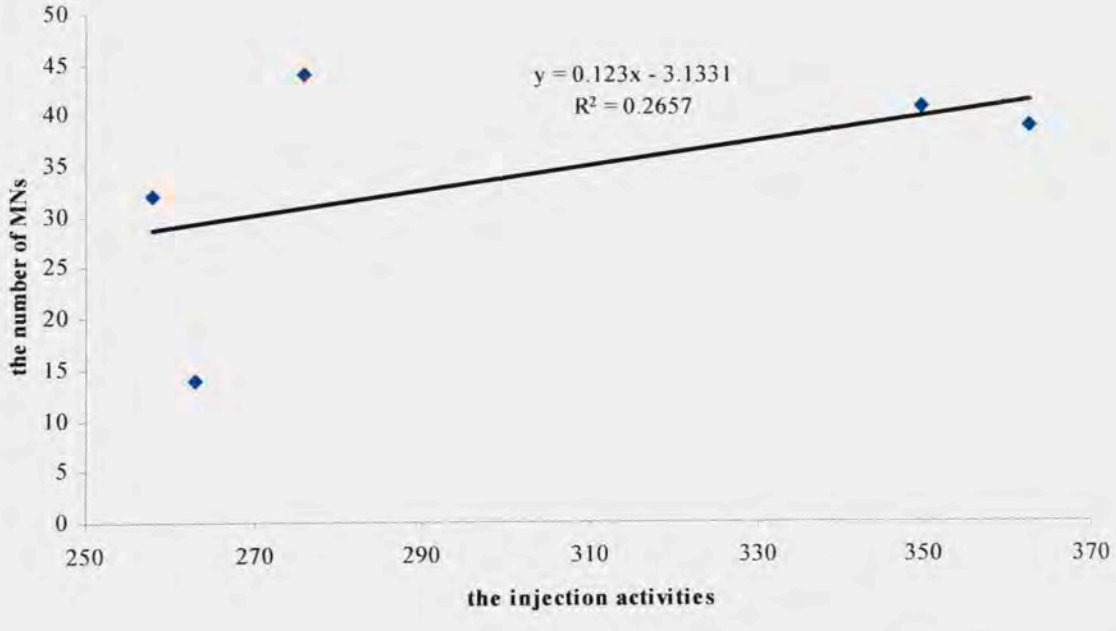

Figure 7-5 A dose response was observed. The number of MNs increased while the activities raised.

Dose calculation according to the MIRD formalism

Method: Described in Chapter 2.4.7. A 70 kg man has 5 L of blood, we assume that all the activity injected in patient remains in the blood. A = 300 MBq/5L =60 KBq/mL, E = 10.33 MeV. 1 mL of blood was used for micronuclei assy.

Results: The average absorbed dose for 1 mL of blood of 5 treated patients is 0.1 ± 0.016Gy according to the MIRD formula.

7.3 Discussion

Some of the studied patients had received chemotherapy at a certain time before ^{213}Bi-9.2.27. Chemotherapy inhibits cell division when cells are stimulated by the phytohaemaglutinin that is added to the culture medium (Monsieurs et al., 2001). For patients 6 and 7, we were not able to induce 1000 cells to divide in each fraction, and therefore their data have to be excluded from this study. Patient 1 blood samples for absorbed dose calculation was collected half hour behind schedule compare to the other patients, so the activity in early time was uncertain. These data for the absorbed dose calculation have been excluded from this study.

The residual damage after ^{213}Bi-9.2.27 therapy was investigated for the first time in the present study. An initial increase in micronucleus yield after administration of ^{213}Bi-9.2.27 was observed in all patients, followed by recovery to the baseline values at 4 weeks post-injection. The biological dosimeter could be used for multiple treatments.

A comparison of the radiation-induced increase in micronuclei after in vivo and in vitro irradiation showed that there was no significant difference between these two conditions (Gantenberg et al., 1991). Therefore the dose response curves obtained after in vitro irradiation can be used for calibration in order to estimate radiation doses after in vivo incubation.

The mean increase in micronuclei yield after in vitro irradiation with 0.5 Gy and 1 Gy ^{60}Co was 40 micronuclei (SD 26) and 97 micronuclei (SD30) respectively (Monsieurs et al., 2001). For the same number of micronuclei induced from ^{60}Co (0.5 Gy; MNs: 40 ± 26) and alpha particles (0.1±0.016 Gy; MNs: 34 ±12) will reflex the RBE value of alpha particle. The RBE value for α particle in this study was 5 ±1.

BIBLIOGRAPHY

Abbas Rizvi, S.M., Sarkar, S., Goozee, G. & Allen, B.J. (2000). Radioimmunoconjugates for targeted alpha therapy of malignant melanoma. *Melanoma Res*, **10,** 281-9.

Adams, G.P. & Schier, R. (1999). Generating improved single-chain Fv molecules for tumor targeting. *Journal of Immunological Methods*, **231,** 249-60.

Agrawal, B., Gendler, S.J. & Longenecker, B.M. (1998). The biological role of mucins in cellular interactions and immune regulation: prospects for cancer immunotherapy. *Molecular Medicine Today*, **4,** 397-403.

Agus, D.B., Bunn, P.A., Jr., Franklin, W., Garcia, M. & Ozols, R.F. (2000). HER-2/neu as a therapeutic target in non-small cell lung cancer, prostate cancer, and ovarian cancer. *Seminars in Oncology*, **27,** 53-63; discussion 92-100.

Akiyama, T., Sudo, C., Ogawara, H., Toyoshima, K. & Yamamoto, T. (1986). The product of the human c-erbB-2 gene: a 185-kilodalton glycoprotein with tyrosine kinase activity. *Science*, **232,** 1644-6.

Al-Ejeh, F., Croucher, D. & Ranson, M. (2004). Kinetic analysis of plasminogen activator inhibitor type-2: urokinase complex formation and subsequent internalisation by carcinoma cell lines. *Experimental Cell Research*, **297,** 259-71.

Allen, B. & Blagojevic, N. (1997). Alpha and beta emitting radiolanthanides in targeted cancer therapy. *Nucl Med Commun*, **20,** 205-207.

Allen, B.J. (1999). Can alpha-immunotherapy succeed where other systemic modalities have failed? *Nuclear Medicine Communications*, **20,** 205-7.

Allen, B.J. & Blagojevic, N. (1996). Alpha- and beta-emitting radiolanthanides in targeted cancer therapy: the potential role of terbium-149. *Nucl Med Commun*, **17,** 40-7.

Allen, B.J., Raja, C., Rizvi, S., Li, Y., Tsui, W., Graham, P., Thompson, J.F., Reisfeld, R.A. & Kearsley, J. (2005). Intralesional targeted alpha therapy for metastatic melanoma. *Cancer Biol Ther*, **4,** 1318-24.

Allen, B.J., Raja, C., Rizvi, S., Li, Y., Tsui, W., Zhang, D., Song, E., Qu, C.F., Kearsley, J., Graham, P. & Thompson, J. (2004). Targeted alpha therapy for cancer. *Phys Med Biol*, **49,** 3703-12.

Allen, B.J., Rizvi, S., Li, Y., Tian, Z. & Ranson, M. (2001). In vitro and preclinical targeted alpha therapy for melanoma, breast, prostate and colorectal cancers. *Crit Rev Oncol Hematol*, **39,** 139-46.

Allen, B.J., Tian, Z., Rizvi, S.M., Li, Y. & Ranson, M. (2003a). Preclinical studies of targeted alpha therapy for breast cancer using 213Bi-labelled-plasminogen activator inhibitor type 2. *British Journal of Cancer*, **88,** 944-50.

Almqvist, Y., Orlova, A., Sjostrom, A., Jensen, H.J., Lundqvist, H., Sundin, A. & Tolmachev, V. (2005). In vitro characterization of 211 At-labeled antibody A33--a potential therapeutic agent against metastatic colorectal carcinoma. *Cancer Biother Radiopharm*, **20,** 514-23.

Andersson, M., Carstensen, B. & Visfeldt, J. (1993). Leukemia and other related hematological disorders among Danish patients exposed to Thorotrast. *Radiat Res*, **134,** 224-33.

Andreasen, P.A., Kjoller, L., Christensen, L. & Duffy, M.J. (1997). The urokinase-type plasminogen activator system in cancer metastasis: a review. *International Journal of Cancer*, **72,** 1-22.

Apostolidis, C., Molinet, R., McGinley, J., Abbas, K., Mollenbeck, J. & Morgenstern, A. (2005). Cyclotron production of Ac-225 for targeted alpha therapy. *Applied Radiation & Isotopes*, **62,** 383-7.

Arano, Y., Uezono, T., Akizawa, H., Ono, M., Wakisaka, K., Nakayama, M., Sakahara, H., Konishi, J. & Yokoyama, A. (1996). Reassessment of diethylenetriaminepentaacetic acid (DTPA) as a chelating agent for indium-111 labeling of polypeptides using a newly synthesized monoreactive DTPA derivative. *Journal of Medicinal Chemistry*, **39,** 3451-60.

Aurlien, E., Larsen, R.H., Akabani, G., Olsen, D.R., Zalutsky, M.R. & Bruland, O.S. (2000). Exposure of human osteosarcoma and bone marrow cells to tumour-targeted alpha-particles and gamma-irradiation: analysis of cell survival and microdosimetry. *Int J Radiat Biol*, **76,** 1129-41.

Avichezer, D., Springer, G.F., Schechter, B. & Arnon, R. (1997). Immunoreactivities of polyclonal and monoclonal anti-T and anti-Tn antibodies with human carcinoma cells, grown in vitro and in a xenograft model.[erratum appears in

Int J Cancer 1997 Sep 4;72(5):918]. *International Journal of Cancer.*, **72,** 119-27.

Azure, M.T., Archer, R.D., Sastry, K.S., Rao, D.V. & Howell, R.W. (1994). Biological effect of lead-212 localized in the nucleus of mammalian cells: role of recoil energy in the radiotoxicity of internal alpha-particle emitters. *Radiat Res*, **140,** 276-83.

Back, T., Andersson, H., Divgi, C.R., Hultborn, R., Jensen, H., Lindegren, S., Palm, S. & Jacobsson, L. (2005). 211At Radioimmunotherapy of Subcutaneous Human Ovarian Cancer Xenografts: Evaluation of Relative Biologic Effectiveness of an {alpha}-Emitter In Vivo. *J Nucl Med*, **46,** 2061-2067.

Bajou, K., Noel, A., Gerard, R.D., Masson, V., Brunner, N., Holst-Hansen, C., Skobe, M., Fusenig, N.E., Carmeliet, P. & Collen et, a. (1998). Absence of host plasminogen activator inhibitor 1 prevents cancer invasion and vascularization. *Nature Medicine*, **4,** 923-928.

Ballangrud, A.M., Yang, W.-H., Charlton, D.E., McDevitt, M.R., Hamacher, K.A., Panageas, K.S., Ma, D., Bander, N.H., Scheinberg, D.A. & Sgouros, G. (2001). Response of LNCaP Spheroids after Treatment with an {{alpha}}-Particle Emitter (213Bi)-labeled Anti-Prostate-specific Membrane Antigen Antibody (J591). *Cancer Res*, **61,** 2008-2014.

Barendsen, G.W. (1994). The relationships between RBE and LET for different types of lethal damage in mammalian cells: biophysical and molecular mechanisms. *Radiat Res*, **139,** 257-70.

Baruch, A., Hartmann, M., Yoeli, M., Adereth, Y., Greenstein, S., Stadler, Y., Skornik, Y., Zaretsky, J., Smorodinsky, N.I., Keydar, I. & Wreschner, D.H. (1999). The breast cancer-associated MUC1 gene generates both a receptor and its cognate binding protein. *Cancer Research*, **59,** 1552-61.

Baselga, J., Norton, L., Albanell, J., Kim, Y.M. & Mendelsohn, J. (1998). Recombinant humanized anti-HER2 antibody (Herceptin) enhances the antitumor activity of paclitaxel and doxorubicin against HER2/neu overexpressing human breast cancer xenografts.[erratum appears in Cancer Res 1999 Apr 15;59(8):2020]. *Cancer Research*, **58,** 2825-31.

Behr, T.M., Behe, M., Stabin, M.G., Wehrmann, E., Apostolidis, C., Molinet, R., Strutz, F., Fayyazi, A., Wieland, E., Gratz, S., Koch, L., Goldenberg, D.M. & Becker, W. (1999a). High-linear energy transfer (LET) alpha versus low-LET

beta emitters in radioimmunotherapy of solid tumors: therapeutic efficacy and dose-limiting toxicity of 213Bi- versus 90Y-labeled CO17-1A Fab' fragments in a human colonic cancer model. *Cancer Res*, **59,** 2635-43.

Behr, T.M. & Boerman, O.C. (1999). 13th Meeting of the International Research Group on Immunoscintigraphy and Immunotherapy (IRIST). 7-8 May 1999, Gottingen, Germany. *Eur J Nucl Med*, **26,** 950-2.

Behr, T.M., Goldenberg, D.M. & Becker, W. (1998). Reducing the renal uptake of radiolabeled antibody fragments and peptides for diagnosis and therapy: present status, future prospects and limitations. *European Journal of Nuclear Medicine.*, **25,** 201-12.

Behr, T.M., Liersch, T., Greiner-Bechert, L., Griesinger, F., Behe, M., Markus, P.M., Gratz, S., Angerstein, C., Brittinger, G., Becker, H., Goldenberg, D.M. & Becker, W. (2002). Radioimmunotherapy of small-volume disease of metastatic colorectal cancer. *Cancer*, **94,** 1373-81.

Behr, T.M., Sgouros, G., Stabin, M.G., Behe, M., Angerstein, C., Blumenthal, R.D., Apostolidis, C., Molinet, R., Sharkey, R.M., Koch, L., Goldenberg, D.M. & Becker, W. (1999b). Studies on the red marrow dosimetry in radioimmunotherapy: an experimental investigation of factors influencing the radiation-induced myelotoxicity in therapy with beta-, Auger/conversion electron-, or alpha-emitters. *Clin Cancer Res*, **5,** 3031s-3043s.

Behr, T.M., Sharkey, R.M., Sgouros, G., Blumenthal, R.D., Dunn, R.M., Kolbert, K., Griffiths, G.L., Siegel, J.A., Becker, W.S. & Goldenberg, D.M. (1997). Overcoming the nephrotoxicity of radiometal-labeled immunoconjugates: improved cancer therapy administered to a nude mouse model in relation to the internal radiation dosimetry. *Cancer*, **80,** 2591-610.

Behr, T.M., Wormann, B., Gramatzki, M., Riggert, J., Gratz, S., Behe, M., Griesinger, F., Sharkey, R.M., Kolb, H.J., Hiddemann, W., Goldenberg, D.M. & Becker, W. (1999c). Low- versus high-dose radioimmunotherapy with humanized anti-CD22 or chimeric anti-CD20 antibodies in a broad spectrum of B cell-associated malignancies. *Clinical Cancer Research*, **5,** 3304s-3314s.

Bernard, B.F., Krenning, E.P., Breeman, W.A., Rolleman, E.J., Bakker, W.H., Visser, T.J., Macke, H. & de Jong, M. (1997). D-lysine reduction of indium-111 octreotide and yttrium-90 octreotide renal uptake. *Journal of Nuclear Medicine*, **38,** 1929-33.

Bethge, W.A., Wilbur, D.S., Storb, R., Hamlin, D.K., Santos, E.B., Brechbiel, M.W., Fisher, D.R. & Sandmaier, B.M. (2003). Selective T-cell ablation with bismuth-213-labeled anti-TCR{alpha}{beta} as nonmyeloablative conditioning for allogeneic canine marrow transplantation. *Blood*, **101,** 5068-5075.

Boll, R.A., Malkemus, D. & Mirzadeh, S. (2005). Production of actinium-225 for alpha particle mediated radioimmunotherapy. *Applied Radiation & Isotopes*, **62,** 667-79.

Borchardt, P.E., Yuan, R.R., Miederer, M., McDevitt, M.R. & Scheinberg, D.A. (2003). Targeted actinium-225 in vivo generators for therapy of ovarian cancer. *Cancer Res*, **63,** 5084-90.

Borgfeldt, C., Bendahl, P.O., Gustavsson, B., Langstrom, E., Ferno, M., Willen, R., Grenman, S. & Casslen, B. (2003). High tumor tissue concentration of urokinase plasminogen activator receptor is associated with good prognosis in patients with ovarian cancer. *International Journal of Cancer*, **107,** 658-65.

Borstnar, S., Vrhovec, I., Svetic, B. & Cufer, T. (2002). Prognostic value of the urokinase-type plasminogen activator, and its inhibitors and receptor in breast cancer patients. *Clinical Breast Cancer*, **3,** 138-46.

Bossard, C., Bieche, I., Le Doussal, V., Lidereau, R. & Sabourin, J.C. (2005). Real-time RT-PCR: a complementary method to detect HER-2 status in breast carcinoma. *Anticancer Research*, **25,** 4679-83.

Boxenbaum, H. (1984). Interspecies pharmacokinetic scaling and the evolutionary-comparative paradigm. *Drug Metabolism Reviews*, **15,** 1071-121.

Bramwell, M.E., Wiseman, G. & Shotton, D.M. (1986). Electron-microscopic studies of the CA antigen, epitectin. *Journal Of Cell Science*, **86,** 249-261.

Brechbiel, M. & Gansow, O. (1992). Synthesis of C-functionalized trans-cyclohexyldiethylenetriaminepentaacetic acids for labeling of monoclonal antibodies with the bismuth-212-a particle emitter. *J Chem Soc Perkin Trans*, **1,** 1173-8.

Brechbiel, M.W. & Gansow, O.A. (1991). Backbone-substituted DTPA ligands for 90Y radioimmunotherapy. *Bioconjug Chem*, **2,** 187-94.

Briand, G.G. & Burford, N. (1999). Bismuth compounds and preparations with biological or medicinal relevance. *Chem Rev*, **99,** 2601-58.

Brown, R.E. (2002). HER-2/neu-Positive breast carcinoma: molecular concomitants by proteomic analysis and their therapeutic implications. *Annals of Clinical & Laboratory Science*, **32,** 12-21.

Bumol, T.F. & Reisfeld, R.A. (1982). Unique Glycoprotein-Proteoglycan Complex Defined by Monoclonal Antibody on Human Melanoma Cells. *PNAS*, **79,** 1245-1249.

Bumol, T.F., Walker, L.E. & Reisfeld, R.A. (1984). Biosynthetic studies of proteoglycans in human melanoma cells with a monoclonal antibody to a core glycoprotein of chondroitin sulfate proteoglycans. *J. Biol. Chem.*, **259,** 12733-12741.

Burchell, J., Gendler, S., Taylor-Papadimitriou, J., Girling, A., Lewis, A., Millis, R. & Lamport, D. (1987). Development and characterization of breast cancer reactive monoclonal antibodies directed to the core protein of the human milk mucin. *Cancer Research*, **47,** 5476-5482.

Caron, P.C., Co, M.S., Bull, M.K., Avdalovic, N.M., Queen, C. & Scheinberg, D.A. (1992). Biological and immunological features of humanized M195 (anti-CD33) monoclonal antibodies. *Cancer Res*, **52,** 6761-7.

Caron, P.C., Jurcic, J.G., Scott, A.M., Finn, R.D., Divgi, C.R., Graham, M.C., Jureidini, I.M., Sgouros, G., Tyson, D., Old, L.J. & et al. (1994). A phase 1B trial of humanized monoclonal antibody M195 (anti-CD33) in myeloid leukemia: specific targeting without immunogenicity. *Blood*, **83,** 1760-8.

Chekenya, M., Rooprai, H.K., Davies, D., Levine, J.M., Butt, A.M. & Pilkington, G.J. (1999). The NG2 chondoitin sulfate proteoglycan: role in malignant progression of human brain tumours. *International Journal of Developmental Neuroscience*, **17,** 421-435.

Chen, D.J., Tsuboi, K., Nguyen, T. & Yang, T.C. (1994). Charged-particle mutagenesis II. Mutagenic effects of high energy charged particles in normal human fibroblasts. *Adv Space Res*, **14,** 347-54.

Choi, D.H., Kim, S., Rimm, D.L., Carter, D. & Haffty, B.G. (2005). Immunohistochemical biomarkers in patients with early-onset breast carcinoma by tissue microarray. *Cancer Journal*, **11,** 404-11.

Christensen, L., Wiborg Simonsen, A.C., Heegaard, C.W., Moestrup, S.K., Andersen, J.A. & Andreasen, P.A. (1996). Immunohistochemical localization of urokinase-type plasminogen activator, type-1 plasminogen-activator inhibitor,

urokinase receptor and alpha(2)-macroglobulin receptor in human breast carcinomas. *International Journal of Cancer*, **66,** 441-52.

Co, M.S., Avdalovic, N.M., Caron, P.C., Avdalovic, M.V., Scheinberg, D.A. & Queen, C. (1992). Chimeric and humanized antibodies with specificity for the CD33 antigen. *J Immunol*, **148,** 1149-54.

Cobb, L.M., Harrison, A. & Butler, S.A. (1988). Toxicity of astatine-211 in the mouse. *Hum Toxicol*, **7,** 529-34.

Cohen, J.A., Weiner, D.B., More, K.F., Kokai, Y., Williams, W.V., Maguire, H.C., Jr., LiVolsi, V.A. & Greene, M.I. (1989). Expression pattern of the neu (NGL) gene-encoded growth factor receptor protein (p185neu) in normal and transformed epithelial tissues of the digestive tract. *Oncogene*, **4,** 81-8.

Coussens, L., Yang-Feng, T.L., Liao, Y.C., Chen, E., Gray, A., McGrath, J., Seeburg, P.H., Libermann, T.A., Schlessinger, J., Francke, U. & et al. (1985). Tyrosine kinase receptor with extensive homology to EGF receptor shares chromosomal location with neu oncogene. *Science*, **230,** 1132-9.

Couturier, O., Faivre-Chauvet, A., Filippovich, I.V., Thedrez, P., Sai-Maurel, C., Bardies, M., Mishra, A.K., Gauvrit, M., Blain, G., Apostolidis, C., Molinet, R., Abbe, J.C., Bataille, R., Wijdenes, J., Chatal, J.F. & Cherel, M. (1999). Validation of 213Bi-alpha radioimmunotherapy for multiple myeloma. *Clin Cancer Res*, **5,** 3165s-3170s.

Couturier, O., Supiot, S., Degraef-Mougin, M., Faivre-Chauvet, A., Carlier, T., Chatal, J.-F., Davodeau, F. & Cherel, M. (2005). Cancer radioimmunotherapy with alpha-emitting nuclides. *European Journal of Nuclear Medicine & Molecular Imaging*, **32,** 601-14.

Creemers, G.J., Bolis, G., Gore, M., Scarfone, G., Lacave, A.J., Guastalla, J.P., Despax, R., Favalli, G., Kreinberg, R., Van Belle, S., Hudson, I., Verweij, J. & Ten Bokkel Huinink, W.W. (1996). Topotecan, an active drug in the second-line treatment of epithelial ovarian cancer: results of a large European phase II study. *J Clin Oncol*, **14,** 3056-61.

Davis, I.A. & Kennel, S.J. (1999). Radioimmunotherapy using vascular targeted 213Bi: the role of tumor necrosis factor alpha in the development of pulmonary fibrosis. *Clin Cancer Res*, **5,** 3160s-3164s.

de The, H., Chomienne, C., Lanotte, M., Degos, L. & Dejean, A. (1990). The t(15;17) translocation of acute promyelocytic leukaemia fuses the retinoic acid receptor alpha gene to a novel transcribed locus. *Nature*, **347,** 558-61.

DeNardo, S.J., Kroger, L.A. & DeNardo, G.L. (1999). A new era for radiolabeled antibodies in cancer? *Curr Opin Immunol*, **11,** 563-9.

Denton, G. & Price, M.R. (1995). Immune Responses to the MUC1 Mucin. *Pathol Oncol Res*, **1,** 27-31.

Devine, P.L. & McKenzie, I.F. (1992). Mucins: structure, function, and associations with malignancy. *BioEssays: News And Reviews In Molecular, Cellular And Developmental Biology*, **14,** 619-625.

Devys, A., Thedrez, P., Gautherot, E., Faivre-Chauvet, A., Sai-Maurel, C., Rouvier, E., Auget, J.L., Barbet, J. & Chatal, J.F. (1996). Comparative targeting of human colon-carcinoma multicell spheroids using one- and two-step (bispecific antibody) techniques. *International Journal of Cancer*, **67,** 883-91.

Dublin, E., Hanby, A., Patel, N.K., Liebman, R. & Barnes, D. (2000). Immunohistochemical expression of uPA, uPAR, and PAI-1 in breast carcinoma. Fibroblastic expression has strong associations with tumor pathology. *American Journal of Pathology*, **157,** 1219-27.

Eisenmann, K.M., McCarthy, J.B., Simpson, M.A., Keely, P.J., Guan, J.L., Tachibana, K., Lim, L., Manser, E., Furcht, L.T. & Iida, J. (1999). Melanoma chondroitin sulphate proteoglycan regulates cell spreading through Cdc42, Ack-1 and p130cas. *Nat Cell Biol*, **1,** 507-13.

Elgqvist, J., Bernhardt, P., Hultborn, R., Jensen, H., Karlsson, B., Lindegren, S., Warnhammar, E. & Jacobsson, L. (2005). Myelotoxicity and RBE of 211At-Conjugated Monoclonal Antibodies Compared with 99mTc-Conjugated Monoclonal Antibodies and 60Co Irradiation in Nude Mice. *J Nucl Med*, **46,** 464-471.

Engelholm, L.H., Nielsen, B.S., Dano, K. & Behrendt, N. (2001). The Urokinase Receptor Associated Protein (uPARAP/Endo180): A Novel Internalization Receptor Connected to the Plasminogen Activation System. *Trends in Cardiovascular Medicine*, **11,** 7-13.

Essand, M., Gronvik, C., Hartman, T. & Carlsson, J. (1995). Radioimmunotherapy of prostatic adenocarcinomas: effects of 131I-labelled E4 antibodies on cells at

different depth in DU 145 spheroids. *International Journal of Cancer.*, **63,** 387-94.

Fenech, M. (2000). The in vitro micronucleus technique. *Mutation Research*, **455,** 81-95.

Feng, H., Ghazizadeh, M., Konishi, H. & Araki, T. (2002). Expression of MUC1 and MUC2 mucin gene products in human ovarian carcinomas. *Jpn J Clin Oncol*, **32,** 525-9.

Ferrone, S., Temponi. M, Gargiulo. D, Scassellati. G.A, Cavaliere.R & P.G., N. (1988). *Selection and utilization of monoclonal antibody defined melanoma associated antigens for immunoscintigraphy in patients with melanoma. Radiolabeled Monoclonal Antibodies for Imaging and Therapy.* . Vol. 152.S.C. Plenum Publishing Corp: New York/London.

Fisher, J.L., Field, C.L., Zhou, H., Harris, T.L., Henderson, M.A. & Choong, P.F. (2000). Urokinase plasminogen activator system gene expression is increased in human breast carcinoma and its bone metastases--a comparison of normal breast tissue, non-invasive and invasive carcinoma and osseous metastases. *Breast Cancer Research & Treatment*, **61,** 1-12.

Folkard, M., Vojnovic, B., Prise, K.M., Bowey, A.G., Locke, R.J., Schettino, G. & Michael, B.D. (1997). A charged-particle microbeam: I. Development of an experimental system for targeting cells individually with counted particles. *Int J Radiat Biol*, **72,** 375-85.

Friedberg, E.C., Bardwell, A.J., Bardwell, L., Feaver, W.J., Kornberg, R.D., Svejstrup, J.Q., Tomkinson, A.E. & Wang, Z. (1995). Nucleotide excision repair in the yeast Saccharomyces cerevisiae: its relationship to specialized mitotic recombination and RNA polymerase II basal transcription. *Philos Trans R Soc Lond B Biol Sci*, **347,** 63-8.

Gantenberg, H.W., Wuttke, K., Streffer, C. & Muller, W.U. (1991). Micronuclei in human lymphocytes irradiated in vitro or in vivo. *Radiation Research*, **128,** 276-81.

Gavrieli, Y., Sherman, Y. & Ben-Sasson, S.A. (1992). Identification of programmed cell death in situ via specific labeling of nuclear DNA fragmentation. *Journal of Cell Biology.*, **119,** 493-501.

Gendler, S., Taylor-Papadimitriou, J., Duhig, T., Rothbard, J. & Burchell, J. (1988). A highly immunogenic region of a human polymorphic epithelial mucin

expressed by carcinomas is made up of tandem repeats. *Journal of Biological Chemistry.*, **263,** 12820-3.

Gendler, S.J., Lancaster, C.A., Taylor-Papadimitriou, J., Duhig, T., Peat, N., Burchell, J., Pemberton, L., Lalani, E.N. & Wilson, D. (1990). Molecular cloning and expression of human tumor-associated polymorphic epithelial mucin. *The Journal Of Biological Chemistry*, **265,** 15286-15293.

Gendler, S.J., Spicer, A.P., Lalani, E.N., Duhig, T., Peat, N., Burchell, J., Pemberton, L., Boshell, M. & Taylor-Papadimitriou, J. (1991). Structure and biology of a carcinoma-associated mucin, MUC1. *Am Rev Respir Dis*, **144,** S42-7.

Giuntoli, R.L., 2nd, Rodriguez, G.C., Whitaker, R.S., Dodge, R. & Voynow, J.A. (1998). Mucin gene expression in ovarian cancers. *Cancer Research*, **58,** 5546-50.

Gleave, M., Tolcher, A., Miyake, H., Nelson, C., Brown, B., Beraldi, E. & Goldie, J. (1999). Progression to androgen independence is delayed by adjuvant treatment with antisense Bcl-2 oligodeoxynucleotides after castration in the LNCaP prostate tumor model. *Clin Cancer Res*, **5,** 2891-8.

Goddu, S.M., Rao, D.V. & Howell, R.W. (1994). Multicellular dosimetry for micrometastases: dependence of self-dose versus cross-dose to cell nuclei on type and energy of radiation and subcellular distribution of radionuclides. *Journal of Nuclear Medicine*, **35,** 521-30.

Gold, D.V., Modrak, D.E., Schutsky, K. & Cardillo, T.M. (2004). Combined 90Yttrium-DOTA-labeled PAM4 antibody radioimmunotherapy and gemcitabine radiosensitization for the treatment of a human pancreatic cancer xenograft. *Int J Cancer*, **109,** 618-26.

Goldenberg, D.M. & Sharkey, R.M. (2005). Radioimmunotherapy of non-Hodgkin's lymphoma revisited. *J Nucl Med*, **46,** 383-4.

Goldenberg, M.M. (1999). Trastuzumab, a recombinant DNA-derived humanized monoclonal antibody, a novel agent for the treatment of metastatic breast cancer. *Clinical Therapeutics*, **21,** 309-18.

Grawe, J., Biko, J., Lorenz, R., Reiners, C., Stopper, H., Vershenya, S., Vukicevic, V. & Hempel, K. (2005). Evaluation of the reticulocyte micronucleus assay in patients treated with radioiodine for thyroid cancer. *Mutation Research*, **583,** 12-25.

Guyton, C. (1991). *Textbook of medical physiology*. W.B. Saunders.

Hall, E.J. (1994). *radiobiology for the Radiologist.*

Hamby, C.V., Chinol, M., Palestro, C.J., Manzo, C. & Ferrone, S. (1998). Improved tumor targeting of rhenium-186-labeled anti-human high-m.w. melanoma-associated antigen monoclonal antibody 763.74 following purification with anti-idiotypic monoclonal antibody MK2-23. *Int J Cancer*, **78,** 486-90.

Hamilton TC, Y.R., Louie KG et al. Characterization of a xenograft model of human ovarian carcinoma which produces ascites and intra abdominal carcinomatosis in mice. Cancer Res 1984;44:5286 90.

Hang, M., Ranson, M., Saunders, D., Liang, X., Bunn, C. & Baker, M. (1998). Pharmacokinetics and biodistribution of recombinant human plasminogen activator inhibitor type 2 (PAI-2) in control and tumour xenograft-bearing mice. *Fibrinol Proteol*, **12,** 145-154.

Hanisch, F.G., Stadie, T.R., Deutzmann, F. & Peter-Katalinic, J. (1996). MUC1 glycoforms in breast cancer--cell line T47D as a model for carcinoma-associated alterations of 0-glycosylation. *European Journal Of Biochemistry / FEBS*, **236,** 318-327.

Harms-Ringdahl, M., Nicotera, P. & Radford, I.R. (1996). Radiation induced apoptosis. *Mutation Research*, **366,** 171-9.

Hassfjell, S. & Brechbiel, M.W. (2001). The development of the alpha-particle emitting radionuclides 212Bi and 213Bi, and their decay chain related radionuclides, for therapeutic applications. *Chemical Reviews*, **101,** 2019-36.

Hilden, J.M., Smith, F.O., Frestedt, J.L., McGlennen, R., Howells, W.B., Sorensen, P.H.B., Arthur, D.C., Woods, W.G., Buckley, J., Bernstein, I.D. & Kersey, J.H. (1997). MLL Gene Rearrangement, Cytogenetic 11q23 Abnormalities, and Expression of the NG2 Molecule in Infant Acute Myeloid Leukemia. *Blood*, **89,** 3801-3805.

Horak, E., Hartmann, F., Garmestani, K., Wu, C., Brechbiel, M., Gansow, O.A., Landolfi, N.F. & Waldmann, T.A. (1997). Radioimmunotherapy targeting of HER2/neu oncoprotein on ovarian tumor using lead-212-DOTA-AE1. *J Nucl Med*, **38,** 1944-50.

Howell, R.W., Goddu, S.M., Narra, V.R., Fisher, D.R., Schenter, R.E. & Rao, D.V. (1997). Radiotoxicity of gadolinium-148 and radium-223 in mouse testes: relative biological effectiveness of alpha-particle emitters in vivo. *Radiat Res*, **147,** 342-8.

Howell, R.W., Wessels, B.W., Loevinger, R., Watson, E.E., Bolch, W.E., Brill, A.B., Charkes, N.D., Fisher, D.R., Hays, M.T., Robertson, J.S., Siegel, J.A. & Thomas, S.R. (1999). The MIRD perspective 1999. Medical Internal Radiation Dose Committee. *Journal of Nuclear Medicine*, **40,** 3S-10S.

Hudson, P.J. (1999). Recombinant antibody constructs in cancer therapy. *Current Opinion in Immunology*, **11,** 548-57.

Hughes, O.D., Denley, H. & Kunker, R.B. (2000). MUC1 mucin expression in transitional cell carcinoma of the bladder. *J Urol Path*, **12,** 179-191.

Humm, J.L. (1987). A microdosimetric model of astatine-211 labeled antibodies for radioimmunotherapy. *International Journal of Radiation Oncology, Biology, Physics*, **13,** 1767-73.

Humm, J.L., Roeske, J.C., Fisher, D.R. & Chen, G.T. (1993). Microdosimetric concepts in radioimmunotherapy. *Medical Physics*, **20,** 535-41.

Huneke, R.B., Pippin, C.G., Squire, R.A., Brechbiel, M.W., Gansow, O.A. & Strand, M. (1992). Effective alpha-particle-mediated radioimmunotherapy of murine leukemia. *Cancer Res*, **52,** 5818-20.

Iida, J., Meijne, A.M.L., Knutson, J.R., Furcht, L.T. & McCarthy, J.B. (1996). Cell surface chondroitin sulfate proteoglycans in tumor cell adhesion, motility and invasion. *Seminars in Cancer Biology*, **7,** 155-162.

Iida, J., Pei, D., Kang, T., Simpson, M.A., Herlyn, M., Furcht, L.T. & McCarthy, J.B. (2001). Melanoma Chondroitin Sulfate Proteoglycan Regulates Matrix Metalloproteinase-dependent Human Melanoma Invasion into Type I Collagen. *J. Biol. Chem.*, **276,** 18786-18794.

Iida, J., Skubitz, A.P., Furcht, L.T., Wayner, E.A. & McCarthy, J.B. (1992). Coordinate role for cell surface chondroitin sulfate proteoglycan and alpha 4 beta 1 integrin in mediating melanoma cell adhesion to fibronectin. *J. Cell Biol.*, **118,** 431-444.

Imam, S.K. (2001). Advancements in cancer therapy with alpha-emitters: a review. *International Journal of Radiation Oncology, Biology, Physics*, **51,** 271-8.

Ishikawa, Y., Wada, I. & Fukumoto, M. (2001). Alpha-particle carcinogenesis in Thorotrast patients: epidemiology, dosimetry, pathology, and molecular analysis. *J Environ Pathol Toxicol Oncol*, **20,** 311-5.

Jaggi, J.S., Kappel, B.J., McDevitt, M.R., Sgouros, G., Flombaum, C.D., Cabassa, C. & Scheinberg, D.A. (2005a). Efforts to control the errant products of a targeted in vivo generator. *Cancer Research*, **65,** 4888-95.

Jaggi, J.S., Seshan, S.V., McDevitt, M.R., LaPerle, K., Sgouros, G. & Scheinberg, D.A. (2005b). Renal Tubulointerstitial Changes after Internal Irradiation with {alpha}-Particle-Emitting Actinium Daughters. *J Am Soc Nephrol*, **16,** 2677-2689.

Jaggi, J.S., Seshan, S.V., McDevitt, M.R., Sgouros, G., Hyjek, E. & Scheinberg, D.A. (2006). Mitigation of radiation nephropathy after internal alpha-particle irradiation of kidneys. *International Journal of Radiation Oncology, Biology, Physics*, **64,** 1503-12.

Jurcic, J.G., Caron, P.C., Nikula, T.K., Papadopoulos, E.B., Finn, R.D., Gansow, O.A., Miller, W.H., Jr., Geerlings, M.W., Warrell, R.P., Jr., Larson, S.M. & et al. (1995). Radiolabeled anti-CD33 monoclonal antibody M195 for myeloid leukemias. *Cancer Res*, **55,** 5908s-5910s.

Jurcic, J.G., Larson, S.M., Sgouros, G., McDevitt, M.R., Finn, R.D., Divgi, C.R., Ballangrud, A.M., Hamacher, K.A., Ma, D., Humm, J.L., Brechbiel, M.W., Molinet, R. & Scheinberg, D.A. (2002). Targeted alpha particle immunotherapy for myeloid leukemia. *Blood*, **100,** 1233-1239.

Jurcic, J.G., Scheinberg, D.A. & Houghton, A.N. (1997). Monoclonal antibody therapy of cancer. *Cancer Chemother Biol Response Modif*, **17,** 195-216.

Kageshita, T., Kuriya, N., Ono, T., Horikoshi, T., Takahashi, M., Wong, G.Y. & Ferrone, S. (1993). Association of high molecular weight melanoma-associated antigen expression in primary acral lentiginous melanoma lesions with poor prognosis. *Cancer Res*, **53,** 2830-2833.

Kamikawa, T., Amenomori, M., Itoh, T., Momoi, H., Hiai, H., Machinami, R., Ishikawa, Y., Mori, T., Shimahara, Y., Yamaoka, Y. & Fukumoto, M. (1999). Analysis of genetic changes in intrahepatic cholangiocarcinoma induced by thorotrast. *Radiat Res*, **152,** S118-24.

Kaptain, S., Tan, L.K. & Chen, B. (2001). Her-2/neu and breast cancer. *Diagn Mol Pathol*, **10,** 139-52.

Kaspersen, F.M., Bos, E., Doornmalen, A.V., Geerlings, M.W., Apostolidis, C. & Molinet, R. (1995). Cytotoxicity of 213Bi- and 225Ac-immunoconjugates. *Nucl Med Commun*, **16,** 468-76.

Kennel, S.J., Boll, R., Stabin, M., Schuller, H.M. & Mirzadeh, S. (1999a). Radioimmunotherapy of micrometastases in lung with vascular targeted 213Bi. *British Journal of Cancer*, **80,** 175-84.

Kennel, S.J., Lankford, T.K., Foote, L.J., Davis, I.A., Boll, R.A. & Mirzadeh, S. (1999b). Combination vascular targeted and tumor targeted radioimmunotherapy. *Cancer Biother Radiopharm*, **14,** 371-9.

Kennel, S.J., Lee, R., Bultman, S. & Kabalka, G. (1990). Rat monoclonal antibody distribution in mice: an epitope inside the lung vascular space mediates very efficient localization. *International Journal of Radiation Applications & Instrumentation - Part B, Nuclear Medicine & Biology*, **17,** 193-200.

Kennel, S.J., Stabin, M., Roeske, J.C., Foote, L.J., Lankford, P.K., Terzaghi-Howe, M., Patterson, H., Barkenbus, J., Popp, D.M., Boll, R. & Mirzadeh, S. (1999c). Radiotoxicity of bismuth-213 bound to membranes of monolayer and spheroid cultures of tumor cells. *Radiation Research*, **151,** 244-56.

Klapper, L.N., Kirschbaum, M.H., Sela, M. & Yarden, Y. (2000). Biochemical and clinical implications of the ErbB/HER signaling network of growth factor receptors. *Advances in Cancer Research*, **77,** 25-79.

Konecny, G., Untch, M., Pihan, A., Kimmig, R., Gropp, M., Stieber, P., Hepp, H., Slamon, D. & Pegram, M. (2001). Association of urokinase-type plasminogen activator and its inhibitor with disease progression and prognosis in ovarian cancer. *Clinical Cancer Research*, **7,** 1743-9.

Konno, H., Abe, J., Kaneko, T., Baba, M., Shoji, A., Sunayama, K., Kamiya, K., Tanaka, T., Suzuki, S., Nakamura, S. & Urano, T. (2001). Urokinase receptor and vascular endothelial growth factor are synergistically associated with the liver metastasis of colorectal cancer. *Japanese Journal of Cancer Research*, **92,** 516-23.

Kozak, R.W., Atcher, R.W., Gansow, O.A., Friedman, A.M., Hines, J.J. & Waldmann, T.A. (1986). Bismuth-212-labeled anti-Tac monoclonal antibody: alpha-particle-emitting radionuclides as modalities for radioimmunotherapy. *Proceedings of the National Academy of Sciences of the United States of America*, **83,** 474-8.

Kruithof, E.K., Baker, M.S. & Bunn, C.L. (1995). Biological and clinical aspects of plasminogen activator inhibitor type 2. *Blood*, **86,** 4007-4024.

Kuhn, W., Pache, L., Schmalfeldt, B., Dettmar, P., Schmitt, M., Janicke, F. & Graeff, H. (1994). Urokinase (uPA) and PAI-1 predict survival in advanced ovarian cancer patients (FIGO III) after radical surgery and platinum-based chemotherapy. *Gynecologic Oncology*, **55,** 401-9.

Li, Y., Cozzi, P.J., Qu, C.F., Zhang, D.Y., Abbas Rizvi, S.M., Raja, C. & Allen, B.J. (2004). Cytotoxicity of human prostate cancer cell lines in vitro and induction of apoptosis using 213Bi-Herceptin alpha-conjugate. *Cancer Lett*, **205,** 161-71.

Li, Y., Kuwahara, H., Ren, J., Wen, G. & Kufe, D. (2001a). The c-Src Tyrosine Kinase Regulates Signaling of the Human DF3/MUC1 Carcinoma-associated Antigen with GSK3beta and beta -Catenin. *J. Biol. Chem.*, **276,** 6061-6064.

Li, Y., Ren, J., Yu, W.-h., Li, Q., Kuwahara, H., Yin, L., Carraway, K.L., III & Kufe, D. (2001b). The Epidermal Growth Factor Receptor Regulates Interaction of the Human DF3/MUC1 Carcinoma Antigen with c-Src and beta -Catenin. *J. Biol. Chem.*, **276,** 35239-35242.

Li, Y., Rizvi, S.M., Ranson, M. & Allen, B.J. (2002). 213Bi-PAI2 conjugate selectively induces apoptosis in PC3 metastatic prostate cancer cell line and shows anti-cancer activity in a xenograft animal model. *British Journal of Cancer*, **86,** 1197-203.

Liersch, T., Meller, J., Kulle, B., Behr, T.M., Markus, P., Langer, C., Ghadimi, B.M., Wegener, W.A., Kovacs, J., Horak, I.D., Becker, H. & Goldenberg, D.M. (2005). Phase II trial of carcinoembryonic antigen radioimmunotherapy with 131I-labetuzumab after salvage resection of colorectal metastases in the liver: five-year safety and efficacy results. *J Clin Oncol*, **23,** 6763-70.

Liewendahl, K. & Pyrhonen, S. (1993). Radioimmunodetection and radioimmunotherapy of malignant melanoma. A review. *Acta Oncol*, **32,** 717-21.

Ligtenberg, M., Buijs, F., Vos, H. & Hilkens, J. (1992). Suppression of cellular aggregation by high levels of episialin. *Cancer Res*, **52,** 2318-2324.

Liu, L., Barth, R.F., Adams, D.M., Soloway, A.H. & Reisfeld, R.A. (1995). Bispecific antibodies as targeting agents for boron neutron capture therapy of brain tumors. *Journal of Hematotherapy*, **4,** 477-83.

Lundgren, C.H., Sawa, H., Sobel, B.E. & Fujii, S. (1994). Modulation of expression of monocyte/macrophage plasminogen activator activity and its implications for attenuation of vasculopathy. *Circulation*, **90,** 1927-34.

Macklis, R.M., Kinsey, B.M., Kassis, A.I., Ferrara, J.L., Atcher, R.W., Hines, J.J., Coleman, C.N., Adelstein, S.J. & Burakoff, S.J. (1988). Radioimmunotherapy with alpha-particle-emitting immunoconjugates. *Science*, **240,** 1024-6.

Macklis, R.M., Lin, J.Y., Beresford, B., Atcher, R.W., Hines, J.J. & Humm, J.L. (1992). Cellular kinetics, dosimetry, and radiobiology of alpha-particle radioimmunotherapy: induction of apoptosis. *Radiat Res*, **130,** 220-6.

Madrazo, A., Schwarz, G. & Churg, J. (1975). Radiation nephritis: a review. *Journal of Urology.*, **114,** 822-7.

Majumdar, M., Vuori, K. & Stallcup, W.B. (2003). Engagement of the NG2 proteoglycan triggers cell spreading via rac and p130cas. *Cellular Signalling*, **15,** 79-84.

Marian Teresa Santini & Rainaldi, G. (1999). Three-dimensional spheroid model in tumor biology. *pathbiology*, **67,** 148-157.

Martell, A.E. & Smith, R.M. (1974). *Critical Stability Constants; Plenum Press: New York, 1974; Vol. 1.* . Vol. 1. Plenum Press: New York,: New York.

Matsuishi, T., Terasawa, K., Yoshida, I., Yano, E., Yamashita, F., Hidaka, T., Ishihara, O., Yoshino, M., Nonaka, I., Kurokawa, T. & Nakamura, Y. (1982). Vacuolar myopathy with type 2 A fiber atrophy and type 2 B fiber deficiency. A case of childhood form acid alpha-1,4-glucosidase deficiency. *Neuropediatrics*, **13,** 173-6.

McDermott, K.M., Crocker, P.R., Harris, A., Burdick, M.D., Hinoda, Y., Hayashi, T., Imai, K. & Hollingsworth, M.A. (2001). Overexpression of MUC1 reconfigures the binding properties of tumor cells. *Int J Cancer*, **94,** 783-91.

McDevitt, M.R., Barendswaard, E., Ma, D., Lai, L., Curcio, M.J., Sgouros, G., Ballangrud, A.M., Yang, W.H., Finn, R.D., Pellegrini, V., Geerlings, M.W., Jr., Lee, M., Brechbiel, M.W., Bander, N.H., Cordon-Cardo, C. & Scheinberg, D.A. (2000). An alpha-particle emitting antibody ([213Bi]J591) for radioimmunotherapy of prostate cancer. *Cancer Res*, **60,** 6095-100.

McDevitt, M.R., Finn, R.D., Ma, D., Larson, S.M. & Scheinberg, D.A. (1999). Preparation of alpha-emitting 213Bi-labeled antibody constructs for clinical use. *Journal of Nuclear Medicine*, **40,** 1722-7.

McDevitt, M.R., Sgouros, G., Finn, R.D., Humm, J.L., Jurcic, J.G., Larson, S.M. & Scheinberg, D.A. (1998). Radioimmunotherapy with alpha-emitting nuclides. *Eur J Nucl Med*, **25,** 1341-51.

McGuire, W.P. (1993). Primary treatment of epithelial ovarian malignancies. *Cancer.*, **71,** 1541-50.

McLendon, R.E., Archer, G.E., Larsen, R.H., Akabani, G., Bigner, D.D. & Zalutsky, M.R. (1999). Radiotoxicity of systemically administered 211At-labeled human/mouse chimeric monoclonal antibody: a long-term survival study with histologic analysis. *Int J Radiat Oncol Biol Phys*, **45,** 491-9.

Menard, S., Tagliabue, E., Campiglio, M. & Pupa, S.M. (2000). Role of HER2 gene overexpression in breast carcinoma. *Journal of Cellular Physiology*, **182,** 150-62.

Michael A. Burg, K.A.G.W.B.S. (1998). Expression of the NG2 proteoglycan enhances the growth and metastatic properties of melanoma cells. *Journal of Cellular Physiology*, **177,** 299-312.

Milenic, D.E., Garmestani, K., Brady, E.D., Albert, P.S., Ma, D., Abdulla, A. & Brechbiel, M.W. (2005). Alpha-particle radioimmunotherapy of disseminated peritoneal disease using a (212)Pb-labeled radioimmunoconjugate targeting HER2. *Cancer Biother Radiopharm*, **20,** 557-68.

Milenic, D.E., Roselli, M., Mirzadeh, S., Pippin, C.G., Gansow, O.A., Colcher, D., Brechbiel, M.W. & Schlom, J. (2001). In vivo evaluation of bismuth-labeled monoclonal antibody comparing DTPA-derived bifunctional chelates. *Cancer Biotherapy & Radiopharmaceuticals*, **16,** 133-46.

Miseljic, S., Galandiuk, S., Myers, S.D. & Wittliff, J.L. (1995). Expression of urokinase-type plasminogen activator and plasminogen activator inhibitor in colon disease. *J Clin Lab Anal*, **9,** 413-7.

Mishra, A.K., Iznaga-Escobar, N., Figueredo, R., Jain, V.K., Dwarakanath, B.S., Perez-Rodriguez, R., Sharma, R.K. & Mathew, T.L. (2002). Preparation and comparative evaluation of 99mTc-labeled 2-iminothiolane modified antibodies and CITC-DTPA immunoconjugates of anti-EGF-receptor antibodies. *Methods Find Exp Clin Pharmacol*, **24,** 653-60.

Mogensen, C.E. & Solling. (1977). Studies on renal tubular protein reabsorption: partial and near complete inhibition by certain amino acids. *Scandinavian Journal of Clinical & Laboratory Investigation*, **37,** 477-86.

Mommers, E.C., Leonhart, A.M., von Mensdorff-Pouilly, S., Schol, D.J., Hilgers, J., Meijer, C.J., Baak, J.P. & van Diest, P.J. (1999). Aberrant expression of MUC1 mucin in ductal hyperplasia and ductal carcinoma In situ of the breast. *International Journal of Cancer*, **84,** 466-9.

Monsieurs, M.A., Bacher, K., Brans, B., Vral, A., De Ridder, L., Dierckx, R.A. & Thierens, H.M. (2003). Patient dosimetry for 131I-lipiodol therapy. *European Journal of Nuclear Medicine & Molecular Imaging*, **30,** 554-61.

Monsieurs, M.A., Thierens, H.M., Vral, A., Brans, B., De Ridder, L. & Dierckx, R.A. (2001). Patient dosimetry after 131I-MIBG therapy for neuroblastoma and carcinoid tumours. *Nuclear Medicine Communications*, **22,** 367-74.

Morgan, A.C., Jr., Galloway, D.R. & Reisfeld, R.A. (1981). Production and characterization of monoclonal antibody to a melanoma specific glycoprotein. *Hybridoma*, **1,** 27-36.

Murray, A., Simms, M.S., Scholfield, D.P., Vincent, R.M., Denton, G., Bishop, M.C., Price, M.R. & Perkins, A.C. (2001). Production and characterization of 188Re-C595 antibody for radioimmunotherapy of transitional cell bladder cancer. *J Nucl Med*, **42,** 726-32.

Newman, H.C., Prise, K.M., Folkard, M. & Michael, B.D. (1997). DNA double-strand break distributions in X-ray and alpha-particle irradiated V79 cells: evidence for non-random breakage. *Int J Radiat Biol*, **71,** 347-63.

Niehans, G.A., Singleton, T.P., Dykoski, D. & Kiang, D.T. (1993). Stability of HER-2/neu expression over time and at multiple metastatic sites. *Journal of the National Cancer Institute*, **85,** 1230-5.

Nielsen, J.S., Jakobsen, E., Holund, B., Bertelsen, K. & Jakobsen, A. (2004). Prognostic significance of p53, Her-2, and EGFR overexpression in borderline and epithelial ovarian cancer. *International Journal of Gynecological Cancer*, **14,** 1086-96.

Nikula, T.K., McDevitt, M.R., Finn, R.D., Wu, C., Kozak, R.W., Garmestani, K., Brechbiel, M.W., Curcio, M.J., Pippin, C.G., Tiffany-Jones, L., Geerlings, M.W., Sr., Apostolidis, C., Molinet, R., Geerlings, M.W., Jr., Gansow, O.A. & Scheinberg, D.A. (1999). Alpha-emitting bismuth cyclohexylbenzyl DTPA constructs of recombinant humanized anti-CD33 antibodies: pharmacokinetics, bioactivity, toxicity and chemistry. *Journal of Nuclear Medicine*, **40,** 166-76.

Nishiyama, A. (2001). NG2 cells in the brain: a novel glial cell population. *Hum Cell*, **14,** 77-82.

Norenberg, J.P., Krenning, B.J., Konings, I.R.H.M., Kusewitt, D.F., Nayak, T.K., Anderson, T.L., de Jong, M., Garmestani, K., Brechbiel, M.W. & Kvols, L.K. (2006). 213Bi-[DOTA0, Tyr3]Octreotide Peptide Receptor Radionuclide Therapy of Pancreatic Tumors in a Preclinical Animal Model. *Clin Cancer Res*, **12,** 897-903.

Ohara, H., Okazaki, N., Monobe, M., Watanabe, S., Kanayama, M. & Minamihisamatsu, M. (1998). Induction of asymmetrical type of chromosomal aberrations in cultured human lymphocytes by ion beams of different energies at varying LET from HIMAC and RRC. *Adv Space Res*, **22,** 1673-82.

Oosterkamp, H.M., Scheiner, L., Stefanova, M.C., Lloyd, K.O. & Finstad, C.L. (1997). Comparison of MUC-1 mucin expression in epithelial and non-epithelial cancer cell lines and demonstration of a new short variant form (MUC-1/Z). *Int J Cancer*, **72,** 87-94.

Osako, M., Yonezawa, S., Siddiki, B., Huang, J., Ho, J.J., Kim, Y.S. & Sato, E. (1993). Immunohistochemical study of mucin carbohydrates and core proteins in human pancreatic tumors. *Cancer*, **71,** 2191-9.

Palm, S., Andersson, H., Back, T., Claesson, I., Delle, U., Hultborn, R., Jacobsson, L., Kopf, I. & Lindegren, S. (2000). In vitro effects of free 211At,211At-albumin and 211At-monoclonal antibody compared to external photon irradiation on two human cancer cell lines. *Anticancer Res*, **20,** 1005-12.

Pandey, P., Kharbanda, S. & Kufe, D. (1995). Association of the DF3/MUC1 breast cancer antigen with Grb2 and the Sos/Ras exchange protein. *Cancer Res*, **55,** 4000-4003.

Pearse, H. (1994). The kidney. In *Moss' radiation oncology: rationale, technique, results.*, JD, C. (ed) pp. 499-517: St. Louis: Mosby, .

Pemberton, L.F., Rughetti, A., Taylor-Papadimitriou, J. & Gendler, S.J. (1996). The Epithelial Mucin MUC1 Contains at Least Two Discrete Signals Specifying Membrane Localization in Cells. *J. Biol. Chem.*, **271,** 2332-2340.

Persson, M.I., Gedda, L., Jensen, H.J., Lundqvist, H., Malmstrom, P.U. & Tolmachev, V. (2006). Astatinated trastuzumab, a putative agent for radionuclide immunotherapy of ErbB2-expressing tumours. *Oncol Rep*, **15,** 673-80.

Pluschke, G., Vanek, M., Evans, A., Dittmar, T., Schmid, P., Itin, P., Filardo, E.J. & Reisfeld, R.A. (1996). Molecular cloning of a human melanoma-associated chondroitin sulfate proteoglycan. *PNAS*, **93,** 9710-9715.

Press, O.W., Eary, J.F., Gooley, T., Gopal, A.K., Liu, S., Rajendran, J.G., Maloney, D.G., Petersdorf, S., Bush, S.A., Durack, L.D., Martin, P.J., Fisher, D.R., Wood, B., Borrow, J.W., Porter, B., Smith, J.P., Matthews, D.C., Appelbaum, F.R. & Bernstein, I.D. (2000). A phase I/II trial of iodine-131-tositumomab (anti-CD20), etoposide, cyclophosphamide, and autologous stem cell transplantation for relapsed B-cell lymphomas. *Blood*, **96,** 2934-42.

Price, M.R., Pugh, J.A., Hudecz, F., Griffiths, W., Jacobs, E., Symonds, I.M., Clarke, A.J., Chan, W.C. & Baldwin, R.W. (1990). C595--a monoclonal antibody against the protein core of human urinary epithelial mucin commonly expressed in breast carcinomas. *British Journal of Cancer.*, **61,** 681-6.

Qu, C.F., Song, E.Y., Li, Y., Rizvi, S.M., Raja, C., Smith, R., Morgenstern, A., Apostolidis, C. & Allen, B.J. (2005). Pre-clinical Study of (213)Bi Labeled PAI2 for the Control of Micrometastatic Pancreatic Cancer. *Clin Exp Metastasis*, **22,** 575-86.

Raju, M.R., Eisen, Y., Carpenter, S. & Inkret, W.C. (1991). Radiobiology of alpha particles. III. Cell inactivation by alpha-particle traversals of the cell nucleus. *Radiation Research*, **128,** 204-9.

Ranson, M., Tian, Z., Andronicos, N.M., Rizvi, S. & Allen, B.J. (2002). In vitro cytotoxicity of bismuth-213 (213Bi)-labeled-plasminogen activator inhibitor type 2 (alpha-PAI-2) on human breast cancer cells. *Breast Cancer Research & Treatment*, **71,** 149-59.

Riss, T.L. & Moravec, R.A. (2004). Use of multiple assay endpoints to investigate the effects of incubation time, dose of toxin, and plating density in cell-based cytotoxicity assays. *Assay Drug Dev Technol*, **2,** 51-62.

Rizvi, S.M., Allen, B.J., Tian, Z., Goozee, G. & Sarkar, S. (2001). In vitro and preclinical studies of targeted alpha therapy (TAT) for colorectal cancer. *Colorectal Dis*, **3,** 345-53.

Rizvi, S.M., Li, Y., Jun Song, E.Y., Qu, C.F., Raja, C., Morgenstern, A., Apostolidis, C. & Allen, B.J. (2006). Preclinical Studies of Bismuth-213 Labeled Plasminogen Activator Inhibitor Type 2 (PAI2) in a Prostate Cancer Nude Mouse Xenograft Model. *Cancer Biol Ther*, **5,** 386-93.

Rizvi, S.M., Sarkar, S., Goozee, G. & Allen, B.J. (2000). Radioimmunoconjugates for targeted alpha therapy of malignant melanoma. *Melanoma Res*, **10,** 281-9.

Roeske, J.C. & Stinchcomb, T.G. (1997). Dosimetric framework for therapeutic alpha-particle emitters. *Journal of Nuclear Medicine*, **38,** 1923-9.

Roselli, M., Milenic, D.E., Brechbiel, M.W., Mirzadeh, S., Pippin, C.G., Gansow, O.A., Colcher, D. & Schlom, J. (1999). In vivo comparison of CHX-DTPA ligand isomers in athymic mice bearing carcinoma xenografts. *Cancer Biotherapy & Radiopharmaceuticals*, **14,** 209-20.

Rubin, I. & Yarden, Y. (2001). The basic biology of HER2. *Annals of Oncology
<I>as of 2002, published by Oxford University Press</I>*, **12,** 3-8.

Ruegg, C.L., Anderson-Berg, W.T., Brechbiel, M.W., Mirzadeh, S., Gansow, O.A. & Strand, M. (1990). Improved in vivo stability and tumor targeting of bismuth-labeled antibody. *Cancer Research*, **50,** 4221-6.

Russ, G.A., Bigler, R., Tilbury, R., Woodard, H. & Laughlin, J. (1975). Metabolic studies with radiobismuth. I. Retention and distribution of 206Bi in the normal rat. *Radiat Res*, **63,** 443-54.

Rutgers, D.H., van Oostrum, I.E., Noorman van der Dussen, M.F. & Wils, I.S. (1989). Relationship between cell kinetics and radiation-induced arrest of proliferating cells in G2: relevance to efficacy of radiotherapy. *Analytical Cellular Pathology.*, **1,** 53-62.

Safa, M.M. & Foon, K.A. (2001). Adjuvant immunotherapy for melanoma and colorectal cancers. *Semin Oncol*, **28,** 68-92.

Satoh, S., Hinoda, Y., Hayashi, T., Burdick, M.D., Imai, K. & Hollingsworth, M.A. (2000). Enhancement of metastatic properties of pancreatic cancer cells by MUC1 gene encoding an anti-adhesion molecule. *International Journal of Cancer*, **88,** 507-18.

Schaefer, N.G., Pestalozzi, B.C., Knuth, A. & Renner, C. (2006). Potential use of humanized antibodies in the treatment of breast cancer. *Expert Review of Anticancer Therapy*, **6,** 1065-74.

Schechter, A.L., Hung, M.C., Vaidyanathan, L., Weinberg, R.A., Yang-Feng, T.L., Francke, U., Ullrich, A. & Coussens, L. (1985). The neu gene: an erbB-homologous gene distinct from and unlinked to the gene encoding the EGF receptor. *Science*, **229,** 976-8.

Scheinberg, D.A., Lovett, D., Divgi, C.R., Graham, M.C., Berman, E., Pentlow, K., Feirt, N., Finn, R.D., Clarkson, B.D., Gee, T.S. & et al. (1991). A phase I trial of monoclonal antibody M195 in acute myelogenous leukemia: specific bone marrow targeting and internalization of radionuclide. *J Clin Oncol*, **9,** 478-90.

Scheinberg, D.A., Strand, M. & Gansow, O.A. (1982). Tumor imaging with radioactive metal chelates conjugated to monoclonal antibodies. *Science*, **215,** 1511-3.

Schmalfeldt, B., Kuhn, W., Reuning, U., Pache, L., Dettmar, P., Schmitt, M., Janicke, F., Hofler, H. & Graeff, H. (1995). Primary tumor and metastasis in ovarian cancer differ in their content of urokinase-type plasminogen activator, its receptor, and inhibitors types 1 and 2. *Cancer Res*, **55,** 3958-63.

Schroeder, J.A., Thompson, M.C., Gardner, M.M. & Gendler, S.J. (2001). Transgenic MUC1 Interacts with Epidermal Growth Factor Receptor and Correlates with Mitogen-activated Protein Kinase Activation in the Mouse Mammary Gland. *J. Biol. Chem.*, **276,** 13057-13064.

Schwartz, J.L., Ashman, C.R., Atcher, R.W., Sedita, B.A., Shadley, J.D., Tang, J., Whitlock, J.L. & Rotmensch, J. (1991). Differential locus sensitivity to mutation induction by ionizing radiations of different LETs in Chinese hamster ovary K1 cells. *Carcinogenesis*, **12,** 1721-6.

Seidl, C., Schrock, H., Seidenschwang, S., Beck, R., Schmid, E., Abend, M., Becker, K.F., Apostolidis, C., Nikula, T.K., Kremmer, E., Schwaiger, M. & Senekowitsch-Schmidtke, R. (2005). Cell death triggered by alpha-emitting 213Bi-immunoconjugates in HSC45-M2 gastric cancer cells is different from apoptotic cell death. *Eur J Nucl Med Mol Imaging*, **32,** 274-85.

Sgouros, G., Ballangrud, A.M., Jurcic, J.G., McDevitt, M.R., Humm, J.L., Erdi, Y.E., Mehta, B.M., Finn, R.D., Larson, S.M. & Scheinberg, D.A. (1999). Pharmacokinetics and dosimetry of an alpha-particle emitter labeled antibody: 213Bi-HuM195 (anti-CD33) in patients with leukemia. *J Nucl Med*, **40,** 1935-46.

Sgouros, G., Graham, M.C., Divgi, C.R., Larson, S.M. & Scheinberg, D.A. (1993). Modeling and dosimetry of monoclonal antibody M195 (anti-CD33) in acute myelogenous leukemia. *J Nucl Med*, **34,** 422-30.

Sgouros, G. & Scheinberg, D.A. (1993). Treatment of leukemia with radiolabeled monoclonal antibodies. *Cancer Treat Res*, **68,** 23-64.

Simms, M.S., Perkins, A.C., Price, M.R., Scholfield, D.P. & Bishop, M.C. (2001). 99mTechnetium-C595 radioimmunoscintigraphy: a potential staging tool for bladder cancer. *BJU Int*, **88,** 686-91.

Skirnisdottir, I., Sorbe, B. & Seidal, T. (2001). The growth factor receptors HER-2/neu and EGFR, their relationship, and their effects on the prognosis in early stage (FIGO I-II) epithelial ovarian carcinoma. *International Journal of Gynecological Cancer*, **11,** 119-29.

Slamon, D.J., Godolphin, W., Jones, L.A., Holt, J.A., Wong, S.G., Keith, D.E., Levin, W.J., Stuart, S.G., Udove, J., Ullrich, A. & et al. (1989). Studies of the HER-2/neu proto-oncogene in human breast and ovarian cancer. *Science*, **244,** 707-12.

Slikkerveer, A., Jong, H.B., Helmich, R.B. & de Wolff, F.A. (1992). Development of a therapeutic procedure for bismuth intoxication with chelating agents. *Journal of Laboratory & Clinical Medicine*, **119,** 529-37.

Song, Y.J., Qu, C.F., Rizvi, S.M.A., Li, Y., Robertson, G., Raja, C., Morgenstern, A., Apostolidis, C., Perkins, A.C. & Allen, B.J. (2006). Cytotoxicity of PAI2, C595 and Herceptin vectors labeled with the alpha-emitting radioisotope Bismuth-213 for ovarian cancer cell monolayers and clusters. *Cancer Letters*, **234,** 176-183.

Sparks, R. (1999). Comparison of the effectiveness of some common animal data scaling techniques in estimationg human organ self absorbed dose. *6th International Radiopharmaceutical Dosimetry Symposium*, **99,** 705-716.

Speidel, M.T., Holmquist, B., Kassis, A.I., Humm, J.L., Berman, R.M., Atcher, R.W., Hines, J.J. & Macklis, R.M. (1993). Morphological, biochemical, and molecular changes in endothelial cells after alpha-particle irradiation. *Radiat Res*, **136,** 373-81.

Spencer, D.I., Missailidis, S., Denton, G., Murray, A., Brady, K., Matteis, C.I., Searle, M.S., Tendler, S.J. & Price, M.R. (1999). Structure/activity studies of the anti-MUC1 monoclonal antibody C595 and synthetic MUC1 mucin-core-related peptides and glycopeptides. *Biospectroscopy*, **5,** 79-91.

Spicer, A.P., Duhig, T., Chilton, B.S. & Gendler, S.J. (1995). Analysis of mammalian MUC1 genes reveals potential functionally important domains. *Mamm Genome*, **6,** 885-8.

Stallcup, W.B. (2002). The NG2 proteoglycan: Past insights and future prospects. *Journal of Neurocytology*, **31,** 423 ppl=-435.

Stinchcomb, T.G. & Roeske, J.C. (1992). Analytic microdosimetry for radioimmunotherapeutic alpha emitters. *Medical Physics*, **19,** 1385-93.

Supiot, S., Faivre-Chauvet, A., Couturier, O., Heymann, M.F., Robillard, N., Kraeber-Bodere, F., Morandeau, L., Mahe, M.A. & Cherel, M. (2002). Comparison of the biologic effects of MA5 and B-B4 monoclonal antibody labeled with iodine-131 and bismuth-213 on multiple myeloma. *Cancer*, **94,** 1202-9.

Thomas, P.A., Tracy, B.L., Ping, T., Wickstrom, M., Sidhu, N. & Hiebert, L. (2003). Relative biological effectiveness (RBE) of 210Po alpha-particles versus X-rays on lethality in bovine endothelial cells. *Int J Radiat Biol*, **79,** 107-18.

Tzahar, E. & Yarden, Y. (1998). The ErbB-2/HER2 oncogenic receptor of adenocarcinomas: from orphanhood to multiple stromal ligands. *Biochimica et Biophysica Acta*, **1377,** M25-37.

Urban, J.L. & Schreiber, H. (1992). Tumor antigens. *Annual Review of Immunology*, **10,** 617-44.

van de Wiel-van Kemenade, E., Ligtenberg, M., de Boer, A., Buijs, F., Vos, H., Melief, C., Hilkens, J. & Figdor, C. (1993a). Episialin (MUC1) inhibits cytotoxic lymphocyte-target cell interaction. *J Immunol*, **151,** 767-776.

van de Wiel-van Kemenade, E., Ligtenberg, M.J., de Boer, A.J., Buijs, F., Vos, H.L., Melief, C.J., Hilkens, J. & Figdor, C.G. (1993b). Episialin (MUC1) inhibits cytotoxic lymphocyte-target cell interaction. *Journal of Immunology.*, **151,** 767-76.

van der Burg, M.E., Henzen-Logmans, S.C., Berns, E.M., van Putten, W.L., Klijn, J.G. & Foekens, J.A. (1996). Expression of urokinase-type plasminogen activator (uPA) and its inhibitor PAI-1 in benign, borderline, malignant primary and metastatic ovarian tumors. *Int J Cancer*, **69,** 475-9.

Vandenbulcke, K., Thierens, H., Offner, F., Janssens, A., de Gelder, V., Bacher, K., Philippe, J., De Vos, F., Dierckx, R., Apostolidis, C., Morgenstern, A. & Slegers, G. (2004). Importance of receptor density in alpha radioimmunotherapy in B cell malignancies: an in-vitro study. *Nucl Med Commun*, **25,** 1131-6.

Vandenbulcke, K., Vos, F., Offner, F., PhilippÃ©, J., Apostolidis, C., Molinet, R., Nikula, T., Bacher, K., Gelder, V., Vral, A., Lahorte, C., Thierens, H.,

Dierckx, R. & Slegers, G. (2003). In vitro evaluation of ²¹³Bi-rituximab versus external gamma irradiation for the treatment of B-CLL patients: relative biological efficacy with respect to apoptosis induction and chromosomal damage. *European Journal of Nuclear Medicine and Molecular Imaging*, **30,** 1357-1364.

Vaughan, A.T., Bateman, W.J. & Fisher, D.R. (1982). The in vivo fate of a 211At labelled monoclonal antibody with known specificity in a murine system. *International Journal of Radiation Oncology, Biology, Physics*, **8,** 1943-6.

Wang, Y., Kristensen, G.B., Helland, A., Nesland, J.M., Borresen-Dale, A.-L. & Holm, R. (2005). Protein expression and prognostic value of genes in the erb-b signaling pathway in advanced ovarian carcinomas. *American Journal of Clinical Pathology*, **124,** 392-401.

Wesseling, J., van der Valk, S., Vos, H., Sonnenberg, A. & Hilkens, J. (1995). Episialin (MUC1) overexpression inhibits integrin-mediated cell adhesion to extracellular matrix components. *J. Cell Biol.*, **129,** 255-265.

Wiseman, G.A., White, C.A., Witzig, T.E., Gordon, L.I., Emmanouilides, C., Raubitschek, A., Janakiraman, N., Gutheil, J., Schilder, R.J., Spies, S., Silverman, D.H. & Grillo-Lopez, A.J. (1999). Radioimmunotherapy of relapsed non-Hodgkin's lymphoma with zevalin, a 90Y-labeled anti-CD20 monoclonal antibody. *Clin Cancer Res*, **5,** 3281s-3286s.

Wong, J.Y., Shibata, S., Williams, L.E., Kwok, C.S., Liu, A., Chu, D.Z., Yamauchi, D.M., Wilczynski, S., Ikle, D.N., Wu, A.M., Yazaki, P.J., Shively, J.E., Doroshow, J.H. & Raubitschek, A.A. (2003). A Phase I trial of 90Y-anti-carcinoembryonic antigen chimeric T84.66 radioimmunotherapy with 5-fluorouracil in patients with metastatic colorectal cancer. *Clin Cancer Res*, **9,** 5842-52.

Wu, C., Kobayashi, H., Sun, B., Yoo, T.M., Paik, C.H., Gansow, O.A., Carrasquillo, J.A., Pastan, I. & Brechbiel, M.W. (1997). Stereochemical influence on the stability of radio-metal complexes in vivo. Synthesis and evaluation of the four stereoisomers of 2-(p-nitrobenzyl)-trans-CyDTPA. *Bioorg Med Chem*, **5,** 1925-34.

Wu, L.J., Randers-Pehrson, G., Xu, A., Waldren, C.A., Geard, C.R., Yu, Z. & Hei, T.K. (1999). Targeted cytoplasmic irradiation with alpha particles induces mutations in mammalian cells. *Proc Natl Acad Sci U S A*, **96,** 4959-64.

Yamada, Y., Oghiso, Y., Enomoto, H. & Ishigure, N. (2002). Induction of micronuclei in a rat alveolar epithelial cell line by alpha particle irradiation. *Radiat Prot Dosimetry*, **99,** 219-22.

Yang, J., Price, M.A., Neudauer, C.L., Wilson, C., Ferrone, S., Xia, H., Iida, J., Simpson, M.A. & McCarthy, J.B. (2004). Melanoma chondroitin sulfate proteoglycan enhances FAK and ERK activation by distinct mechanisms. *J. Cell Biol.*, **165,** 881-891.

Yao, Z., Zhang, M., Garmestani, K., Axworthy, D.B., Mallett, R.W., Fritzberg, A.R., Theodore, L.J., Plascjak, P.S., Eckelman, W.C., Waldmann, T.A., Pastan, I., Paik, C.H., Brechbiel, M.W. & Carrasquillo, J.A. (2004). Pretargeted alpha emitting radioimmunotherapy using (213)Bi 1,4,7,10-tetraazacyclododecane-N,N',N",N"'-tetraacetic acid-biotin. *Clin Cancer Res*, **10,** 3137-46.

Yokota, T., Milenic, D.E., Whitlow, M. & Schlom, J. (1992). Rapid tumor penetration of a single-chain Fv and comparison with other immunoglobulin forms. *Cancer Research*, **52,** 3402-8.

Zajchowski, D., Band, V., Pauzie, N., Tager, A., Stampfer, M. & Sager, R. (1988). Expression of growth factors and oncogenes in normal and tumor-derived human mammary epithelial cells. *Cancer Res*, **48,** 7041-7.

Zalutsky, M.R. (2005). Current Status of Therapy of Solid Tumors: Brain Tumor Therapy. *J Nucl Med*, **46,** 151S-156.

Zanzonico, P.B. (2000). Internal radionuclide radiation dosimetry: a review of basic concepts and recent developments. *Journal of Nuclear Medicine*, **41,** 297-308.

Zhang, M., Yao, Z., Garmestani, K., Axworthy, D.B., Zhang, Z., Mallett, R.W., Theodore, L.J., Goldman, C.K., Brechbiel, M.W., Carrasquillo, J.A. & Waldmann, T.A. (2002). Pretargeting radioimmunotherapy of a murine model of adult T-cell leukemia with the alpha-emitting radionuclide, bismuth 213. *Blood*, **100,** 208-16.

Zhao, Y.L., Piao, C.Q., Hall, E.J. & Hei, T.K. (2001). Mechanisms of radiation-induced neoplastic transformation of human bronchial epithelial cells. *Radiat Res*, **155,** 230-234.

Zhou, H., Randers-Pehrson, G., Waldren, C.A., Vannais, D., Hall, E.J. & Hei, T.K. (2000). Induction of a bystander mutagenic effect of alpha particles in mammalian cells. *Proc Natl Acad Sci U S A*, **97,** 2099-104.

Zidenberg-Cherr, S., Parks, N.J. & Keen, C.L. (1987). Tissue and subcellular distribution of bismuth radiotracer in the rat: considerations of cytotoxicity and microdosimetry for bismuth radiopharmaceuticals. *Radiat Res*, **111,** 119-29.

Zotter, S., Hageman, P.C., Lossnitzer, A., van den Tweel, J., Hilkens, J., Mooi, W.J. & Hilgers, J. (1988). Monoclonal antibodies to epithelial sialomucins recognize epitopes at different cellular sites in adenolymphomas of the parotid gland. *International Journal of Cancer Supplement*, **3,** 38-44.

APPENDICES

I. APPENDIX I----Buffer and Medium Preparation

I.1 Inactive fetal bovine serum (FBS)

Endogenous bovine complement factors contained in fetal bovine serum can affect cell growth. In order to inactivate the endogenous bovine complement factors, heat inactivation of fetal bovine serum (FBS)(Life Technologies, MD, USA; or CSL VIC Australia) was performed by incubating FBS at 56° for 30 min in a water bath.

I.2 Dulbecco's phosphate buffered saline (DPBS)

DPBS powder (Life Technologies) was dissolved in 900 mL of deionizing water. The medium was diluted to 1 L and stirred until dissolved and immediately transferred to sterile containers by membrane filtration using a 0.2 μm filter and kept at 4°.

I.3 Cell culture medium

Different culture media were used for different cell lines. After dissolving the sachet powder as described below, the medium was subsequently filter-sterilised using a 0.2 μm filter.

I.3.1 Roswell park memorial institute (RPMI - 1640) medium

To prepare RPMI – 1640 medium, a sachet of RPMI – 1640 powder (Life Technologies), was dissolved in 1 L of deionizing water. This powder contains 2 mM L-glutamine, 10 mM HEPES, 1 mM sodium bicarbonate.

I.3.2 McCoy's 5a Medium

To prepare McCoy's 5a medium, a sachet of McCoy's 5a medium powder (Life Technologies), was dissolved in 1 L of deionizing water. This powder contains 1.5 mM L-glutamine, 2.2 g/L sodium bicarbonate.

I.3.3 MCDB 105 medium

To prepare MCDB 105 medium, a sachet of MCDB 105 medium powder (Sigma), was dissolved in 1 Liter of deionizing water. This powder contains L-glutamine, 25 mM HEPES.

I.3.4 Medium 109

To prepare Medium 109, a sachet of Medium 109 powder (Sigma), was dissolved in 1 L of deionizing water. This powder contains L-glutamine.

I.3.5 DMEM

To prepare DMEM, a sachet of DMEM powder (Life Technology), was dissolved in 1 L of deionizing water. This powder contains L-glutamine, 25 mM HEPES.

I.4 Cytochalasin B (Cyt B) (sigma #6762)

Cytochalasin B was used for micronuclei assay. This material is highly toxic, a possible teratogen with a risk of irreversible effects. It must always be purchased in sealed vials. The preparation of this reagent must be carried out in a cytoguard cabinet and the following personal protection must be used: Gown, P2 dusk mask, double nitrile gloves and safety glasses.

5 mg solid of Cyt B was dissolved in 8.3 mL Dimethyl Sulphoxide (DMSO) and dispensed 50 µL aliquots into tubes. Tubes were stored at –20°C for 12 months.

I.5 Phytohaemagglutinin (PHA) (sigma #)

The preparation of this reagent has been modified slightly from the product insert to suit the needs of the laboratory.

45 mg solid was dissolved in 20 mL sterile isotonic saline to obtain a final concentration of 2.25 mg/mL and dispensed in 500 µL aliquots into vials. Vials were stored at 4 °C for up to 6 months. The 500 µL aliquots were single use only. Any remaining solution in the vial was discarded.

I.6 0.05 M Tris-buffered saline (TBS)

- Weigh 60.5g tris (121.1g/mol), and dissolve in 1L distil water.
- Adjust PH to 7.6 with 37% hydrochloric acid (HCl) to obtain 0.5M tris buffer.
- Prepare 0.9% saline 900 mL.
- Addition of 100 mL of 0.5M PH 7.6 tris buffer into 0.9% saline.

II. APPENDIX II-----Cancer cell culture

II.1 Culture frozen cells

1. Thaw the frozen vial by gentle agitation in 37°C water bath. To reduce the possibility of contamination, keep the O-ring and cap out of the water. Thawing takes approximately 2 minutes.

2. The vial is removed from the water bath as soon as the contents are thawed, and decontaminated by dipping in or spraying with 70% ethanol. All of the operation from this point on is carried out under strict aseptic conditions.

3. The vial contents are transferred to a 75 cm^2 tissue culture flask and diluted with the recommended complete culture medium.

4. The cell culture at 37°C is incubated in a suitable medium. A 5% CO_2 in air atmosphere was used.

II.2 Subculturing Procedure

Volumes used in this protocol are for 75-cm^2 flask; proportionally reduce or increase amount of dissociation medium for culture vessels of other sizes.

1. Culture medium removed and discarded.
2. Briefly rinse the cell layer twice with PBS solution to remove all traces of serum, which contains trypsin inhibitor.
3. Add 8-10 mL of 0.25% (w/v) trypsin- 0.03 (w/v) EDTA solution to flask and observed cells under an inverted microscope until cell layer was dispersed. (Usually using 5 to 15 minutes)
4. Transfer detached cells and solution to a 50mL of tube which containing 5 mL of medium, centrifuge at 1000g for 5 minutes.
5. Discard the suspended part.

6. Add completed growth medium into the tube, aspirate cells by gently pipetting the cell pellet.
7. Add 8.0 to 10.0mL of completed growth medium and appreciated aliquots of the cell suspension into new culture flask.
8. Incubate cultures at 37°C.

III. APPENDIX III-----Labelling Protocols

III.1 Standard radioleblelling protocol

1. The chelator was prepared by adding 1 mg of cDTPA to 1 mL of chloroform. 100 μL of the chelator was purified under a stream of nitrogen until chloroform was evaporated to dryness.
2. To the purified chelator, 1 mg of the antibody C595 was added and the contents were incubated for one hour at room temperature. This gave the chelator: antibody ratio of 20: 1 which minimizes the use of antibody but still is as effective as possible.
3. A PD10 column (Amersham, Australia) was prepared by pre-equilibrating it with CH_3COONa, 0.5 M, pH 5.5 buffer. Acidic pH was used as it was found to be more conducive for labeling without degrading the antibody.
4. The contents from "Step 2" above were passed through the column as prepared in "Step 3". All the fractions collected were in 1mL aliquots and were subjected to protein estimation.
5. Concentration of the chelated antibody/protein was then determined using available protein assay methods (Micro BCA™ Protein Assay Reagent Kit from Pierce - Progen Code 0023235).

6. This purified conjugated antibody was used for labeling with Bi-213 in a concentration of 1: 1ratio. For ITLC a solvent of sodium acetate (0.5M, pH 5.5) was used.

7. The resultant AC was subjected to purification on PD10 column pre-equilibrated with PBS (pH 7.02). The fractions of 1 mL were collected and protein estimation was done again for each fraction.

III.2 Instant Thin Layer Chromatography (ITLC)

ITLC was used to test the labeling efficacy. The ITLC strip was cut to a size of 1 x 9 cm and marked at 1.5 cm distance. The specimen application was at 1.5 cm from the origin and the strip was cut into 4 equal parts from the point of sample application.

The strip was cut in 4 parts and counted for radioactivity. Each part represents a fraction. A schematic drawing of the strip is shown below.

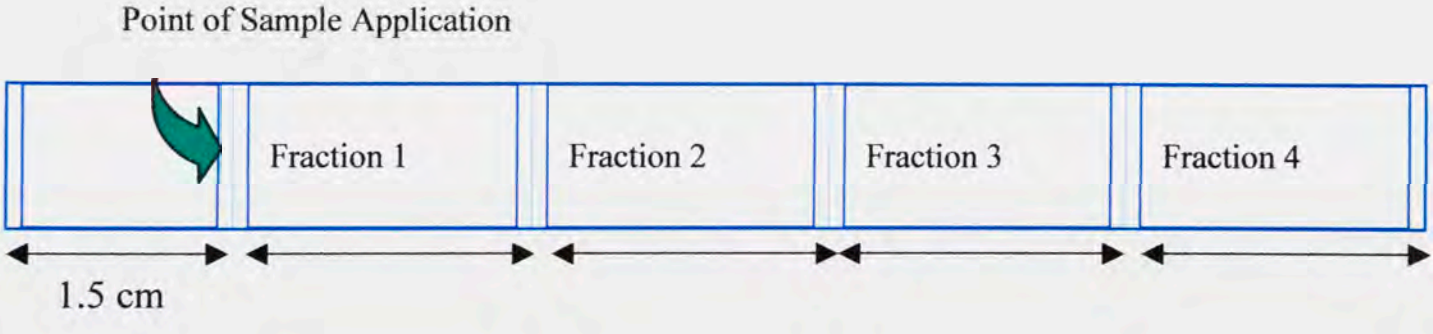

III.3 Modification of the protocol for PAI2

The protocol was modified to achieve higher labeling efficacy as follows:

(1) The conjugation method was altered by using a 50:1 ratio of the cDTPA in Dimethylsulfoxide (DMSO) (Abbas Rizvi et al., 2000). After one-hour incubation, the contents were buffer exchanged with PBS (pH 7.2) by using a

PD-10 column. The conjugated protein was then concentrated to the required concentration by using Centricon 30 filter.

(2) The conjugated PAI-2 was labeled with the isotope, after adjusting the pH to 5.5 with either acetate or citrate buffer. The ITLC was done as per procedure described above.

III.4 Serum stability of alpha conjugates test

Stability of the AC is of prime importance as an unstable AC will lose any free or loosely bound isotope and can irradiate the organs that should not be irradiated, for instance stem cells.

Serum was always taken from a freshly drawn blood specimen. The AC was incubated with serum at 37°C in a 1 : 100 ratio for AC and serum respectively. A sample was drawn out immediately as the zero-time specimen and was subjected to ITLC. The contents were subjected to occasional shaking and periodic samples at 45-minute for ^{213}Bi labeled antibody or protein. The drawn out specimen was subjected to ITLC.

III.5 Yttrium-90-PAI2 labelling protocol (Kukis et al., 1998)

Yttrium–90 in 1.16 M HCl was buffered in 4 M ammonium acetate (pH 7.3) and then DOPA-PAI2 in 0.1 M ammonium acetated (pH 5) were added. The final concentration of ammonium acetate was 0.4-0.5, and the final pH was 7. Radioleblelling solutions were incubated at 37C for 30 minutes DTPA (0.1 M) in 0.5 M ammonium acetate (pH 5) was added to a final concentration of 10 mM. The FTPA challenged radioleblelling solution was incubated at room temperature for 15 minutes and then purified and transferred to saline by G-25 molecular sieving chromatography or centrifuged column gel filtration. The radioimmunoconjugates were examined by ITLC.